Universidade de São Paulo
Instituto de Física

Termodinâmica de Vaidya-de Sitter e aplicações

Thiago de Lima Campos

Orientador: Prof. Dr. Carlos Molina Mendes

Dissertação de mestrado apresentada ao Instituto de Física da Universidade de São Paulo, como requisito parcial para a obtenção do título de Mestre em Ciências.

Banca Examinadora:
Prof. Dr. Carlos Molina Mendes - Orientador (EACH/USP)
Prof. Dr. Rodrigo Nemmen da Silva (IAG/USP)
Prof. Dr. George Emanual Avraam Matsas (IFT/UNESP)

São Paulo
2021

FICHA CATALOGRÁFICA
Preparada pelo Serviço de Biblioteca e Informação
do Instituto de Física da Universidade de São Paulo

Campos, Thiago de Lima

Termodinâmica de Vaidya-de Sitter e aplicações. São Paulo, 2021.

Dissertação (Mestrado) – Universidade de São Paulo. Instituto de Física. Depto. de Física Matemática.

Orientador(a): Prof. Dr. Carlos Molina Mendes

Área de Concentração: Física

Unitermos: 1. Relatividade (física); 2. Buracos negros; 3. Termodinâmica.

USP/IF/SBI-088/2021

University of São Paulo
Physics Institute

Thermodynamics of Vaidya-de Sitter and applications

Thiago de Lima Campos

Supervisor: Prof. Dr. Carlos Molina Mendes

Dissertation submitted to the Physics Institute of the University of São Paulo in partial fulfillment of the requirements for the degree of Master of Science.

Examining Committee:
Prof. Dr. Carlos Molina Mendes - Orientador (EACH/USP)
Prof. Dr. Rodrigo Nemmen da Silva (IAG/USP)
Prof. Dr. George Emanual Avraam Matsas (IFT/UNESP)

São Paulo
2021

Aos meus avós.

Acknowledgements

To Camila for always being by my side.

To my parents for encouraging me to move to São Paulo to get my master's degree.

To my friends for the good moments together at the university.

To Carlos for all his help and patience during the development of this project.

This work was carried out with the support of CNPq, Conselho Nacional de Desenvolvimento Científico e Tecnológico - Brasil. Hence, I also thank the CNPq for the financial support.

We accept the reality of the world with which we're presented. It's as simple as that.

The Truman Show

Abstract

In this project, black holes in an environment of positive cosmological constant will be investigated, emphasizing the thermodynamic characteristics of the system. Specifically, we are interested in the Vaidya-de Sitter solution, which represents a generalization of Schwarzschild-de Sitter with accretion or emission of radiation. A thermodynamic analysis for both spacetimes will be conducted, where the formalism proposed by Hayward *et al.* will be employed. For this reason, the Hayward black-hole thermodynamics is going to be studied in details. This method is suitable for the investigation of spherically symmetric dynamical geometries which possess trapping horizons. Once the characterization of the relevant spacetimes is performed, the results obtained will be applied in a model of a primordial black hole. A function for the mass parameter is assumed and, then, it is measured how important thermodynamic quantities evolve according to the cosmic time.

Keywords: black-hole thermodynamics, Hayward thermodynamics, Schwarzschild-de Sitter spacetime, Vaidya-de Sitter spacetime, primordial black holes.

Resumo

Neste projeto, serão investigados buracos negros em um ambiente de constante cosmológica positiva, enfatizando as características termodinâmicas do sistema. Especificamente, estamos interessados na solução de Vaidya-de Sitter, que representa uma generalização de Schwarzschild-de Sitter com acreção ou emissão de radiação. Será realizada uma análise termodinâmica para ambos os espaços-tempos, onde será empregado o formalismo proposto por Hayward *et al.*. Por esse motivo, a termodinâmica de Hayward para buracos negros será estudada em detalhes. Este método é adequado para a investigação de geometrias dinâmicas e esfericamente simétricas que possuem *trapping horizons*. Uma vez realizada a caracterização dos espaços-tempos de interesse, os resultados obtidos serão aplicados em um modelo de um buraco negro primordial. Uma função para o parâmetro de massa é assumida e, então, será acompanhado como grandezas termodinâmicas importantes evoluem de acordo com o tempo cósmico.

Palavras-chave: termodinâmica de buracos negros, termodinâmica de Hayward, espaço-tempo Schwarzschild-de Sitter, espaço-tempo Vaidya-de Sitter, buracos negros primordiais.

Contents

Chapter 1

Introduction

The proposal that black holes present a thermodynamic behavior was not an immediate result but, instead, it was an idea developted during the 1970s. Along those years, laws of black-hole mechanics in an apparent analogy to those from classical thermodynamics were discovered. The first one to be derived is known as the Area Theorem (or the Second Law) and was proved by S. Hawking in 1972. It showed that, under physically reasonable assumptions, the area of the event horizon could not decrease [25]. The resemblance with the second law of classical thermodynamics was pointed out by J. Bekenstein who proposed that this area should measure, somehow, the entropy contained in the black hole [7].

In 1974, J. Bardeen, B. Carter and S. Hawking presented the other three laws of black-hole mechanics in [16] and their apparent similarity to the laws of classical thermodynamics were mentioned. The missing connection that made possible the reinterpretation of these laws as thermodynamic ones came when Hawking showed, one year latter, that a black hole is evaporating as particles in a thermal spectrum are emitted from the event horizon [26]. Then, the apparent result that a black hole has zero temperature is, in fact, not true.

It is known that classical thermodynamics is a description of macroscopic effects caused by a large set of interacting small particles. For instance, the entropy assigned for a thermodynamic system is directly related to the number of accessible states for the constituent particles. Therefore, a lot of the interest behind the study of black-hole thermodynamics is explained by the expectation that it is an effective theory of an unknown quantum gravity theory and, hence, it could lead to the discovery of new physics.

The laws of the Bekenstein-Hawking black-hole thermodynamics developted during the 1970s are remarkable results. On the other hand, one of its limitations is that it is only applicable to stationary geometries. It was motivated to extend their work to dynamical spacetimes that S. Hayward published in 1994 and 1998 the generalized laws of black-hole mechanics [28, 30].

Dynamical solutions in General Relativity usually behave in a distinctive way when compared to the stationary ones. Some quantities that are defined for the latter geometries are particular for time-symmetric and asymptotically flat spacetimes, therefore, they do not exist in more general scenarios. Thus, one of S. Hayward's challenges was to find the right counterparts for objects in the Bekenstein-Hawking theory in order to develop his generalized work. One of this changes is a key point in Hayward's theory: the role of the event horizon in the usual black-hole thermodynamics is now played by trapping horizons. Unlike the usual definition for the boundary of a black-hole, trapping horizons are quasi-local structures in the sense that can be defined based on the information available in limited regions of the spacetime. Therefore, it is, in principle, possible to locate a black hole given a finite set of observers.

Although Hayward's work is limited to spherically symmetric spacetimes, it supports solutions that are not time-symmetric. For instance, it can be used in order to study the thermodynamics of a black hole rapidly evaporating via the Hawking Radiation. Other scenarios in which the Hayward black-hole thermodynamics are useful are those where there is a black hole immersed in a dynamical cosmological background. An important example of such solution for the Einstein Equation is the Schwarzschild-de Sitter spacetime, which considers a static and compact spherical object in an environment of accelerated cosmic expansion. An even more interesting situation is when the black hole itself is dynamical, evaporating and/or accreting radiation, in the same background. In this case, the geometry is known as Vaidya-de Sitter.

There is one class of black holes that are subjected to the dynamics of the universe since its early times. These primordial black holes, as they are called, are understood as those who could have been formed before the first stars. They are hypothetical and their existence have been considered since the the 1960s due to the works of I. Novikov and Y. Zel'dovich [66] and, also, S. Hawking [24]. There are proposals in which primordial black holes come in a large variety of mass intervals [13]. Those small enough would be under a strong evaporation process and, therefore, Hayward's work should be an adequate theory in order to study their thermodynamics.

Although de Sitter is a possible asymptotic geometry for our universe in the far future according to the FLRW cosmological model, treating the black hole in a de Sitter background may lead to interesting results as it accounts for the expansion of the spacetime. Furthermore, considering the cosmological environment in which the black hole is immersed could lead to a procedure that can be generalized to take into account the other contents present in the universe.

In this work, we propose to study the Hayward black-hole thermodynamics and to apply it to a dynamical black hole in a universe filled with a positive cosmological constant, that is, the Vaidya-de Sitter spacetime. This work is intended to be self-contained as much as possible so that not only Hayward's formalism and its application is presented in details but also that it can be useful as a possible reference in the subject. In order for this goal to be fully accomplished, the content of this work is divided in five chapters.

Chapter 2 (Geometry and General Relativity) is a brief collection of the main definitions and results of differential geometry and General Relativity. It is intended to be written in the right balance between concise and clearness so that it can be useful as a review for the mathematics and physical interpretations of Einstein's theory. Next, in Chapter 3 (Spherically symmetric solutions) we start to develop a groundwork for this dissertation. Symmetries related to the intrinsic geometry of a spacetime are defined and a special focus is given to the spherical one. This is justified by the fact that, as already pointed out, it is only in spherical symmetric spacetimes that Hayward's work is applicable. Then, three geometries which represent limit cases for Vaidya-de Sitter are studied separately. These are the de Sitter, Schwarzschild and Vaidya solutions.

It is in Chapter 4 (Black-hole thermodynamics) where the Bekenstein-Hawking and the Hayward theories are presented. However, before each theory is properly discussed, the characterization of horizons in General Relativity is given in details. Event and trapping horizons are defined and their main distinctions pointed out. Then, the black-hole thermodynamics are introduced starting, as it should be, with the one developed during the 1970s. For both theories, the focus is given towards presenting and proving the usual and the generalized laws of black-hole mechanics. How the transition for a true thermodynamics is given via the Hawking Radiation is also discussed.

In Chapter 5 (Applications of the Hayward thermodynamics), it will be studied, for the Schwarzschild-de Sitter and Vaidya-de Sitter geometries, the thermodynamics of the trapping horizons either relative to the presence of a black hole or defining a cosmological horizon due to the expansion of the spacetime. The relevant thermodynamic quantities are calculated and interpreted for a general mass parameter and cosmological constant, also, when possible, compared with their counterparts from the Bekenstein-Hawking theory. It is derived that, given the definition for the energy of a black hole used in the Hayward thermodynamics [29] (and assuming further conditions), no phase transition occurs for these geometries. Another interesting result shown is that defining a total energy, according to the same description, and a total entropy, the Hawking Radiation takes the system to a state where these quantities are, respectively, minimized and maximized, as it is expected for an isolated system in classical thermodynamics.

Once the thermodynamic characterization of these geometries is well understood, the next goal is to apply the results in more concrete physical cases. This is what is done in Chapter 6 (Primordial black holes), where the specific scenario chosen is the primordial black holes. For that, we propose a simplified model for the dynamics of a black hole immersed in an environment of positive cosmological constant and study how it evolves according to the cosmological time. Similarly to the work of W. Hiscock [35], the region outside the black hole is taken as a Vaidya-de Sitter spacetime with massless particles being emitted from its trapping horizon. One of the main challenges in this proposal is to find how the dynamics in this model can be measured as a function of the time used in cosmology, with respect to which the chronology of the universe is studied.

The physical constants c, G, k_B and $\hbar$ are set equal to one unless otherwise stated. The signature for the metric is $(- \ + \ + \ +)$ and the tensor notation followed is the same as the one used in [17].

Chapter 2

Geometry and General Relativity

We intend with this chapter to present a collection of the main definitions in Differential Geometry and General Relativity in a direct but clear manner. The goals are to make this work self-contained as much as possible and also that the reader can return here whenever necessary to recall some definition. Section 2.1 treats of smooth manifolds, which is the background structure of spacetimes, and tensor fields, that are coordinate independent objects defined on the manifold used to express the laws of physics in General Relativity. In Section 2.2, it is added a metric tensor to the manifold so that it becomes a spacetime. A way to differentiate tensors and some physical interpretations of the spacetime are also discussed. Lastly, in Section 2.3 the curvature tensor is presented as well as the Einstein Equation, which relates the curvature of the spacetime with its energy-momentum content.

2.1 Manifolds and tensors

An n-dimensional **smooth manifold** (to be called just manifold) M is a topological space such that for each point $p \in M$ there is an open set U_α containing p and a homeomorphism $\varphi_\alpha : U_\alpha \to \mathbb{R}^n$, such that the transition functions (change of coordinates) $\varphi_\alpha \circ \varphi_\beta^{-1}$ are diffeomorphisms. The combination $(U_\alpha, \varphi_\alpha)$ is called a **chart** and φ_α a chart function. This one can be seen as n real functions $x^\mu : U_\alpha \to \mathbb{R}$ called the **coordinate functions**.

In General Relativity, the spacetime is taken as a smooth manifold. This assumption assures that any function and curve defined on the geometry can be continuously differentiated as many times as it is needed. It is also expected to hold at large enough scales and to break down at quantum distances, in which the spacetime itself could be quantized [33].

A map $f : V \subset M \to \mathbb{R}$ is said to be a **smooth function**, $C^\infty(M)$, if for any

$U_\alpha \cap V \neq 0$, $f \circ \varphi_\alpha^{-1} : \mathbb{R}^n \to \mathbb{R}$ is smooth. This definition of smooth functions on a manifold transforms the chart functions into diffeomorphisms.

A **vector field** v on M is a map $v : C^\infty(M) \to C^\infty(M)$ which is linear and satisfies the Leibniz law:

$$\begin{aligned} v(\alpha f + \beta g) &= \alpha v(f) + \beta v(g), \\ v(fg) &= v(f)g + f v(g), \end{aligned} \tag{2.1}$$

where $f, g \in C^\infty(M)$ and $\alpha, \beta \in \mathbb{R}$. The vector space of all vector fields on M is denoted by TM and is called the vector bundle.

From this definition, partial derivatives $\partial_\mu : C^\infty(\mathbb{R}^n) \to C^\infty(\mathbb{R}^n)$ are vector fields on $\mathbb{R}^n$. It is an important theorem that partial derivatives form a basis [8] and, therefore, any vector field on $\mathbb{R}^n$ can be written as a linear combination of them:

$$v = v^\mu \partial_\mu, \tag{2.2}$$

where v^μ are smooth functions on $\mathbb{R}^n$. Therefore, when working on a chart of the manifold, that is, on an open set $O_\alpha \subset \mathbb{R}^n$ such that $\varphi_\alpha(U_\alpha) = O_\alpha$, we can use (2.2).

Given a point $p \in M$, a vector field gives a function $v_p : C^\infty(M) \to \mathbb{R}$ defined by $v_p(f) = \big[v(f)\big](p)$. The function v_p is called a **tangent vector** at p and vector space of all tangent vectors at this point is called the tangent space at p, T_pM.

An **1-form** θ is a map $\theta : TM \to C^\infty(M)$, which is linear over smooth functions:

$$\theta(fv + gw) = f\theta(v) + g\theta(w). \tag{2.3}$$

An 1-form defines a **covariant vector** at each point through $\theta_p(v_p) = \big[\theta(v)\big](p)$. The vector space of 1-forms over M are denoted T^*M and is called the cotangent bundle and the vector field of cotangent vectors on a point p is denoted T_p^*M. As the 1-form is a function of vector fields, we can invert the definition so that $v : T^*M \to C^\infty(M)$ and $v(\theta) = \theta(v)$.

From the definition of 1-forms and defining the **differential** of f, df, by $df(v) = v(f)$, which is also an 1-form, the differentials $dx^\mu : T\mathbb{R}^n \to C^\infty(\mathbb{R}^n)$ form a basis [8] and any 1-form on $\mathbb{R}^n$ can be written as

$$\theta = \theta_\mu dx^\mu, \tag{2.4}$$

where $\theta_\mu \in C^\infty(\mathbb{R}^n)$. Then, when working on the charts of a manifold, we can use (2.4).

Vector fields and 1-forms are special types of tensor fields. A (r, s) tensor bundle is the tensor product of r copies of TM and s copies of T^*M. An element of this tensor bundle is called a **tensor field** of rank (r, s) and, by definition, scalar fields are $(0, 0)$ tensors.

A tensor field T is, then, a C^∞-multilinear function $T : \otimes^r T^*M \otimes \otimes^s TM \to C^\infty(M)$. When working in a chart,

$$T = T^{\mu_1 \dots \mu_r}{}_{\nu_1 \dots \nu_s} \partial_{\mu_1} \otimes \dots \otimes \partial_{\mu_r} \otimes dx^{\nu_1} \otimes \dots \otimes dx^{\nu_s}, \tag{2.5}$$

where $T^{\mu_1 \dots \mu_r}{}_{\nu_1 \dots \nu_s} \in C^\infty(\mathbb{R}^n)$ are the components of T.

It is a principle in general relativity that the laws of physics should be written in coordinate-invariant equations as there is no preferable coordinate system (observer) to describe nature. This is known as General Covariance. Since tensors are independent of a particular chart, they are appropriate objects to write equations in Einstein's theory.

2.2 Semi-Riemannian geometry and spacetime

A **semi-Riemannian metric** (which will be called just metric) is a tensor field of rank (0,2), that is, a C^∞-bilinear map $g : TM \otimes TM \to C^\infty$ which is symmetric and nondegenerate:

$$\begin{aligned} &g(v, w) = g(w, v), \\ &g(v, w) = 0 \text{ for all } w \implies v = 0. \end{aligned} \tag{2.6}$$

Given a metric, we can always a construct at each point of M an orthonormal basis (also called as tetrad basis), $\{n_\mu\}$. If $g(n_\alpha, n_\alpha) = 1$ for p vectors in this basis and there are q vectors such that $g(n_\beta, n_\beta) = -1$, then it is said that the signature of the metric is (p, q).

A metric is added to the spacetime in order for observers to be able to compute distances, time intervals and angles between vectors. Moreover, in Einstein's theory the spacetime is a 4-dimensional semi-Riemannian manifold, that is a manifold equipped with a metric tensor of signature (3,1).

If $g(v, v) > 0$, then the tangent vectors of v (and v itself) are called **spacelike**. If $g(v, v) < 0$, then they are called **timelike**. And if $g(v, v) = 0$, they are **null**. In General Relativity particles can only travel along curves[1] whose tangent vectors are all timelike (or null for massless particles)[2]. These are called timelike (or null) curves and similarly are defined the spacelike curves. The elapsed **proper time** τ of a timelike curve $\gamma(t) : [a, b] \subset \mathbb{R} \to M$ is

$$\tau = \int_b^a \sqrt{-g(\gamma', \gamma')} dt, \tag{2.7}$$

[1] A **curve** is a map $\gamma : U \subset \mathbb{R} \to M$ whose tangent vector is given by $\gamma'(f) = \frac{d}{dt}(f \circ \gamma)$ for any smooth function f.

[2] In Chapter 4, it will be seen how causal relations between events of a spacetime are determined by the metric tensor.

which is the time measured by the clock of an observer following this curve on the spacetime.

The metric tensor also defines an isomorphism between TM and T^*M:

$$g : v \mapsto g(v,\ ), \tag{2.8}$$

and, for that reason, we can define in a chart, unambiguously, $v_\mu \equiv g_{\mu\nu} v^\nu$. This procedure is called lowering the index (similarly, we can define the raising of an index with the inverse of the metric tensor, $g^{\mu\nu}$).

A **connection** D on a manifold is a map

$$D : \bigotimes^{r} T^*M \otimes \bigotimes^{s+1} TM \longrightarrow \bigotimes^{r} T^*M \otimes \bigotimes^{s} TM \tag{2.9}$$

satisfying, by definition,

$$\begin{aligned}
&D_v(T_1 + T_2) = D_v T_1 + D_v T_2, \\
&D_v(fT) = v(f)T + f D_v T, \\
&D_{fv_1+v_2} T = f D_{v_1} T + D_{v_2} T, \\
&D_v(T_1 \otimes T_2) = D_v(T_1) \otimes T_2 + T_1 \otimes D_v(T_2), \\
&\mathrm{C}(D_v T) = D_v\big[\mathrm{C}(T)\big],
\end{aligned} \tag{2.10}$$

where $v, v_1, v_2 \in TM$, $f \in C^\infty(M)$ and $\mathrm{C}(T)$ is the contraction of (sum over) a covariant and a contravariant index. Notice that the connection is only C^∞-linear in its argument that has v (or $v_1 + v_2$) as its input and, therefore, D could not be turned into a tensor.

For a manifold representing spacetime, there is a preferable type of connection, usually denoted ∇, known as the **Levi-Civita connection**, which is metric compatible and torsion free. That is

$$\begin{aligned}
&u\big[g(v,w)\big] = g(\nabla_u v, w) + g(v, \nabla_u w), \\
&[v,w] = \nabla_v w - \nabla_w v,
\end{aligned} \tag{2.11}$$

where $v, w, u \in TM$.

These properties together imply that, when working on a chart, the action of ∇_v on the bases $\{\partial_\mu\}$ and $\{dx^\mu\}$ is uniquely given by

$$\begin{aligned}
&\nabla_v \partial_\mu = v^\nu \Gamma^\sigma{}_{\nu\mu} \partial_\sigma, \\
&\nabla_v dx^\mu = -v^\nu \Gamma^\mu{}_{\nu\sigma} dx^\sigma,
\end{aligned} \tag{2.12}$$

where we have **Christoffel symbols**

$$\Gamma^{\sigma}{}_{\nu\mu} = \frac{1}{2} g^{\sigma\rho} (\partial_{\nu} g_{\mu\rho} + \partial_{\mu} g_{\nu\rho} - \partial_{\rho} g_{\nu\mu}). \tag{2.13}$$

Since the action of ∇ is determined by how it acts on the basis, we conclude that the Levi-Civita connection is unique. For instance, if T is of rank (1,1) the components of $\nabla_{\mu} T \equiv \nabla_{\partial_{\mu}} T$ are

$$\left(\nabla_{\sigma} T\right)^{\mu}_{\nu} \equiv \nabla_{\sigma} T^{\mu}_{\nu} = \partial_{\sigma} T^{\mu}_{\nu} + \Gamma^{\mu}{}_{\sigma\rho} T^{\rho}_{\nu} - \Gamma^{\rho}{}_{\sigma\nu} T^{\mu}_{\rho}. \tag{2.14}$$

Although a connection is not itself a tensor field, given a tensor T of rank (r,s), we can define a tensor field of rank $(r, s+1)$, called the **covariant derivative** of T. In a chart, this is given by

$$\nabla T = dx^{\mu} \otimes \nabla_{\mu} T. \tag{2.15}$$

We know how this tensor acts since the components of $\nabla_{\mu} T$ are uniquely defined due to the previous discussion. Moreover, as it is apparent in (2.14), the covariant derivative of T on the direction of v, that is, $\nabla_{v} T$, is a generalization of the usual directional derivative for a semi-Riemannian manifold in an arbitrary coordinate system (the Christoffel symbols are needed to tell how the basis changes from point to point).

Given a curve $\gamma : \mathbb{R} \to M$, it is said that a tensor is **parallel transported** along γ if

$$\nabla_{\gamma'} T = 0. \tag{2.16}$$

One important class of curves are the **geodesics**, which are the ones whose tangent vectors are parallel transported along their integral curves[3]:

$$\nabla_{\gamma'} \gamma' = 0. \tag{2.17}$$

The geodesic equation is given in a chart by

$$\frac{d^2 \gamma^{\mu}}{dt^2} + \Gamma^{\mu}{}_{\nu\lambda} \frac{d\gamma^{\nu}}{dt} \frac{d\gamma^{\lambda}}{dt} = 0, \tag{2.18}$$

where $\gamma^{\mu} \equiv x^{\mu} \circ \gamma$. Geodesics are the analogous of straight lines for curved geometries and in General Relativity they are the (timelike or null) paths followed by free-falling (that is, unaccelerated) particles.

When working in a chart, the properties that define the Levi-Civita connection (2.11)

[3]Equation (2.17) is, actually, only true if $\gamma(t)$ is **affinely-parametrized**. Other parametrizations yield $\nabla_{\gamma'} \gamma' = \alpha \gamma'$, where α is a function on the curve.

assume the form

$$\begin{aligned}\nabla_\rho g_{\mu\nu} &= 0,\\ \Gamma^\rho{}_{\mu\nu} &= \Gamma^\rho{}_{\nu\mu},\end{aligned} \tag{2.19}$$

from where the geometric interpretation about the metric compatibility is straightforward: parallel transport preserves lengths and angles.

2.3 Curvature and the Einstein Equation

The **curvature** F of a connection D is a map $F : \otimes^3 TM \to TM$ which is C^∞-linear in all its slots and defined by

$$F(v,w)u = D_v D_w u - D_w D_v u - D_{[v,w]}u. \tag{2.20}$$

If the connection is the Levi-Civita one, then it is called the **Riemann curvature** and denoted by R. It can also be seen as a tensor of rank (1,3) $F : \otimes^3 TM \otimes T^*M \to C^\infty(M)$ defined such that

$$R(\theta, v, w, u) = \theta\big[R(v,w)u\big]. \tag{2.21}$$

And, for that reason, it is called the Riemann curvature tensor.

The components of the Riemann tensor, which, by definition

$$R^\alpha{}_{\beta\gamma\delta} \equiv dx^\alpha\big[R(\partial_\beta, \partial_\gamma)\partial_\delta\big], \tag{2.22}$$

are calculated from the Christoffel symbols (which depend only on the metric tensor):

$$R^\alpha{}_{\beta\gamma\delta} = \partial_\beta \Gamma^\alpha{}_{\gamma\delta} - \partial_\gamma \Gamma^\alpha{}_{\beta\delta} + \Gamma^\sigma{}_{\gamma\delta}\Gamma^\alpha{}_{\beta\sigma} - \Gamma^\sigma{}_{\beta\delta}\Gamma^\alpha{}_{\gamma\sigma}. \tag{2.23}$$

Other tensors are obtained contracting the Riemann tensor:

Ricci tensor: $R_{\beta\delta} \equiv R^\alpha{}_{\beta\alpha\delta}$, (2.24)

Ricci scalar or **curvature scalar**: $R \equiv R^\alpha{}_\alpha$. (2.25)

The **Einstein Equation** relates the "matter" in the spacetime to the curvature it produces:

$$R_{\mu\nu} - \frac{1}{2}R g_{\mu\nu} + \Lambda g_{\mu\nu} = 8\pi T_{\mu\nu}, \tag{2.26}$$

The validity of (2.26) has been proved by a large number of experiments until the current days. Three of them, called the classical tests of General Relativity were proposed by Einstein himself. These are the deflection of light as it passes near to a massive compact object, the precession of perihelia in Mercury's orbit and the gravitational redshift [17].

Equation (2.26) can also be written as

$$R_{\mu\nu} = 8\pi\left(T_{\mu\nu} - \frac{1}{2}Tg_{\mu\nu}\right) + \Lambda g_{\mu\nu}. \tag{2.27}$$

$T_{\mu\nu}$ is the **energy-momentum tensor** ($T \equiv T^{\mu}{}_{\mu}$), which is symmetric and corresponds to the content present in the spacetime, and Λ is a scalar called the cosmological constant.

The tensor $G_{\mu\nu} \equiv R_{\mu\nu} - \frac{1}{2}Rg_{\mu\nu}$ is known as the **Einstein tensor** and it is symmetric of zero divergence

$$\nabla^{\mu}G_{\mu\nu} = 0. \tag{2.28}$$

From (2.26), the divergence of $T_{\mu\nu}$ also vanishes and this is the local conservation of energy-momentum of General Relativity. The physical (local) interpretation for the components of the energy-momentum tensor are

$$\begin{aligned}
T^{00} =& \text{ energy density,} \\
T^{0i} =& \text{ energy flux across a surface of constant spatial coordinate } x^i, \\
T^{i0} =& \text{ density of momentum in the direction of } \partial_i, \\
T^{ij} =& \text{ flux of momentum in the direction of } \partial_i \text{ across a surface of} \\
& \text{ constant spatial coordinate } x^j.
\end{aligned} \tag{2.29}$$

These can be summarized as: $T^{\mu\nu}$ corresponds locally to the flux of energy-momentum in the direction of ∂_μ across a surface of constant x^ν. If there is a coordinate system (chart) where $T^{0i} = T^{i0}$ and T^{ij} (for $i \neq j$) are equal to zero, then it is said, respectively, that this fluid has no heat conduction and no viscosity. From the Einstein Equation, there are only geometrical constraints on the possible fluids. Thus, in order to restrict the possible energy-momentum tensors, it is usually imposed energy conditions which seem to be in accordance to classical physics [17]. There are several of these constraints and we are not going to present them here, instead, they will be cited along this work whenever any of them is important.

From the Einstein Equation, a spacetime is characterized by its metric tensor in General Relativity. Then, two models for the spacetime are considered locally equivalent if they are isometric in these regions (as defined in Section 3.1) and, for this reason, it is said that the General Relativity is an isometric invariant theory. Furthermore, it is only physically important to consider spacetime as a connected manifold, but, when solving the Einstein Equation (that is, finding a metric tensor given an energy-momentum tensor), it is not rare to find disconnected regions. So, they shall be consider different spacetimes unless it can be found a larger geometry with submanifolds isometric to the previous disconnected components. If this happens, it is said the spacetime has been extended. The importance of extending a spacetime is to make sure that is not possible for any geodesic, defined for all values of its affine parameter, to end at an event, unless this event represents a curvature singularity. If this is the case, then it is said that the spacetime is maximally extended. Such geometries are recurrent in the studies of causal relations in a spacetime as it will be seen in this work.

Chapter 3

Spherically symmetric solutions

The aim of this work is to study the thermodynamics of the Vaidya-de Sitter spacetime through the theory developted by S. Hayward. The present chapter is the first step towards this goal. We are going to introduce the de Sitter spacetime, representing a universe of positive cosmological constant in vacuum, which is studied in details in Section 3.2. Then, the Schwarzschild geometry, a solution for a spherical object (possibly a black hole) of constant mass in empty space, is presented in Section 3.3. After that, a generalization of this solution for a dynamical mass, the Vaidya spacetime, is analyzed in Section 3.4. In this way, we study each geometry separately so that, latter in this work, they are combined as Schwarzschild-de Sitter and, more importantly, Vaidya-de Sitter.

One major feature of all the spacetimes cited above is that they are spherically symmetric. Such geometries are the only ones in which Hayward's theory is applicable and, therefore, this chapter starts, in Section 3.1, discussing the symmetries related to the metric, focusing on the spherical symmetry.

3.1 Symmetries

In order to talk about symmetries on a spacetime we must be able to compare tensors on different points of a manifold. Specifically, if the symmetry is from the intrinsic geometry and also continuous, we need to compare the metric on points arbitrarily close. Defining a rigorous way to do this is where we start in this section.

Let $\phi : M \to N$ be a smooth map between two manifolds[1]. Then, the **pushforward** of a vector field $w \in TM$ defines a vector field, denoted $\phi_* w$, in TN :

$$\phi_* w(f) \equiv w(f \circ \phi), \tag{3.1}$$

[1]A map ϕ between two manifolds M and N is smooth if, for any charts φ_α in M and ψ_β in N, the map $\psi_\beta \circ \phi \circ \varphi_\alpha^{-1} : \mathbb{R}^n \to \mathbb{R}^n$ is C^∞.

where f is any smooth real function in N. And the **pullback** of a 1-form $\theta \in T^*N$ defines a 1-form, denoted $\phi^*\theta$, in T^*M :

$$\phi^*\theta(u) \equiv \theta(\phi_* u), \tag{3.2}$$

where u is any vector field in TM.

Moreover, if ϕ is a diffeomorphism, we can define the pullback of general tensor fields. In order to see how it works, let T be a tensor field of rank $(1,1)$ over a manifold N, v a vector field on TM and ω a 1-form on T^*M. Then, the pullback of T is defined by

$$\phi^*T(v,\omega) \equiv T\big[\phi_* v, (\phi^{-1})^*\omega\big]. \tag{3.3}$$

From this definition, a generalization for tensor fields of arbitrary rank is straightforward.

A diffeormorphism allow us to compare a tensor on a point $p \in M$ to another tensor on $\phi(p) \in N$. If this tensor is the metric, then we can already define **isometric** manifolds as those which are connected by a diffeomorphism $\phi : M \to N$, called an isometry, such that $\phi^* g_N(v,w) = g_M(v,w)$, where g_N and g_M are the metric tensors on the manifolds M and N and $v, w \in TM$ are arbitrary.

If the diffeomorphism takes a point on a manifold to another point on the same manifold, that is, $\phi : M \to M$, then this gives a way to compare tensors of distinct points on the same geometry. Therefore, we are able to define two other symmetries which are specially important in cosmology. The first one is **homogeneity**, which is the property that every point is equivalent. In mathematical rigour, given any two points p and q, there is an isometry $\phi : M \to M$ such that $\phi(p) = q$. And the second one is **isotropy**, which is the property that every direction is equivalent. Formally, for any point p and tangent vectors $v_p, w_p \in T_pM$, there is an isometry $\phi : M \to M$ such that $\phi_* v_p$ is parallel to w_p [17].

Moreover, if there is a way to compare tensors arbitrarily close, then this would give us a way of differentiation. In the following, it is presented how this derivative can be defined.

A vector field in an open set $\mathcal{O}$ of a manifolds M generates a congruence of integral curves parametrized, by definition, by λ: ϕ_λ. Through any point $p \in \mathcal{O}$ passes an unique curve $\phi_\lambda(p)$ which can always be reparametrized such that $\phi_0(p) = p$. In this way, ϕ_λ can be interpreted as a function $\phi_\lambda : \mathbb{R} \times M \to M$ which, when specified a point, defines a curve through it or, when specified a real value for the parameter, defines a function (actually, a diffeomorphism) which takes each point to another one, over the same curve, with a parametric distance of λ.

Given a one-parameter family of diffeomorphisms, such as defined above, we can take the limit $\lambda \to 0$ and compare two arbitrarily close tensors on points of the same curve. Then, if ϕ_λ is generated by a vector field K, this defines the **Lie derivative** of a tensor T on the direction of K at a point p :

$$\mathcal{L}_K T(p) \equiv \lim_{\lambda \to 0} \frac{\phi_\lambda^* T\big[\phi_\lambda(p)\big] - T(p)}{\lambda}. \tag{3.4}$$

If there is a connection in the manifold, then the Lie derivative can be written in terms of covariant derivatives [17]. For our purposes in this work, it is enough to write how it acts on arbitrary real function f and vector field v. These are, respectively,

$$\mathcal{L}_K f = K(f), \tag{3.5}$$

$$\mathcal{L}_K v = [v, K]. \tag{3.6}$$

Moreover, the Lie derivative of the metric tensor is also important for us. From the compatibility of $g_{\mu\nu}$ with the metric, we have

$$(\mathcal{L}_K g)_{\mu\nu} \equiv \mathcal{L}_K g_{\mu\nu} = 2\nabla_{(\mu} K_{\nu)}. \tag{3.7}$$

If the derivative vanishes, $\mathcal{L}_K g_{\mu\nu} = 0$, which implies in

$$\nabla_{(\mu} K_{\nu)} = 0, \tag{3.8}$$

then it is said that K, called a **Killing vector field**, is the generator of continuous isometries in M and (3.8) is known as the **Killing equation**.

One important property is that if K is a Killing vector field, then there is always a coordinate system such that it assumes the form of a coordinate vector $\frac{\partial}{\partial x^*}$ and no component of the metric will be a function of x^*. And the converse is also true. This gives a practical way to identify Killing fields given a metric as will be seen when we study specific solutions for the Einstein Equation.

The existence of Killing vector fields is used to classify spacetimes. For instance, if a region of a spacetime has a timelike Killing vector field, denoted χ^μ, than this region is called **stationary** [17]. Moreover, if these timelike Killing fields are orthogonal to a family of spacelike hypersurfaces, that is, if $\chi_{[\mu}\nabla_\nu \chi_{\sigma]} = 0$ [17], this region is called **static**. Many times, when the Killing vector field is timelike in infinity, it is said that the spacetime itself is stationary (or static).

Killing vectors define a surface that is recurrent in the study of black holes and specially important for the Bekenstein-Hawking thermodynamics: the **Killing horizon**. That is a null hypersurface such that the normal null vector field is of Killing-type. Since the Killing horizon is characterized for being the 3-dimensional surface where $K^\mu K_\mu = 0$, in which K^μ is the orthogonal Killing vector field, the vector field $\nabla^\mu(K^\nu K_\nu)$ is also normal to the horizon and we can write

$$\nabla^\mu(K^\nu K_\nu) \overset{h}{=} -2\kappa K^\mu \tag{3.9}$$

(only on the horizon and, therefore, we use the symbol $\overset{h}{=}$) for some function κ, whose actual value depends on the normalization of the Killing vector field. For static and asymptotically flat spacetimes, it is usually taken a normalization such that at infinity $K^\mu K_\mu = -1$. However, in this work we are going to work with the de Sitter geometry, which has an asymptotic structure different than the one from Minkowski (as we shall see in Section 3.2). Therefore, we will always talk about a κ for a previously specified Killing vector field and will only ask for its normalization to be such that κ is positive. Then, this function is called **surface gravity**[2].

The surface gravity is greatly important in the Bekenstein-Hawking thermodynamics for black holes. Therefore, we will derive an equation from where κ can be straightforwardly computed from. In order to do this, we use the Killing equation $\nabla_{(\mu}K_{\nu)} = 0$ and the condition for a vector field to be normal to a hypersurface $K_{[\mu}\nabla_\nu K_{\sigma]} = 0$. These two equations together give a condition for the Killing vector field on the Killing horizon:

$$K_\sigma \nabla_\mu K_\nu + K_\mu \nabla_\nu K_\sigma + K_\nu \nabla_\sigma K_\mu \overset{h}{=} 0. \tag{3.10}$$

We know from (3.9) $K^\nu \nabla^\mu K_\nu \overset{h}{=} -\kappa K^\mu$, which suggests contracting the previous equation with $\nabla^\mu K^\nu$:

$$\begin{aligned}
(\nabla^\mu K^\nu)K_\sigma \nabla_\mu K_\nu + (\nabla^\mu K^\nu)K_\mu \nabla_\nu K_\sigma + (\nabla^\mu K^\nu)K_\nu \nabla_\sigma K_\mu \\
\overset{h}{=} K_\sigma(\nabla^\mu K^\nu)\nabla_\mu K_\nu + \kappa K^\nu \nabla_\nu K_\sigma - \kappa K^\mu \nabla_\sigma K_\mu \\
\overset{h}{=} K_\sigma(\nabla^\mu K^\nu)\nabla_\mu K_\nu - 2\kappa K^\nu \nabla_\sigma K_\nu \\
\overset{h}{=} K_\sigma(\nabla^\mu K^\nu)\nabla_\mu K_\nu + 2\kappa^2 K_\sigma \overset{h}{=} 0.
\end{aligned} \tag{3.11}$$

And we have:

$$\kappa^2 = -\frac{1}{2}(\nabla^\mu K^\nu)\nabla_\mu K_\nu. \tag{3.12}$$

As the existence of timelike Killing vector fields are used in order to classify the spacetimes which possess time translation symmetry, geometries with other kinds of Killing fields will be symmetric in other ways. The symmetry which is mostly important in this work is the spherical one since the Hayward black-hole thermodynamics is exclusive for

[2]The name surface gravity is due to the fact that for a static black hole in an asymptotically flat spacetime, and choosing the normalization $K^\mu K_\mu = -1$ at infinity, κ is the acceleration of a static observer near the Killing horizon that is measured by an observer at infinity [63].

the spacetimes in which it is present. So, in the rest of this section we are going to properly introduce the spherical symmetry.

A spacetime M is said to be **spherically symmetric** if it has three spacelike Killing vector fields, K_1, K_2 and K_3, that satisfy the Lie Algebra of $SO(3)$ [55]:

$$[K_i, K_j] = -\epsilon_{ijk}{}^{3} K_k, \tag{3.13}$$

and such that the set of integral curves generated by them determine 2-dimensional surfaces (or isolated points).

This definition implies that if a spacetime is spherically symmetric, then each point is contained in a submanifold isometric to the 2-sphere and, therefore, the metric of M can be described in a coordinate system such that this isometry is made explicit [55, 63]:

$$ds^2 = h_{ab}dx^a dx^b + r^2 d\Omega^2, \tag{3.14}$$

where r is a function of the non-angular coordinates and

$$d\Omega^2 \equiv d\theta^2 + \sin^2\theta d\phi^2. \tag{3.15}$$

Further comments are necessary about the function r, which is called **areal radius** for reasons we shall now clarify. For a 2-sphere embedded[4] in $\mathbb{R}^3$ the radius is the distance, measured with the metric of euclidean space, from any point of the surface to its center. However, the lesson of differential geometry is that in order to study manifolds they do not need to be embedded on a higher dimension and, thus, the radius loses its usual meaning. Nonetheless, we can intrinsically measure the area of the sphere and the result is still $A = 4\pi r^2$. Therefore, the physical meaning of r comes from the area of the sphere and, for this reason, it is usually called areal radius. Then, a spherically symmetric spacetime can be seen as a 2-dimensional surface (to be called **bidimensional effective surface**) such that on each point there is a 2-sphere of areal radius r.

In the present work, it will be useful to consider the line element of a static and

[3]The Levi-Civita symbol is defined as

$$\epsilon_{ijk} = \begin{cases} +1 & \text{for an even permutation of (1,2,3),} \\ -1 & \text{for an odd permutation of (1,2,3),} \\ 0 & \text{otherwise.} \end{cases}$$

[4]A manifold S is said to be embedded in another manifold M if there is a diffeomorphism such as $\phi : S \to \phi[S] \subset M$. The embedding is said to be isometric if ϕ is also an isometry. By an embedding we will always mean an isometric embedding.

spherically symmetric spacetime written in a form similar to

$$ds^2 = -A(r)dw^2 \pm 2\sqrt{\frac{A(r)}{B(r)}}dwdr + r^2 d\Omega^2. \tag{3.16}$$

Therefore, we present a condition that assures a surface in a geometry described by the metric above to be a Killing horizon for the Killing vector field ∂_w (which we know it is indeed a Killing field since the components of the metric tensor are all independent of the coordinate w). For that, it should be noticed that

$$(\partial_w)_\mu = g_{\mu\nu}(\partial_w)^\nu = g_{\mu w} = g_{ww}\partial_\mu w + g_{rw}\partial_\mu r. \tag{3.17}$$

Then, the 1-form $(\partial_w)_\mu$ is orthogonal to surfaces of constant radius r_K if

$$g_{ww}(r_K) = A(r_K) = 0 \tag{3.18}$$

and

$$\lim_{r\to r_K} \frac{A(r)}{B(r)} \text{ converges to a non-zero value.} \tag{3.19}$$

So, as long as

$$A(r)B(r) > 0 \text{ for all } r \text{ in some neighborhood of } r_K, \tag{3.20}$$

and (3.18 - 3.19) are true, the 2-sphere of radius r_K is a Killing horizon for the Killing vector field ∂_w.

3.2 de Sitter spacetime

The **de Sitter spacetime** is a solution for the Einstein Equation which is completely homogeneous and isotropic with constant positive curvature. Both these properties together imply that the spacetime is **maximally symmetric** [17]. This name refers to the fact that a maximally symmetric space, by definition, has the maximum number of linear independent Killing vector fields, which is $n(n+1)/2$, where n is the dimension of the manifold. And this kind of spacetimes are characterized for having the Riemann curvature tensor satisfying [17]

$$R_{\rho\sigma\mu\nu} = \frac{R}{n(n-1)}(g_{\rho\mu}g_{\sigma\nu} - g_{\rho\nu}g_{\sigma\mu}). \tag{3.21}$$

And contracting ρ and μ (for $n=4$), the Ricci tensor satisfies

$$R_{\sigma\nu} = \frac{1}{4}Rg_{\sigma\nu}. \tag{3.22}$$

From the metric compatibility (2.19), we have $\nabla_\rho R_{\mu\nu} = \frac{1}{4}(\partial_\rho R) g_{\mu\nu}$. Which becomes $\nabla^\nu R_{\mu\nu} = \frac{1}{4}(\partial^\nu R) g_{\mu\nu}$, when a contraction is made. However, the Einstein tensor is divergence-free (2.28), which implies $\nabla^\nu R_{\mu\nu} = \frac{1}{2}(\partial^\nu R) g_{\mu\nu}$. Comparing the previous two results, it is straightforward to conclude $\partial_\mu R = 0$. Therefore, a feature of a maximally symmetric geometry is that it has constant curvature. The converse, on the other hand, is not true. For the Schwarzschild spacetime, for instance, the Ricci scalar is zero everywhere.

If we rewrite equation (3.22) as

$$R_{\mu\nu} - \frac{1}{2} R g_{\mu\nu} + \frac{1}{4} R g_{\mu\nu} = 0, \tag{3.23}$$

it becomes clear that the maximally symmetric spacetime gives a metric tensor which solves the vacuum Einstein equation (2.26) for a cosmological constant satisfying $\Lambda = \frac{R}{4}$. Moreover, this is the value of the cosmological constant for any solution of the Einstein equation with an energy-momentum tensor of vanishing trace. Then, maximally symmetric spacetimes can be classified according to the sign of the Ricci scalar. If $R = 0$ we have Minkowski space, for $R < 0$ the space is called anti-de Sitter and $R > 0$ is the de Sitter spacetime.

In this work, we are going to be interested in the de Sitter geometry, which, as it has been seen above, can be defined as the (vacuum) maximally symmetric geometry of positive cosmological constant. In the rest of this section, the metric tensor of de Sitter is going to be presented in different coordinate systems, each serving a specific purpose. We start with the ones that gives the best geometrical view for it, in which the de Sitter spacetime is defined as the hyperboloid [23]

$$-v^2 + w^2 + x^2 + y^2 + z^2 = a^2, \tag{3.24}$$

(where $a \equiv \sqrt{3/\Lambda}$) embedded in a flat five-dimensional Minkowski space

$$ds^2 = -dv^2 + dw^2 + dx^2 + dy^2 + dz^2. \tag{3.25}$$

If the embedding is made by a function such that, in local coordinates,

$$\begin{aligned}
v &= a \sinh \frac{\tau}{a}, & w &= a \cosh \frac{\tau}{a} \cos \chi, \\
x &= a \cosh \frac{\tau}{a} \sin \chi \cos \theta, & y &= a \cosh \frac{\tau}{a} \sin \chi \sin \theta \cos \phi, \\
z &= a \cosh \frac{\tau}{a} \sin \chi \sin \theta \sin \phi, & &
\end{aligned} \tag{3.26}$$

then the induced metric on the hyperboloid in (t, χ, θ, ϕ) coordinates is

$$ds^2 = -d\tau^2 + a^2 \cosh^2 \frac{\tau}{a}[d\chi^2 + \sin^2 \chi(d\theta^2 + \sin^2 \theta d\phi^2)], \tag{3.27}$$

with ranges

$$\begin{aligned} -\infty < \tau < \infty, \qquad & 0 < \chi < \pi, \\ 0 < \theta < \pi, \qquad & 0 < \phi < 2\pi. \end{aligned} \tag{3.28}$$

We recognize inside brackets in (3.27) the line element of a 3-sphere and, therefore, the de Sitter spacetime can be given the topology of $\mathbb{R} \times S^3$. At the time coordinate $\tau = 0$, the 3-sphere has its minimum size, with a radius of a, and, as the time coordinate increases, the 3-sphere expands. So, we can physically interpret this metric of being from an expanding universe starting from $\tau = 0$ [5].

Another coordinate system in which the de Sitter geometry is commonly presented in the literature comes from taking the following functions for the embedding [23]:

$$\begin{aligned} v &= \sqrt{a^2 - r^2} \sinh \frac{t}{a}, \qquad & w &= \sqrt{a^2 - r^2} \cosh \frac{t}{a}, \\ x &= r \cos \theta, & y &= r \sin \theta \cos \phi, \\ z &= r \sin \theta \sin \phi. \end{aligned} \tag{3.29}$$

In the (t, r, θ, ϕ) coordinates, the line element becomes

$$ds^2 = -\left(1 - \frac{\Lambda}{3} r^2\right) dt^2 + \left(1 - \frac{\Lambda}{3} r^2\right)^{-1} dr^2 + r^2(d\theta^2 + \sin^2 \theta d\phi^2), \tag{3.30}$$

with ranges

$$\begin{aligned} -\infty < t < \infty, \qquad & 0 < r < a, \\ 0 < \theta < \pi, \qquad & 0 < \phi < 2\pi. \end{aligned} \tag{3.31}$$

It is possible to obtain the same metric (3.30), but the range of the radial coordinate being the interval $a < r < \infty$, if we consider the embedding made via

$$\begin{aligned} v &= \sqrt{r^2 - a^2} \cosh \frac{t}{a}, \qquad & w &= \sqrt{r^2 - a^2} \sinh \frac{t}{a}, \\ x &= r \cos \theta, & y &= r \sin \theta \cos \phi, \\ z &= r \sin \theta \sin \phi. \end{aligned} \tag{3.32}$$

[5] The effect of the cosmological constant causing the expansion of the spacetime is intuitive when we see that de Sitter is a special case for the FLRW geometries (this is discussed in Chapter 6) in which the only fluid is the dark energy, having a positive energy density ρ and negative pressure $p = -\rho$ [17].

In what follows we are going to show that these are the line elements of distinct regions of the same extended geometry.

One interesting feature for this coordinate system[6] is that it covers only a static patch of the de Sitter spacetime. This is due to the fact that, in the submanifold covered, ∂_t is a timelike Killing vector field. Furthermore, it can be seen that there is a coordinate singularity for $r = a = \sqrt{3/\Lambda}$ and, in order to extend the manifold, we are going to follow an approach which was first done for the Schwarzschild spacetime. We start going to the tortoise coordinates, defined by:

$$\frac{dr_*}{dr} = \frac{1}{1 - \frac{\Lambda}{3}r^2}. \tag{3.33}$$

In terms of the coordinates (t, r_*, θ, ϕ), the de Sitter metric becomes

$$ds^2 = -\left(1 - \frac{\Lambda}{3}r^2\right)(dt^2 + dr_*^2) + r^2 d\Omega^2. \tag{3.34}$$

After this change of coordinates, the spacetime appears to be no longer singular as the coordinate singularity is taken to infinity. Then, the next step is to define coordinates adapted to null radial geodesics:

$$du = dt - dr_* = dt - \frac{dr}{1 - \frac{\Lambda}{3}r^2}, \tag{3.35}$$

$$dv = dt + dr_* = dt + \frac{dr}{1 - \frac{\Lambda}{3}r^2}. \tag{3.36}$$

For instance, the line element of de Sitter in the coordinates (u, r, θ, ϕ)[7] becomes

$$ds^2 = -\left(1 - \frac{\Lambda}{3}r^2\right)du^2 - 2du dr + r^2 d\Omega^2, \tag{3.37}$$

with ranges

$$\begin{aligned} -\infty < u < \infty, \qquad & 0 < r < \infty, \\ 0 < \theta < \pi, \qquad & 0 < \phi < 2\pi. \end{aligned} \tag{3.38}$$

The patch of the de Sitter spacetime covered by the (t, r, θ, ϕ) coordinates is isometric to the geometry covered by the (u, r, θ, ϕ) coordinates restricted to $0 < r < \sqrt{3/\Lambda}$. And, if we also consider the region of de Sitter covered by (t, r, θ, ϕ) for $r > \sqrt{3/\Lambda}$, this is isometric to the new manifold also for $r > \sqrt{3/\Lambda}$. Therefore, we have found an extension

[6] Any diagonal metric similar to (3.30) is going to be said to be written in Schwarzschild-like coordinates since it is in this form that the Schwarzschild spacetime is usually presented.

[7] Any metric in the form of (3.37) is going to be said to be written in outgoing Eddington-Finkelstein-like coordinates. Similarly, the coordinates (v, r, θ, ϕ) are going to be called ingoing Eddington-Finkelstein-like coordinates.

which is not singular at $r = \sqrt{3/\Lambda}$.

Since we have a coordinate system that covers the previous coordinate singularity, we can now make computations on this hypersurface. We notice that the coordinates of (3.37) are similar to the ones of (3.16) and, thus, from the discussion in the end of Section 3.1, the 2-sphere of radius $\sqrt{3/\Lambda}$ defines a Killing horizon for the timelike Killing vector field ∂_u.

Equation (3.12) gives a direct way to compute κ, however, for some cases, it is actually easier to use the definition (3.9) in order to calculate the surface gravity. Below we use this method to find the surface gravity relative to the timelike Killing vector field $(\partial_u)^\mu \equiv \chi^\mu$ for the metric (3.37):

$$\begin{aligned} -2\kappa\chi^\mu &\overset{h}{=} \partial^\mu(\chi^\nu\chi_\nu) \\ &\overset{h}{=} g^{\mu\rho}\partial_\rho g_{uu} \\ &\overset{h}{=} -g^{\mu r}\partial_r\left(1 - \frac{\Lambda}{3}r^2\right) \\ &\overset{h}{=} g^{\mu r}\frac{2\Lambda}{3}r \\ &\overset{h}{=} -\delta^\mu_u\frac{2\Lambda}{3}r \overset{h}{=} -2\kappa\chi^\mu. \end{aligned} \tag{3.39}$$

This is only true on the horizon, where $r = \sqrt{3/\Lambda}$. Thus,

$$\kappa = \sqrt{\frac{\Lambda}{3}}. \tag{3.40}$$

Although extensions were found through the Killing horizon, the (u, r, θ, ϕ) coordinates and also the (v, r, θ, ϕ) ones do not cover all of the de Sitter spacetime. For this task and in order to study the causal structure of de Sitter, consider the coordinate transformation from (3.27) via [17]

$$\cosh\frac{\tau}{a} = \frac{1}{\cos t'}. \tag{3.41}$$

Then the metric becomes

$$ds^2 = \frac{a^2}{\cos^2 t'}(-dt'^2 + d\chi^2 + \sin^2\chi d\Omega^2), \tag{3.42}$$

with ranges

$$-\frac{\pi}{2} < t' < \frac{\pi}{2}, \qquad 0 < \chi < \pi, \tag{3.43}$$

$$0 < \theta < \pi, \qquad 0 < \phi < 2\pi. \tag{3.44}$$

The metric term inside parenthesis in (3.42) is said to be the line element of the

Einstein static universe. And, because the de Sitter geometry relates to it as $g_{\mu\nu} = \omega^2 \tilde{g}_{\mu\nu}$, where ω is a function of the coordinates, it is said the de Sitter spacetime is conformally related to the Einstein static universe. These conformal relations are specially useful to analyse the causal structure of the spacetime via the Penrose (or conformal) diagrams since the type of a vector (that is, whether it is timelike, null or spacelike) is invariant under these transformations. Furthermore, angles between vectors also do not change and, because the Einstein static universe is conformally related to Minkowski [13], curves at 45^o are null in the conformal diagram of de Sitter.

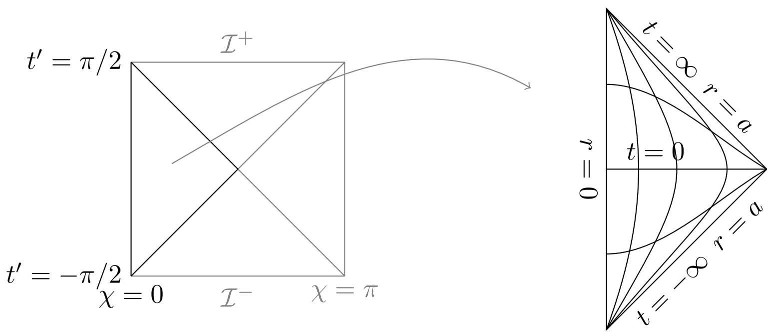

Figure 3.1: First figure is the Penrose diagram for the de Sitter spacetime written in (t', χ, θ, ϕ) coordinates. The second figure is the region of the diagram covered by the (t, r, θ, ϕ) coordinates.

In Figure 3.1, we have the Penrose diagram for the de Sitter spacetime covered by the (t', χ, θ, ϕ) coordinates on the left side and the region which is covered by the (t, r, θ, ϕ) coordinates on the right side [23]. Below it is being pointed out some characteristics of the diagram:

∘ Past and future infinities $(\mathcal{I}^-, \mathcal{I}^+)$ are spacelike.

∘ Given an observer $\mathcal{O}$ at a point p, there will be causal curves, which originate at $\mathcal{I}^-$, that do not intersect the past light cone of p. These causal curves are said to be on the **particle horizon** of $\mathcal{O}$ at this event. In Minkowski, on the other hand, there is no particle horizon.

∘ The boundary of the union of all past light cones of $\mathcal{O}$ along its world-line is called **future event horizon**. Similarly for the future light cone, it is called **past event horizon**.

∘ The Killing horizons (at $r = a = \sqrt{3/\Lambda}$) are also said to be **cosmological horizon**[8]. This means that an observer can cross this hypersurface in one direction but cannot comeback. The existence of a cosmological horizon may be seen as a direct consequence

[8]A formal definition for cosmological horizons will be given in Section 4.1

of the fast expansion and fast contraction of the de Sitter spacetime.

3.3 Schwarzschild spacetime

The **Schwarzschild spacetime** is the geometry generated by a spherical object of constant mass parameter M in vacuum. It is usually written in the diagonal coordinates

$$ds^2 = -\left(1 - \frac{2M}{r}\right)dt^2 + \left(1 - \frac{2M}{r}\right)^{-1} dr^2 + r^2 d\Omega^2, \tag{3.45}$$

from where it is evident its static configuration. The ranges assumed by each coordinate are

$$\begin{aligned} -\infty < t < \infty, \qquad & 2M < r < \infty, \\ 0 < \theta < \pi, \qquad & 0 < \phi < 2\pi. \end{aligned} \tag{3.46}$$

As it happened for de Sitter at the cosmological horizon when used the coordinate system of (3.30), the Schwarzschild spacetime has a coordinate singularity at $r = 2M$ when written as (3.45). Following the steps done for de Sitter of defining the tortoise coordinates and then making transformations similar to (3.35 − 3.36), we define coordinates adapted to null radial geodesics in order to extend the manifold for values of areal radius smaller than $2M$.

With the ingoing Eddington-Finkelstein coordinates, the line element of Schwarzschild becomes

$$ds^2 = -\left(1 - \frac{2M}{r}\right)dv^2 + dvdr + r^2 d\Omega^2, \tag{3.47}$$

with ranges

$$\begin{aligned} -\infty < v < \infty, \qquad & 0 < r < \infty, \\ 0 < \theta < \pi, \qquad & 0 < \phi < 2\pi. \end{aligned} \tag{3.48}$$

In order to understand the causal structure of this geometry, we shall analyse the behavior of the outgoing and ingoing radial null vector fields[9]. These are, respectively:

$$l^\mu = \partial_v + \frac{1}{2}\left(1 - \frac{2M}{r}\right)\partial_r, \tag{3.49}$$

$$n^\mu = -\partial_r. \tag{3.50}$$

[9]This nomenclature does not correspond to the actual behavior for these vector fields on all spacetime as discussed in the next paragraph. However, since it agrees with the expectations from the region covered by the usual Schwarzschild coordinates (3.45), the names are kept to all the geometry.

For $r > 2M$, the outgoing vectors point towards increasing radius. Therefore, observers following timelike paths close enough of l^μ are able to escape to infinity. In the usual coordinates (3.45), since only the region $2M < r < \infty$ is covered, this corresponds to all observers. On the other hand, for $r < 2M$, the vectors of the same vector field are now pointing towards decreasing radius. As the other radial null vector field, n^μ, is in ingoing direction, it is impossible to any observer and even for light-speed particles to escape. Following what is usually done in the literature, we present the qualitative behavior of the null radial vector fields in Figure 3.2.

The region from where l^μ also becomes ingoing such as n^μ, $r = 2M$, is a null hypersurface and is called the (future) event horizon and the region $r < 2M$ corresponds to a black hole[10]. In $r = 0$, there is a singularity, in this case not due to the bad behavior of the coordinate system used, but from the spacetime itself. This can be checked from the computation of the, coordinate independent, curvature scalar $R^{\mu\nu\rho\sigma}R_{\mu\nu\rho\sigma}$, which diverges as $r \to 0$ [17]. Physically, we interpret it as an infinite density point.

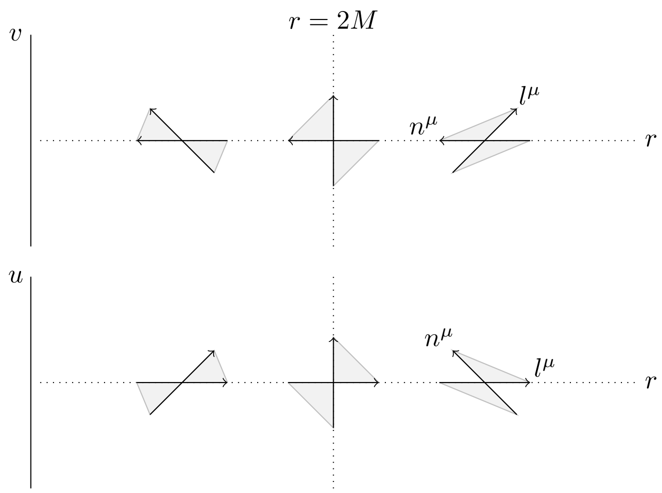

Figure 3.2: Light cones showing the behavior of the ingoing and outgoing null radial vector fields for the regions covered by the ingoing and outgoing Eddington-Finkelstein coordinates.

Since the components of (3.47) are all independent of v, ∂_v is a Killing vector field which, from the discussion on the end of Section 3.1, generates the Killing horizon at $r = 2M$. The computation of the surface gravity relative to $(\partial_v)^\mu \equiv \chi^\mu$ follows from steps similar to the ones made for the de Sitter geometry that led to (3.40):

$$\begin{aligned} -2\kappa\chi^\mu &\overset{h}{=} -g^{\mu r}\partial_r\left(1 - \frac{2M}{r}\right) \\ &\overset{h}{=} -\delta^\mu_v \frac{2M}{r^2}, \end{aligned} \tag{3.51}$$

[10]Proper definitions of event horizons and black holes will be given in Section 4.1.

which is evaluated at the horizon, where $r = 2M$, and thus

$$\kappa = \frac{1}{4M}. \tag{3.52}$$

There is also the coordinate system adapted to the outgoing radial vector fields, that is, the outgoing Eddington-Finkelstein coordinates:

$$ds^2 = -\left(1 - \frac{2M}{r}\right)du^2 - dudr + r^2 d\Omega^2 \tag{3.53}$$

with the ranges assuming the values of

$$\begin{aligned} -\infty < u < \infty, \qquad & 0 < r < \infty, \\ 0 < \theta < \pi, \qquad & 0 < \phi < 2\pi. \end{aligned} \tag{3.54}$$

Similarly, we analyze the outgoing and ingoing radial null vector fields in this region:

$$l^\mu = \partial_r, \tag{3.55}$$

$$n^\mu = \partial_u - \frac{1}{2}\left(1 - \frac{2M}{r}\right)\partial_r. \tag{3.56}$$

For $r > 2M$, the ingoing vectors of n^μ point towards direction of decreasing the areal radius. Therefore, observers in this region can travel close enough to the integral curves of n^μ so that they go towards zero radius. However, for $r < 2M$ both l^μ and n^μ are now in outgoing direction, meaning that any observer, even if in light-speed, must go towards regions of larger radius. It is said that at $r = 2M$ is located a (past) event horizon and at $r < 2M$ there is white hole (see Figure 3.2). For the same previous reason, there is a curvature singularity at $r = 0$.

Although we have presented two extensions for the Schwarzschild spacetime, even a combination of them on the region where they are isometric, $0 < r < 2M$, does not correspond to the maximal extension of this geometry. In Figure 3.3, the Penrose diagram for the maximally extended Schwarzschild spacetime[11] is presented and it is being pointed out some of its important features [23]:

[11]There is a coordinate system named after M. Kruskal which covers all the maximally extended solution. However, such coordinates will not be present here since we are not going to work with its generalization for the spacetimes we are mostly interested, that is, Vaidya and Vaidya-de Sitter.

It is important to cite that Birkhoff's Theorem states that any spherically symmetric solution of the Einstein Equation in vacuum is isometric to a region of the maximally extended Schwarzschild spacetime [27].

∘ Past and future infinities ($\mathcal{I}^-, \mathcal{I}^+$) are null. This is the same asymptotic structure of Minkowski and it is said that Schwarzschild is asymptotically flat.

∘ The (future and past) event horizons at $r = 2M$ are also Killing horizons for the Killing vector fields ∂_v and ∂_u.

∘ Regions I and II, which can be covered by the usual Schwarzschild coordinates, are causally disconnected.

∘ Curvature singularities at $r = 0$ are behind the horizons of black and white holes (BH and WH).

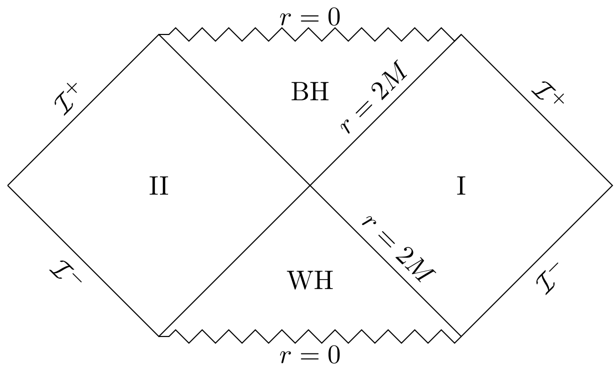

Figure 3.3: Penrose diagram for the maximally extended Schwarzschild spacetime.

3.4 Vaidya spacetime

The **Vaidya spacetime** is a generalization of the Schwarzschild solution which may include the radiation or accretion of massless particles of radial trajectory. This geometry is named after P. Vaidya who published it in 1951 in Schwarzschild-like coordinates [58]:

$$ds^2 = -\frac{\dot{M}^2}{M'^2}\frac{1}{f(t,r)}dt^2 + \frac{1}{f(t,r)}dr^2 + r^2(d\theta^2 + \sin^2\theta d\phi^2), \tag{3.57}$$

where $M(t,r)$ is the mass of the spherical object, M' and $\dot{M}$ are the derivatives with respect to the r and t coordinates respectively, and

$$f(t,r) \equiv 1 - \frac{2M(t,r)}{r}. \tag{3.58}$$

However, this is not the coordinate system in which the Vaidya spacetime is more commonly presented. The most usual ones are the Eddington-Finkelstein-like coordinates, in which the Vaidya solution was first written by Vaidya himself only two years latter, in 1953 [59]. In these coordinates, this metric shows itself, straightforwardly, as a generalization of Schwarzschild for a time-varying mass. First we present it in the ingoing Eddington-Finkelstein-like one:

$$ds^2 = -f(v,r)dv^2 + 2dvdr + r^2(d\theta^2 + \sin^2\theta d\phi^2), \tag{3.59}$$

where

$$f(v,r) \equiv 1 - \frac{2M(v)}{r}, \tag{3.60}$$

with ranges

$$\begin{aligned} -\infty < v < \infty, \qquad & 0 < r < \infty, \\ 0 < \theta < \pi, \qquad & 0 < \phi < 2\pi. \end{aligned} \tag{3.61}$$

We know that the Schwarzschild metric when written as (3.45) has a coordinate singularity at $r = 2M$ and, after changing to Eddington-Finkestein coordinates, it is discovered that this hypersurface is, actually, an event horizon. In order to study the causal structure of the Vaidya spacetime, we need to generalize this treatment for a time changing mass. First we take the hypersurface where $r = 2M(v)$, which is equivalent to take $f(v,r) = 0$. Then, after evaluating the norm of $\partial_\mu f(v,r)$ at $f(v,r) = 0$, we find out that it will be zero only if $\frac{dM}{dv} = 0$, which is the Schwarzschild situation. Therefore, this hypersurface, for more general mass parameter functions, is not null and, thus, cannot be an event horizon.

Nonetheless, similarly to the Schwarzschild case, this is still an interesting surface since it delimits the region, $r < 2M(v)$, where future-pointing radial light rays must follow paths of increasing r coordinate, to the other region, $r > 2M(v)$, where there is no such restriction. This statement can be checked looking at the outgoing and ingoing radial null vector fields [9]:

$$l^\mu = \partial_v + \frac{1}{2}f(v,r)\partial_r, \tag{3.62}$$

$$n^\mu = -\partial_r. \tag{3.63}$$

In this chapter, we are not going to further explore the causal structure of Vaidya. This is going to be done in Chapter 4 for a generalization which includes a positive cosmological constant, that is the Vaidya-de Sitter spacetime. In Appendix B, it is checked (setting $\Lambda = 0$) that the above vector fields are indeed null and satisfy some important properties, for instance, they are generators of geodesics.

We have briefly discussed some of the geometrical structures of the Vaidya spacetime. Now, we must answer for what kind of energy-momentum tensor the metric (3.59) is a solution of the Einstein Equation. This is [37]

$$T^{\mu\nu} = \frac{1}{4\pi r^2}\frac{dM(v)}{dv}n^\mu n^\nu, \tag{3.64}$$

which is the energy-momentum tensor of a pure radiation field [23]. In order to understand the physical content behind (3.64), we must define the simplest type of fluid in General Relativity: the **dust**. This is characterized by the energy-momentum tensor

$$T^{\mu\nu} = \rho\, u^\mu u^\nu, \tag{3.65}$$

where u^μ is the 4-velocity of the particles that constitute this fluid and ρ is the energy density measured by observers with also a 4-velocity of u^μ.

Comparing (3.64) with (3.65), we can interpret the energy-momentum tensor of the Vaidya metric in outgoing Eddington-Finkelstein-like coordinates as the one from a "null-dust". This is regarded as the asymptotic case in which the velocities of the particles of the dust tend to the speed of light, that is, a dust with 4-velocity of n^μ.

Furthermore, the energy density measured in the frame of the fluid (3.64) is

$$\frac{1}{4\pi r^2}\frac{dM(v)}{dv} \tag{3.66}$$

and imposing the null energy condition, $T_{\mu\nu}k^\mu k^\nu \geq 0$, where k^μ is a null vector field, we must have

$$\frac{dM(v)}{dv} \geq 0. \tag{3.67}$$

Therefore, unless the mass parameter is constant, the Vaidya spacetime (3.59) represents a spherically symmetric object increasing its mass due to the accretion of light-speed particles (of radial trajectory).

There is also a Vaidya spacetime with an opposite behavior and, as one could expect, this is written in outgoing Eddington-Finkelstein-like coordinates:

$$ds^2 = -f(u,r)du^2 - 2dudr + r^2(d\theta^2 + \sin^2\theta d\phi^2), \tag{3.68}$$

where

$$f(u,r) \equiv 1 - \frac{2M(u)}{r}, \tag{3.69}$$

with ranges

$$\begin{aligned} -\infty < u < \infty, \qquad & 0 < r < \infty, \\ 0 < \theta < \pi, \qquad & 0 < \phi < 2\pi. \end{aligned} \tag{3.70}$$

For completeness, we present the outgoing and ingoing radial null vector fields for this spacetime

$$l^\mu = \partial_r, \tag{3.71}$$

$$n^\mu = \partial_u - \frac{1}{2} f(u,r)\partial_r, \tag{3.72}$$

which are going to be generalized for Vaidya-de Sitter in the next chapter, where their physical attributes are going to be studied in details.

The energy-momentum tensor for this metric is

$$T^{\mu\nu} = -\frac{1}{4\pi r^2}\frac{dM(u)}{du} l^\mu l^\nu \tag{3.73}$$

and, following the same physical interpretation comparing with the "null-dust" fluid and assuming that the null energy condition holds, which implies

$$\frac{dM(u)}{du} \leq 0, \tag{3.74}$$

we conclude that this solution represents a spherically symmetric object losing its mass through the radiation of massless particles (of radial trajectory).

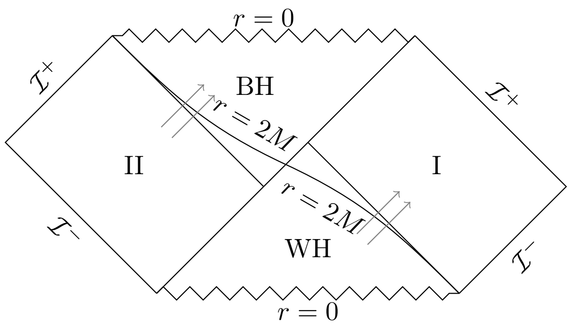

Figure 3.4: Penrose diagram for a maximally extended Vaidya spacetime. The arrows represent the directions of the flux of radiation.

We finish this section (and this chapter) presenting the Penrose diagram for a maximally extended Vaidya spacetime in Figure 3.4 [23]. Most of its features are similar to the ones from the Schwarzschild diagram and below it is pointed out the important differences:

◦ The union of the regions WH and I is the Vaidya geometry covered by the outgoing coordinates and the union of II and BH is the Vaidya spacetime covered by the ingoing ones. These spacetimes do not overlap as it happened in the Schwarzschild extension. The arrows represent the directions of the flux of massless radiation of radial trajectory.

◦ The curved line of $r = 2M$ is not null and do not coincide with the event horizons. The actual shape of this curve depends on how the mass parameters evolve in time and, therefore, it shall be interpreted only as an illustration in the diagram.

Chapter 4

Black-hole thermodynamics

In this chapter, we introduce two different approaches for the thermodynamic description of black holes. The first, which is frequently presented in General Relativity textbooks, is the Bekenstein-Hawking thermodynamics. In a work published in 1972, S. Hawking showed that under physically reasonable assumptions the area of the event horizon of a black hole should never decrease [25]. On the next year, based on S. Hawking's work, J. Bekenstein proposed that the area of the event horizon should be a measure of the entropy contained in the black hole [7]. And around the same time, J. Bardeen, B. Carter and S. Hawking presented the four laws of black-hole mechanics, which among them is the Area Theorem proved by S. Hawking, highlighting their apparent similarity to the laws of classical thermodynamics [16]. In 1975, S. Hawking showed that, for stationary black holes, the event horizon emits particles in a thermal spectrum [26]. Therefore, a temperature could be assigned to the black hole. This is the so-called Hawking radiation and it was due to its discovery that the laws of black-hole mechanics could be reinterpreted as thermodynamic laws.

The other black-hole thermodynamic theory that is considered in this chapter was developed by S. Hayward [28]. He published in 1994 the generalized laws for black hole mechanics [28], which was developted taking as a background not an event horizon, but a trapping horizon. Hayward's work generalizes the Bekenstein-Hawking thermodynamics for spherically symmetric dynamic spacetimes, which means we are no longer restricted to the stationary ones. For this reason, we are able to apply the Hayward thermodynamics to systems where the mass of the black hole varies rapidly, as it may be the case for the Vaidya spacetime of our interest.

Before we get into the discussion of each black-hole thermodynamic theory, it is necessary to rigorously define the terminology involved. For instance, the concepts of event and trapping horizons. This is what it is done in the first section of this chapter, Section 4.1. The Bekenstein-Hawking and the Hayward thermodynamics for black holes are studied in Section 4.2 and Section 4.3, respectively.

4.1 Black holes and the characterization of horizons

Loosely speaking, keeping contact with our physical intuition, a black hole is a region from where nothing can escape to infinity. Of course, in order to do physics, we need a rigorous definition of what a black hole really is. The idea of "escaping to infinity" is related to causal relations between events in the spacetime, therefore, we shall start by introducing a rigorous terminology to talk about how two points may or may not interact with each other. Then, we will be able to formally define a black hole as the absence of causal relation to the "future infinity", which also must be defined.

Two points p and q in a given spacetime M are **causally connected** if they both lie on a timelike (or null) curve. If this curve is future-directed[1] from p to q, then the point q is in the **causal future** of p, $J^+(p)$, that is, the set of all points in M which can be achieved from p following a future-directed curve. The **causal past**, J^-, is defined in a similar way. We can also generalize these definitions to talk about the causal future (or past) of a set of points in the spacetime. For instance, this set may be the future null infinity, which will soon appear in the definition of the black hole. The **future null infinity**, $\mathcal{I}^+$, is the null hypersurface contained in the boundary of a compactified spacetime where all the null curves end. The future null infinity is not present in all spacetimes, but only in the ones that share the same asymptotic structure of Minkowski space, that is, with some simplification, only in the asymptotically-flat geometries [63].

We, then, have introduced the necessary terminology in order to define a **black hole**, B, as the complement of the causal past of the future null infinity, $B = M - J^-(\mathcal{I}^+)$. That is, the set of all points which cannot be causally connected to infinity through future-directed curves. The **event horizon**, H, is defined as the boundary of the black hole[2], $H = \partial(B) = \partial(J^-(\mathcal{I}^+))$.

It is a theorem, due to B. Carter, that if the spacetime is static, then the event horizon must also be a Killing horizon for a vector field χ^μ which is timelike at infinity [62]. This theorem, for instance, is applicable to Schwarzschild. Furthermore, if the spacetime is stationary and has a Killing vector field R^μ related to an axial symmetry (and further geometric conditions are assumed but which shall not be stated here since this work will not be concerned with such spacetimes), then the event horizon is also a Killing horizon for the Killing vector field $K^\mu = \chi^\mu + \Omega_H R^\mu$, where Ω_H is a scalar interpreted as the angular velocity of the event horizon.

One important feature of the previous definition of a black hole is that, in order to locate an event horizon, it is necessary to know the behavior of every single null geodesic of the spacetime for all of their parameters. This property makes an event horizon a

[1] A curve is future-directed if at each point its tangent vector lies in the future-half of the light cone on the tangent space. Similarly a past-directed curve can be defined.

[2] The event horizon, as a causal boundary, is necessarily a null hypersurface [47].

global concept. And it is due to this teleological character that the usual definition of a black hole in terms of the event horizon is, in many circumstances, not a practical one. For this reason, alternative quasi-local definitions are useful, in which by "quasi-local" we mean the property of a quantity or an object to be detected by a set of observers in a finite interval of their proper-time.

In order to make clear the distinction between the nature of an event horizon and a quasi-local horizon, let us consider a spherically symmetric spacetime, which is also the geometry relevant for the Hayward black-hole thermodynamics[3]. If the spacetime has spherical symmetry, there are radial null geodesics in direction of increasing radius, l^μ, which are said to be outgoing, and in direction of decreasing radius, n^μ, called ingoing[4]. As both vector fields are radial, the cross-sectional 2-surfaces they define (A.4) are 2-spheres. And since the expansion scalars will measure the rate of change of these spheres (A.13), what we may intuitively expect is that the event horizon is the region where the expansion scalar in outgoing direction is null: $\theta_l = 0$. However, this is, in fact, not always true.

As it is shown in [47] for the Vaidya spacetime, for example, the condition of vanishing θ_l is satisfied by the spheres of radius $2M(v)$ at each value of time-coordinate v. On the other hand, if we consider the hypersurface defined by the union of all spheres of radius $2M(v)$, for all values of v, the author of [47] shows that this hypersurface is only null if the mass parameter, $M(v)$, is constant. That is, only for the Schwarzschild spacetime the event horizon will have $\theta_l = 0$. Nonetheless, the condition of having null expansion scalar is still a very interesting one and it is the main feature of the, to be defined, trapping horizons.

In order to get to the trapping horizons, we start defining their building block: a **marginal surface**. This is a closed 2-surface with $\theta_l = 0$ or $\theta_n = 0$. An important hypersurface that can already be defined, but that it will not be cited too much on this work, is the **apparent horizon**. This is the outermost 3-surface foliated by marginal surfaces.

It is important to highlight that the definitions of apparent horizons do not coincide in many references. In [63], for example, an apparent horizon is the boundary of the closure of the union of all trapped surfaces (which shall be soon properly defined) and, given further assumptions about its structure, it is proven it has vanishing expansion scalar. The one we are choosing to follow here, as briefly discussed in [10], is usually easier to work with. The existence of different non-equivalent definitions is also recurrent in the theory of trapping horizons. In the present work, we are mostly following Hayward's

[3]The content that follows in this section is heavily dependent on Appendix A, where a study about congruence of null geodesics is introduced and, for instance, the expansion scalar is defined.

[4]It is important to notice that this nomenclature corresponds to the intuitive meaning of the terms only outside the event horizon. However, we will keep the names even in the region inside the black hole.

article [28], but we will also extend the definitions in order to talk about other surfaces which are not considered in his paper.

Before we consider the trapping horizons, we shall talk about trapped surfaces, which capture the intuitive idea of a surface from where nothing can escape from. The usual way to imagine such surfaces is to picture a sphere in Minkowski space. If at each point on the sphere a light ray is simultaneously (relative to some coordinate system) emitted in the direction of increasing radius, then, for each fixed latter time, a larger sphere is produced. The opposite effect happens if the light rays are emitted in direction of decreasing radius. This, seemingly obvious, behavior is also true outside the black hole in the Schwarzschild spacetime, for example. However, inside a black hole, even the light rays that were supposed to follow paths of increasing radius, actually, goes to smaller ones. Such spheres inside a black hole are the called trapped surfaces. The formal definition is: a **future trapped surface** is a closed and spatial 2-surface such that the expansion scalars in directions of surface-normal outgoing and ingoing null geodesics are both negative, $\theta_l, \theta_n < 0$.

When a marginal surface was defined, we did not impose any condition on the non-vanishing expansion scalar, that is, if $\theta_l = 0$, we have said nothing about the behavior of θ_n (and vice-versa). Then, now we begin to classify the different types of marginal surfaces. If a marginal surface has $\theta_n < 0$, it is said to be a **marginally future trapped surface.** A 3-surface foliated by marginally future trapped surfaces is called a **marginally future trapped tube.** This hypersurface represents a limit of some spacetime from where it is impossible to follow paths of increasing radius, but the ingoing paths maintain their natural behavior. Finally, we can define the trapping horizons according to [28].

A **future outer trapping horizon** is a marginally future trapped tube such that in each slice $\mathcal{L}_n\theta_l < 0$. This kind of trapping horizon is typical of black holes as it separates an exterior region where θ_l is positive and it is possible to follow paths of increasing radius from an interior region where θ_l is negative and even the "outgoing" paths are radius-decreasing. Due to this feature, a new and quasi-local definition of a black hole arises, in which the event horizon is replaced by the future outer trapping horizon.

Similarly, a **future inner trapping horizon** is a marginally trapped tube where in each slice $\mathcal{L}_n\theta_l > 0$. This one is related to contracting universes as it represents a boundary from an exterior region, where θ_l is negative, to an interior (lower-radius) region, where θ_l is positive and have its usual behavior. Therefore, a future inner trapping horizon can be used as a definition of a **cosmological horizon** and physically represents the impossibility of going to furthest regions of the spacetime due to its accelerated contraction rate.

Up to this point, we have been considering the marginal surfaces with non-vanishing θ_n. Therefore, we finish the classification of trapping surfaces dealing with the case of past marginal surfaces, in which $\theta_n = 0$. We shall omit some of the details since the new definitions are natural extensions of what we had above. A **past trapped surface** is defined as a close and spatial 2-surface such that both $\theta_n, \theta_l > 0$. A marginal surface on which $\theta_l > 0$ is going to be called a **marginally past trapped surface** and a 3-surface foliated by marginally past trapped surfaces is a **marginally past trapped tube**. If the marginally past trapped tube is such that $\mathcal{L}_l\theta_n < 0$, then it is a **past outer trapping horizon**. Meanwhile, if $\mathcal{L}_l\theta_n > 0$, then it is a **past inner trapping horizon**. As it can be expected, these trapping horizons have opposite behavior to the ones previously defined. Therefore, the past outer one is typical of a white hole and the past inner one is the cosmological horizon of an expanding cosmology.

Since the characterization of trapping horizons is greatly important in this work, we summarize the definitions in Table 4.1.

Table 4.1

	Future trapping horizon		**Past trapping horizon**	
	Outer	**Inner**	**Outer**	**Inner**
$\boldsymbol{\theta_l}$	Zero	Zero	Positive	Positive
$\boldsymbol{\theta_n}$	Negative	Negative	Zero	Zero
$\boldsymbol{\mathcal{L}_n\theta_l}$	Negative	Positive	-	-
$\boldsymbol{\mathcal{L}_l\theta_n}$	-	-	Negative	Positive

In Section 3.1, we have seen another horizon characterization that is recurrent in the study of black holes and a key piece in the Bekenstein-Hawking thermodynamics: the Killing horizon. Moreover, in Section 4.2 we are going to see that the relevant spacetimes for the Bekenstein-Hawking thermodynamics are those stationary. And, on the other hand, the Hayward black-hole thermodynamics can only be applied to spherically-symmetric geometries, whether these are stationary or not. Since Hayward's work is a generalization of the usual black-hole thermodynamics, the spacetimes where both theories coincide are the static and spherically symmetric ones. And it is due to this reason that it is interesting to have an useful condition in order to find trapping horizons for this kind of geometries and see how we can relate them to Killing horizons. As already seen, in this situation we can always write the line element in Schwarzschid-like coordinates [55]:

$$ds^2 = -A(r)dt^2 + \frac{1}{B(r)}dr^2 + r^2 d\Omega^2. \tag{4.1}$$

Or we can work in ingoing Eddington-Finkelstein-like coordinates[5]:

$$ds^2 = -A(r)dv^2 + 2\sqrt{\frac{A(r)}{B(r)}}dvdr + r^2 d\Omega^2, \tag{4.2}$$

as long as we be restricted to the region where $A(r)B(r) > 0$.

If we want to find the trapping horizons for this family of spacetimes, due to the spherical symmetry, we should look for 2-spheres, which have surface-normal radial null vectors

$$n^\mu = -\partial_r, \tag{4.3}$$

$$l^\mu = \sqrt{\frac{B(r)}{A(r)}}\left[\partial_v + \frac{1}{2}\sqrt{A(r)B(r)}\partial_r\right], \tag{4.4}$$

that satisfy $l^\mu n_\mu = -1$. The metric tensor on the cross sectional space (A.4) defined by the previous vector fields is, as it can be checked, indeed a 2-sphere:

$$ds^2 = r^2 d\theta^2 + r^2 \sin^2\theta d\phi^2. \tag{4.5}$$

And the expansion scalars in ingoing and outgoing directions can be computed via (A.13):

$$\theta_n = -\frac{2}{r}, \tag{4.6}$$

$$\theta_l = \frac{B(r)}{r}. \tag{4.7}$$

From (4.7), it seems like the 3-surfaces foliated by 2-spheres of constant radius r_H such that $B(r_H) = 0$ are trapping horizons. However, we must be careful here since the surface where $B(r) = 0$ is a coordinate singularity as a component of the line element (4.2) diverges. Therefore, in order to avoid further difficulties, we impose the condition:

$$\lim_{r\to r_H} \frac{A(r)}{B(r)} \text{ converges to a non-zero value.} \tag{4.8}$$

Then, as long as

$$A(r)B(r) > 0 \text{ for all } r \text{ in some neighborhood of } r_H, \tag{4.9}$$

the 2-sphere of radius r_H such that $B(r_H) = 0$ is a trapping horizon.

Furthermore, we have seen in the end of Section 3.1 that if (4.8) holds and $A(r_H) = 0$, then this surface is a Killing horizon for the Killing vector field ∂_v (3.18). Therefore, under

[5] For outgoing Eddington-Finkelstein-like coordinates, the results we derive can be found with similar calculations.

the assumption of $B(r)$ not diverging at r_H, (4.8) forces $B(r_H)$ to vanish and, thus, this Killing horizon is also a trapping horizon.

This section was focused on characterizing all the horizons that appear in the black-hole thermodynamics we are going to consider. Understanding all these definitions may be cumbersome but it is an important task so that we can start developing each theory. Then, the first to be studied is the Bekenstein-Hawking black-hole thermodynamics.

4.2 Bekenstein-Hawking thermodynamics

In order to present the Bekenstein-Hawking thermodynamics and explore some of its most interesting properties, we have divided this section in three subsections which follow the chronological order of the development of the theory. Subsection 4.2.1 treats about the laws of black-hole mechanics while Subsection 4.2.2 presents the semi-classical result of Hawking radiation, which will imply in the Bekenstein-Hawking black-hole thermodynamics discussed in details in Subsection 4.2.3.

4.2.1 The laws of black-hole mechanics

The laws of black-hole mechanics were published[6] in 1973 by J. Bardeen, B. Carter and S. Hawking [6]. Already in this article the authors drew attention to analogies between their work and the classical thermodynamic laws, specially relating the surface gravity and the area of the event horizon to, respectively, the temperature and the entropy[7] of a thermodynamic system. In what follows we are going to state the four laws of black-hole mechanics and also comment about their proofs.

The **Zeroth Law** asserts that under the conditions:
$>$ The spacetime is stationary and asymptotically flat,
$>$ The dominant energy condition holds, that is, for a timelike (or null) vector field V^μ and an energy-momentum tensor which satisfies the Einstein equation $T^{\mu\nu}$, then $-V^\mu T_{\mu\nu}$ is future-directed and also timelike (or null),
then the surface gravity κ of an event horizon $\mathcal{H}$ is constant.

Proof. Let K^μ be the null Killing vector field which generates the event horizon. First, we show that κ is constant along the Killing vector field K^μ on the horizon. For that, we

[6]The Second Law had already been published by S. Hawking in 1971 [25].
[7]J. Bekenstein had already highlighted the relation between the Area Theorem published by S. Hawking [25] and the entropy of a thermodynamic system [7].

take the Lie derivative $\mathcal{L}_K$ on both sides of (3.9). In components,

$$\begin{aligned}[K, \nabla(K^\nu K_\nu)]^\mu &\stackrel{h}{=} K^\sigma \partial_\sigma \nabla^\mu (K^\nu K_\nu) - \nabla^\sigma (K^\nu K_\nu) \partial_\sigma K^\mu \\ &\stackrel{h}{=} K^\sigma \partial_\sigma (-2\kappa K^\mu) + 2\kappa K^\sigma \partial_\sigma K^\mu \\ &\stackrel{h}{=} -2K^\sigma [(\partial_\sigma \kappa) K^\mu + \kappa(\partial_\sigma K^\mu)] + 2\kappa K^\sigma \partial_\sigma K^\mu \\ &\stackrel{h}{=} -2K^\sigma K^\mu \partial_\sigma k \stackrel{h}{=} 0,\end{aligned} \tag{4.10}$$

and we find

$$\mathcal{L}_K \kappa = 0. \tag{4.11}$$

Then, it is proved that along K^μ the surface gravity κ is constant. Therefore, it is left to be proven that this result also holds in the direction of any other vector field defined on the event horizon $\mathcal{H}$. In order to do that, we need two results which are presented, respectively, in [63] and [18]:

$$\widehat{\nabla_\mu K_\nu} \equiv \widehat{B}_{\nu\mu} \stackrel{h}{=} 0 \implies R_{\mu\nu} K^\mu K^\nu \stackrel{h}{=} 0 \implies T_{\mu\nu} K^\mu K^\nu \stackrel{h}{=} 0, \tag{4.12}$$

$$\mathcal{L}_V \kappa \stackrel{h}{=} -R_{\mu\nu} K^\mu V^\nu \stackrel{h}{=} -8\pi T_{\mu\nu} K^\mu V^\nu, \tag{4.13}$$

both holding on the event horizon and V^μ being a spacelike vector field on $\mathcal{H}$. The "hat" notation that appears in (4.12) means a projection on a 2-surface contained in the horizon and it is explained in details in Appendix A. The result (4.12) is derived from Raychaudhuri's equation (A.14) and (4.13) comes from Einstein equation. It is important to notice that because the event horizon is a null surface, all the tangent vector fields on it are spacelike or K^μ itself.

The result (4.12) tells us that, on the event horizon, $T_{\mu\nu} K^\mu$ is a spacelike vector field or it is proportional to K^ν. On the other hand, due to the dominant energy condition, and the Einstein equation being valid, we know that $-T_{\mu\nu} K^\mu$ cannot be spacelike. Therefore, it must be null and proportional to K^μ. Now, because of (4.13) and $V_\mu K^\mu = 0$, we have

$$\mathcal{L}_V \kappa = 0, \tag{4.14}$$

which shows that the surface gravity κ is also constant in the direction of any tangent vector on $\mathcal{H}$ other than K^μ. $\square$

The **First Law** of black-hole mechanics has two formulations, which, following Wald's nomenclature given at [61], are

Physical Process Version: Take a black hole in a vacuum stationary spacetime with mass M, angular momentum J and event-horizon area A. Disturb it by throwing a small amount of matter across its event horizon and consider that a latter time the black hole sets down to a new stationary configuration given by $M + \delta M$, $J + \delta J$ and $A + \delta A$. Then, the small variations are related by

$$\delta M = \frac{\kappa}{8\pi}\delta A + \Omega_{\mathcal{H}}\delta J, \tag{4.15}$$

where κ is the surface gravity and $\Omega_{\mathcal{H}}$ the angular velocity of the event horizon.

Equilibrium State Version: Take two slightly distinct black holes, each one in a different empty stationary spacetime, such that their mass, angular momentum and event-horizon area differ by δM, δJ and δA. Then, the small variations are also related by (4.15).

The first law of black-hole mechanics was first published in [6], where the equilibrium state version was derived in the presence of matter. Therefore, a more general version of (4.15) was constructed. In the absence of matter and for a chargeless black hole, the first law can be readily checked for the Kerr metric, which is the unique generalization of Schwarzschild including a rotating black hole. For instance, can be found in [17, 63].

In what follows, we derive the physical process version of the first law of black-hole mechanics following what is done in [47, 61].

Proof. We start by taking a small amount of matter, represented by $T_{\mu\nu}$, with mass and angular momentum given by

$$\delta M = -\int_{\mathcal{H}} T_{\mu\nu}\xi^{\mu} d\Sigma^{\nu}, \tag{4.16}$$

$$\delta J = \int_{\mathcal{H}} T_{\mu\nu}\varphi^{\mu} d\Sigma^{\nu}, \tag{4.17}$$

where ξ^{μ} and φ^{μ} are, respectively, the timelike and the rotational Killing vector fields. And we also have the volume element of the event horizon $\mathcal{H}$ is [47]

$$d\Sigma^{\nu} = -\sqrt{g_S}\; K^{\nu} d\lambda dS, \tag{4.18}$$

K^{ν} being the normal null Killing vector field, λ is the parameter of the curves generated by K^{μ} and $\sqrt{g_S}\; dS$ is the volume element of the spatial 2-surface of vectors orthogonal to K^{μ}.

We consider that this matter produces an (also small) change in the metric. We saw in (4.12), from [63], that the expansion scalar and the shear and rotation tensors all vanish on the event horizon. Therefore, since the metric is under a small perturbation, at first order we can neglect the squared terms in Raychaudhuri's equation:

$$K^\mu \nabla_\mu \theta = \kappa\theta - 8\pi T_{\mu\nu} K^\mu K^\nu. \tag{4.19}$$

We recall that it is a theorem that for stationary spacetimes the event horizon is a Killing horizon for the Killing vector field $K^\mu = \xi^\mu + \Omega_{\mathcal{H}} \varphi^\mu$. Using this fact together with (4.19), we have:

$$\begin{aligned}
\delta M - \Omega_{\mathcal{H}} \delta J &= \int_{-\infty}^{\infty} d\lambda \int_S dS \, \sqrt{g_S} \, T_{\mu\nu} K^\mu K^\nu \\
&= -\frac{1}{8\pi} \int_{-\infty}^{\infty} d\lambda \int_S dS \, \sqrt{g_S} \big[K^\mu \nabla_\mu \theta - \kappa\theta \big] \\
&= -\frac{1}{8\pi} \int_{-\infty}^{\infty} d\lambda \int_S dS \, \sqrt{g_S} \left[\frac{d\theta}{d\lambda} - \kappa\theta \right].
\end{aligned} \tag{4.20}$$

In order to continue, it is important to recall that

$$\theta = \frac{\mathcal{L}_K \sqrt{g_S}}{\sqrt{g_S}}, \tag{4.21}$$

where g_S is the determinant of the metric induced on S. Then,

$$\begin{aligned}
\delta M - \Omega_{\mathcal{H}} \delta J = -\frac{1}{8\pi} \int_S dS \, \big[\sqrt{g_S} \, \theta \big]_{-\infty}^{\infty} &+ \frac{1}{8\pi} \int_{-\infty}^{\infty} d\lambda \int_S dS \, \frac{d\sqrt{g_S}}{d\lambda} \theta \\
&+ \frac{\kappa}{8\pi} \int_{-\infty}^{\infty} d\lambda \int_S dS \, \frac{d\sqrt{g_S}}{d\lambda} \\
= \frac{\kappa}{8\pi} \int_{-\infty}^{\infty} d\lambda \int_S dS \, \frac{d\sqrt{g_S}}{d\lambda}& \\
= \frac{\kappa}{8\pi} \int_S dS \, \sqrt{g_S} \big|_{-\infty}^{\infty}& \\
= \frac{\kappa}{8\pi} \big[A(v \to \infty) - A(v \to -\infty) \big]& \\
\equiv \frac{\kappa}{8\pi} \delta A.&
\end{aligned} \tag{4.22}$$

The first equality of (4.22) was obtained via integration by parts. In order to get the second one, it was used the assumption that the black hole evolves to a stationary state for large values of λ and the fact that $\mathcal{L}_K \sqrt{g_S} \, \theta$ is of order θ^2, which is being neglected.

Then we have found the differential relation:

$$\delta M = \frac{\kappa}{8\pi} \delta A + \Omega_{\mathcal{H}} \delta J, \tag{4.23}$$

which is the First Law of black-hole mechanics. □

The **Second Law** states that, under some assumptions regarding the spacetime (to be discussed in the following proof), the spatial area of a black hole cannot decrease, that is, $\delta A \geq 0$ [25].

Due to S. Hawking in 1972 [25], the Second Law, also called the Area Theorem for black holes, was already known before the four laws of black-hole mechanics were published by J. Bardeen, B. Carter and himself in 1973 [6]. Differently from the previous two, the Second Law is more general since it is not restricted to stationary spacetimes. The formal proof for this theorem is beyond the purpose of this work and, therefore, we will only sketch it here.

Proof (sketch). So, in order to give some idea about the proof of the Second Law, first we shall analyze the behavior of an event horizon through Raychaudhuri's equation:

$$K^\mu \nabla_\mu \theta = -\frac{\theta^2}{2} - \widehat{\sigma}^{\mu\nu}\widehat{\sigma}_{\mu\nu} - R_{\mu\nu}K^\mu K^\nu, \tag{4.24}$$

where K^μ is the generator of the horizon and $\widehat{\omega}^{\mu\nu} = 0$ on a hypersurface if and only if K^μ is normal to it (as it is with respect to the event horizon).

If the null-energy condition holds, that is, $R_{\mu\nu}K^\mu K^\nu \geq 0$, and, because $\widehat{\sigma}^{\mu\nu}$ is a spatial tensor, we have that $K^\mu \nabla_\mu \theta \leq 0$. It can be further proven that if in any moment $\theta < 0$, then it must diverge to negative infinity for a finite parameter, this is the Focusing Theorem [47]. This statement is useful for us because the expansion scalar relative to the null geodesics which generate the event horizon cannot diverge in any point of $\mathcal{H}$ [61]. Therefore, for the event horizon we must always have a non-negative θ. Therefore, the straightforward conclusion is that $\delta A \geq 0$. It should still be proven that if new null geodesics enter on $\mathcal{H}$, becoming also generators of the horizon, then, as it could be expected, they would actually contribute to the growth of the spacelike area of the event horizon [27]. □

Originally, the **Third Law** of black-hole mechanics was presented in [6] as the following statement: "it is impossible by any procedure, no matter how idealized, to reduce the surface gravity to zero by a finite sequence of operations".

In opposition to the other laws, these one was not given a proper proof at the time. Actually, not even what exactly was meant by "finite number of operations" was clear in [6], as it was pointed out by W. Israel. A proper proof for the third law was given by him in [36] thirteen years latter of the work of J. Bardeen, B. Carter and S. Hawking. Omitting some technical conditions that escape this work, the third law formulated by Israel states that: if the energy-momentum tensor satisfies the weak energy condition, no continuum process can make the surface gravity vanish for a finite time measured by a set of observers crossing the event horizon.

4.2.2 Hawking radiation

At this point, it is apparent the resemblance between the laws of black-hole mechanics and the laws of classical thermodynamics. The constancy of the surface gravity for a stationary black hole is analogous to the constancy of temperature for a system in thermal equilibrium. The first law of black-hole mechanics tells what is the differential of the mass of a black hole as a function of the spatial area and angular momentum of its event horizon (latter on the electric charge will be considered). But mass is associated to energy and, therefore, this equation is comparable to the first law of thermodynamics. Lastly, probably the most suggestive parallel is between the impossibility of the area of an event horizon to ever decrease and the non-reduction of entropy during an isolated thermodynamic processes.

The comparison between the third law of black-hole mechanics to the third law of classical thermodynamics requires an extra attention. This is due to the fact that this law has different and not equivalent formulations. The most common one, due to M. Planck, states that as the temperature of a thermodynamic system approximates to zero, the entropy also goes to zero. There is no equivalent law for black-hole thermodynamics as a simple counterexample proves: the extreme Kerr black hole ($J = M^2$), whose surface gravity is null but the event horizon has a non-vanishing area. However, there is also the Nernst's formulation of the third law of thermodynamics, which states that the temperature of a thermodynamic system cannot be reduced to zero through a finite number of processes. And this one has some considerable resemblance to the third law given by W. Israel [36].

From the similarities between the Zeroth and Third Laws of black-hole mechanics and the respective ones of classical thermodynamics, two connections are suggested: first between the surface gravity of an event horizon with a thermodynamic temperature and also between the spatial area of the event horizon and the entropy of the black hole. However, classically this is no more than an analogy since a black hole cannot emit any radiation. Thus, its temperature must be zero.

Despite all the interesting similarities between black holes and classical thermodynamics discussed, there was no physical connection between them at the time the laws of black-hole mechanics were first proposed. However, in 1975, S. Hawking coupled Quantum Field Theory to a classical Schwarzschild background and showed that an observer far away from the black hole would perceive a thermal radiation being emitted from its event horizon [26]. And the value of the temperature found is

$$T = \frac{\kappa}{2\pi}, \tag{4.25}$$

where κ is the surface gravity of the event horizon. Therefore, in the work of Hawking, it was found only a few years after the publication of the four laws of black-hole mechanics that the surface gravity is indeed the temperature of the black hole. Thus, it is due to this result that a true black-hole thermodynamic theory can be elaborated, where, from (4.25), we are led to the black-hole entropy:

$$S = \frac{A}{4}. \tag{4.26}$$

4.2.3 Bekenstein-Hawking black-hole thermodynamics

A fundamental idea in classical thermodynamics is the concept of thermodynamic equilibrium, in which a system is completely characterized by a set of extensive parameters: typically (for gases) internal energy U, entropy S, volume V and number of particles N. Therefore, in order for us to be able to build a black-hole thermodynamics, the first step is to ask what can be used to define an equilibrium state for a black hole. The answer to this question comes from the following conjecture [63]:

Black holes have no hair: Black holes in a stationary and asymptotically flat spacetime are completely characterized by three parameters: its mass M, angular momentum J and charge Q.

Furthermore, it is believed that, given enough time, a black hole formed by gravitational collapse should settle down to a stationary configuration. This is not a proved result but it is widely accepted. The idea is that after a gravitational collapse the deviations from stability are radiated away in the form of gravitational waves until the black hole reaches stationarity. A brief discussion about this process and how recent works support this idea can be found in [64]. Furthermore, if all the matter near the black hole falls inside its event horizon, such that any other matter can be considered to be infinitely far away from it, then by the uniqueness theorem of stationary black holes on vacuum, the black hole must be the Kerr-Newman one [61, 49].

We are led to take a stationary black hole as a equilibrium state equivalent (to a certain extent) to the thermodynamic equilibrium. However, it is still important to notice the difference between this definition of equilibrium and the one from classical thermodynamics. As it will be seen latter, the parameters which are used to describe a stationary black-hole, which comes from the No-hair theorem, are not extensive. Therefore, the usual definition of the thermodynamic equilibrium as the state where a set of extensive and intensive parameters are constant is a different notion of equilibrium compared to the stationarity configuration of a black hole. This turns out to be have great importance. As it is presented in [40] by P. Landsberg, if the entropy is not extensive with respect to a set of variables and it is superadditive[8], then it will not be a concave function. What this means is that the entropy cannot be maximized, as it is asked for the equilibrium state in classical thermodynamics.

The differences between taking a stationary configuration for a black hole and the usual thermodynamic equilibrium can be further explored looking at the heat capacity, C, of the Schwarzschild black hole:

$$C \equiv \frac{\partial Q}{\partial T}, \tag{4.27}$$

where Q (not to be confused with the charge of the black hole) is the heat flowing into or out to the thermodynamic system and T its temperature. The calculation is straightforward, we recall that for a quasi-equilibrium process $dQ = TdS$ and make use of the following two results: the surface gravity of the Schwarzschild black hole is given by (3.52) and its mass relates to the area of the event horizon by [53]

$$M^2 = \frac{A}{16\pi}. \tag{4.28}$$

Then, the heat capacity is

$$C = \frac{\partial M}{\partial T} = -8\pi M^2. \tag{4.29}$$

The fact that the heat capacity of the Schwarzschild black hole (4.29) is negative has some important implications towards its behavior. We now present two of them. First, because the Hawking Radiation makes the black hole slowly decrease its mass [63], an isolated black hole shall be completely evaporated after some (long) time since its formation. Therefore, it cannot reach a final state whether it is of equilibrium or not. However, the process is usually slow enough so that for each instant the black hole can be considered to be quasi-stationary [5].

Second, it is possible to put the black hole in thermal equilibrium with an (infinite) heat bath [5], however, the equilibrium is going to be unstable, which is in opposition to the usual cases of classical thermodynamics. In order to perceive this instability, we imagine that a slightly higher amount of radiation enters the black hole, making its mass increase. Then, from (4.29) we see that its temperature decreases, making the radiation which enters the black hole from the thermal bath bigger than the one it is radiated away from the Hawking process. The process follows indefinitely, making the black hole to grow endless. The opposite phenomenon is seen considering a slightly lower

[8]That is, $f(x+y) \geq f(x) + f(y)$.

amount of radiation entering the black hole that is not enough to compensate the Hawking Radiation. Therefore, its mass decreases. Then the negative heat capacity tells us that the temperature of the black hole gets higher, making the Hawking Radiation stronger. Again, this process never stops and the black hole eventually vanishes.

After this discussion about the nature of the equilibrium state for the black-hole thermodynamics, we finish recalling another set of important quantities used in the thermodynamic description of a typical system: the intensive parameters: temperature T, pressure N and chemical potential μ. They can be obtained from the extensive parameters, and therefore, from this perspective, they are not as fundamental as these ones. Equivalently, the counterparts in the black-hole thermodynamics are: surface gravity κ, angular velocity $\Omega_{\mathcal{H}}$ and electric potential $\Phi_{\mathcal{H}}$.

Of course an equilibrium state by itself is not very interesting. If we want to talk about thermodynamic processes, which shall be quasi-static in the sense that the intensive parameters are all well-defined for any moment, a fundamental equation is convenient. This will describe the evolution of a thermodynamic parameter as another set of parameters that characterizes the system evolves. Therefore, the fundamental equation contains all the information about the system under consideration. It will then take an extensive parameter, for instance the energy, and write it as a function of the others: $U = U(S, V, N)$. In the black-hole thermodynamics, we want the mass of the black hole to be a a function of its area, angular momentum and charge: $M = M(A, J, Q)$. In a differential form, this is just the first law of black-hole mechanics:

$$dM = \frac{1}{8\pi}\kappa dA + \Omega_{\mathcal{H}} dJ + \Phi_{\mathcal{H}} dQ, \tag{4.30}$$

where we can associate

$$\frac{\partial M}{\partial A} = \frac{1}{8\pi}\kappa(A, J, Q), \tag{4.31}$$
$$\frac{\partial M}{\partial J} = \Omega_{\mathcal{H}}(A, J, Q), \tag{4.32}$$
$$\frac{\partial M}{\partial Q} = \Phi_{\mathcal{H}}(A, J, Q). \tag{4.33}$$

From (4.31) to (4.33) we have the equations of state, which relate a thermodynamic parameter as a function of others. Each equation of state contains only a partial information about our system. However, the knowledge of all of them is equivalent to having the fundamental thermodynamic equation.

The exact form of the fundamental equation depends on which stationary spacetime we are working with, that is, what is the energy-momentum tensor that enters the Einstein equation. For instance, in the case of vacuum, which we know it must be a (charged)

Kerr spacetime, the fundamental black-hole thermodynamic equation is given by [54]:

$$M = M(A, J, Q) = \sqrt{\frac{A}{16\pi} + \frac{4\pi J^2}{A} + \frac{Q^2}{2} + \frac{\pi Q^4}{A}}. \tag{4.34}$$

From (4.34), it is clear that the black-hole mass is not an extensive parameter of the area, angular momentum and charge. By that, we mean that M is not an homogeneous function of first degree of A, J and Q. Although in some references these parameters are still called extensive, we shall not do it here. By taking partial derivatives of (4.34), it can be found that the surface gravity, angular velocity and electric potential are not homogeneous functions of zeroth degree of A, J, and Q. Thus, we also shall not call them intensive parameters.

In order to continue the presentation of the usual black-hole thermodynamics, let us turn our attentions back to where we started: the Hawking Radiation. We have seen how Hawking's discovery made it possible to develop the thermodynamics of black holes by proving that the surface gravity on the event horizon is really the temperature of the black hole. However, what we have not discussed yet is that the Hawking Radiation also saves the day for the entropy. This is so because, if matter crosses the event horizon, the entropy of the outside universe decreases. Although, one could argue, the total entropy of the universe, including what is inside the horizon, still should increase, for observational purposes this is not what we would want since this information is missed. However, due to (4.26), we can define a generalized entropy S_G such that the information of the entropy inside a black hole can be perceived by us [7]:

$$S_G \equiv S + \frac{A}{4}, \tag{4.35}$$

where S is the entropy of the matter outside of the horizon. This works because when matter crosses the horizon, decreasing the entropy of the outside, the gain in mass of the black hole increases the area of the event horizon. On the other hand, if through the Hawking Radiation the black hole shrinks (which is actually what happens [63]), then its entropy decreases and for the outside universe it increases. This is the balance contained in (4.35) that is consistent with the Second Law.

From classical statistical mechanics, we know that the entropy is a measure of the number of accessible microscopic states for a given configuration of the system. In the case of black-hole thermodynamics, we saw that the configuration is completely determined by the mass, angular momentum and charge of the black hole. On the other hand, it is still not clear how to count the number of microscopic states of a given black hole. Furthermore, classically there is no real reason for the association of the area of the event horizon with the entropy since this connection was only possible due to quantum field effects discovered by Hawking. Therefore, the black-hole thermodynamics can be regarded as an effective theory for an unknown quantum gravity (statistical) theory.

Following what is usually done in the literature, we present the Table 4.2 where important aspects of the black-hole thermodynamics are compared to their classical-thermodynamic counterparts.

Table 4.2

	Thermodynamics	
	Black Holes	**Classical**
Notion of equilibrium	Stationary spacetime	Thermodynamic equilibrium
Parameters needed to describe the equilibrium state	Comes from the No-hair theorem M, J, Q	Extensive parameters U, V, N
Energy / Temperature / Entropy	M / $\frac{\kappa}{2\pi}$ / $\frac{A}{4}$	U / T / S
Zeroth Law	Surface gravity κ is constant on the event horizon for a stationary black hole	Temperature is constant for a system in thermodynamic equilibrium
First Law	$dM = \frac{1}{8\pi}\kappa dA + \Omega_{\mathcal{H}} dJ + \Phi_{\mathcal{H}} dQ$	$dU = TdS - PdV + \mu dN$
Second Law (mechanics law)	$\delta S_G \geq 0 \qquad (\delta A \geq 0)$	$\delta S \geq 0$
Third Law	No continuum process can make the surface gravity vanish for a finite interval of advanced time	No finite quantity of processes can make the temperature of a thermodynamic system vanish

4.3 Hayward thermodynamics

In order to understand why Hayward's work is interesting, let us recall the limitations on the Bekenstein-Hawking thermodynamics. First of all, the thermodynamic quantities are defined based on an event horizon, which, due to the global nature of its definition, cannot be exactly located in a realistic experiment. Moreover, the usual definition of a black hole requires an asymptotically flat spacetime, which may not be the case for our universe. Second, the black hole must be stationary or, at most, quasi-stationary and, therefore, the thermodynamics of dynamical processes is not covered.

Motivated to expand the applicability of a thermodynamic theory for black holes, S. Hayward in 1994 and in 1998 [28, 30] proposed new laws for the black-hole mechanics, called "generalized laws". In his work, the event horizon is no longer the central notion, but the trapping horizons of spherically symmetric spacetimes, which, as we already know, are quasi-locally defined. Since there is no timelike Killing vector unless the spacetime is stationary, S. Hayward employed the Kodama vector in order to define the geometric surface gravity in replace of the usual surface gravity. These subjects are studied, respectively, in Subsection 4.3.1 and in Subsection 4.3.2. In general, there are many different definitions for the energy contained in the black hole, for instance, the most common ones used in the Bekenstein-Hawking thermodynamics are the ADM mass and the Komar mass [63]. In spherically symmetric spacetimes there is a quasi-local definition for the energy known as the Misner-Sharp mass, why is this so and how it is defined is in Subsection 4.3.3. Also, in these geometries a preferable notion of volume exists and will appear in the generalized Hayward First Law, Section 4.3.4.

Quantities associated to the energy-momentum tensor are presented in Subsection 4.3.5. All these objects must be motivated and defined in careful ways. For this reason and because they do not appear in most General Relativity textbooks, this section is organized in many subsections so that we give the proper attention to each quantity. The generalized laws of black-hole mechanics are then presented in Subsection 4.3.6. Finally, then, we get to the Hayward thermodynamics, considered in Subsection 4.3.7

4.3.1 The Kodama vector

The generalized laws of black-hole mechanics developted by S. Hayward in the 1990s [28, 30] are only applicable to spherical symmetric spacetimes. Such geometries were already studied in Section 3.1, but it is worth recalling that in this situation there is always a coordinate system such that the line element can be written in the form

$$ds^2 = h_{ab}dx^a dx^b + r^2 d\Omega^2. \tag{4.36}$$

The areal radius r is a function of the non-angular coordinates and h_{ab} is the metric tensor on the bidimensional effective surface.

As already stated, the Bekenstein-Hawking thermodynamics is only valid for stationary spacetimes, which are characterized by the existence of a timelike Killing vector field ξ^μ. On the other hand, S. Hayward's theory also works for trapping horizons of dynamical spacetimes, such as Vaidya. For this reason Hayward even compared his work as a transition from classical thermostatics to the thermodynamics [30].

If we want to construct a thermodynamics applicable to dynamical geometries, we need a vector field that plays similar functions of ξ^μ so that we can define an analogous quantity for the surface gravity. Such vector is known for spherical geometries and is called the **Kodama vector field** [39]. Its components are defined for a metric of the form (4.36) as

$$K^a \equiv \epsilon^{ab}\nabla_b r \tag{4.37}$$

and $K^\theta = 0 = K^\phi$. The object ϵ^{ab} is the inverse Levi-Civita tensor[9] with respect to the 2-dimensional metric h_{ab}.

In order to explore in which way the Kodama vector generalizes the timelike Killing vector, let us work in a static spacetime, for which the metric can be written in Schwarzschild-like coordinates:

$$ds^2 = -|g_{tt}|dt^2 + g_{rr}dr^2 + r^2 d\Omega^2. \tag{4.38}$$

In this coordinate system, the only non-vanishing component of the Kodama vector field, as it can be computed via (4.37), is

$$K^t = \frac{1}{\sqrt{-g_{tt}g_{rr}}}. \tag{4.39}$$

This shows that, for a static spacetime, at each point the Kodama vector is proportional to the timelike Killing vector $(\partial_t)^\mu$. The condition for both vector fields to coincide (4.39) is $g_{tt}g_{rr} = -1$, which is satisfied, for instance, in the Reissner-Nordströng (charged Schwarzschild) spacetime.

In the Hayward thermodynamics that we shall introduce latter, the trapping horizons play the role of event horizons in the usual black-hole thermodynamics. For this reason, we will now present how to characterize trapped surfaces with respect to the norm of the Kodama vector. For that, it is convenient to change the coordinate system and work with the double null coordinates (ξ^-, ξ^+):

$$ds^2 = -2e^{-f} d\xi^- d\xi^+ + r^2 d\Omega^2, \tag{4.40}$$

where f and r are functions of the null coordinates. We define $\partial_- \equiv \partial_{\xi^-}$ and $\partial_+ \equiv \partial_{\xi^+}$ to represent the future-directed null vector fields pointing toward, respectively, decreasing and increasing areal radius.

In this coordinate system (4.40), the components of the Kodama vector are

$$\begin{aligned} K^+ &= -e^f \partial_- r, \\ K^- &= e^f \partial_+ r, \end{aligned} \tag{4.41}$$

and the others vanish. We compute the norm of the Kodama vector K^μ

$$g_{\mu\nu}K^\mu K^\nu = 2g_{+-}K^+K^- = 2e^f \left[\partial_+ r\ \partial_- r\right]. \tag{4.42}$$

[9]The Levi-Civita tensor, $\epsilon_{\mu\nu}$, also called the volume element, is $\epsilon = \sqrt{h}\, dx^1 \wedge ... \wedge dx^n$, where h is the absolute value of the determinant of the metric and $\{x^1, ..., x^n\}$ are the coordinates of the surface. The wedge product $\wedge$ of two 1-forms, ω and σ, is defined to be $\omega \wedge \sigma = \omega \otimes \sigma - \sigma \otimes \omega$.

In order to relate (4.42) to a trapped surface, the following relation found in [29] is useful:

$$\theta_{\pm} = \frac{2}{r}\partial_{\pm}r. \tag{4.43}$$

Hence we find

$$g_{\mu\nu}K^{\mu}K^{\nu} = \frac{r^2}{2}e^{f}\theta_{+}\theta_{-}. \tag{4.44}$$

It follows that the Kodama vector field is spacelike, null or timelike for, respectively, a trapped, marginal or untrapped surface. This result is consistent, for instance, with the Schwarzschild spacetime since we know the Kodama and the Killing vector fields coincide and inside the event horizon ∂_t becomes spacelike.

4.3.2 Geometric surface gravity

The surface gravity is greatly important in the Bekenstein-Hawking black-hole thermodynamics as it gives the temperature of the black hole. Since in the Hayward thermodynamics the trapping horizons play the role of event horizons, we present now how we to construct a (geometric) surface gravity defined of these hypersurfaces as a generalization, to some extent, of the usual surface gravity. As it was made clear in our previous discussion, in order to accomplish this goal the Kodama vector fields are going to replace of the timelike Killing vector fields.

We begin remembering that the usual surface gravity κ on an event horizon is indirectly defined via (3.9)

$$\frac{1}{2}\chi^{\mu}(\nabla_{\mu}\chi_{\nu} - \nabla_{\nu}\chi_{\mu}) \overset{h}{=} \kappa\chi_{\nu}. \tag{4.45}$$

Let us, then, consider the left hand side of (4.45) replacing the timelike Killing vector for the Kodama one, K^{μ}. In what follows, we make the calculations explicit in order to make clear how concepts that we already understand are connected with the new theory we are developing. Working in the coordinate system of (4.40), we expand the terms that appear inside parenthesis[10]:

$$\begin{aligned}
\nabla_{\mu}K_{\nu} &= g_{\nu\rho}\nabla_{\mu}K^{\rho} \\
&= g_{\nu\rho}\epsilon^{\rho\delta}\nabla_{\mu}\nabla_{\delta}r \\
&= g_{\nu\rho}\epsilon^{\rho\delta}(\partial_{\mu}\partial_{\delta}r - \Gamma^{+}{}_{\mu\delta}\partial_{+}r - \Gamma^{-}{}_{\mu\delta}\partial_{-}r) \\
&= g_{\nu\rho}\big[\epsilon^{\rho+}(\partial_{\mu}\partial_{+}r - \Gamma^{+}{}_{\mu+}\partial_{+}r) + \epsilon^{\rho-}(\partial_{\mu}\partial_{-}r - \Gamma^{-}{}_{\mu-}\partial_{-}r)\big] \\
&= -g_{\nu+}e^{f}(\partial_{\mu}\partial_{-}r - \Gamma^{-}{}_{\mu-}\partial_{-}r) + g_{\nu-}e^{f}(\partial_{\mu}\partial_{+}r - \Gamma^{+}{}_{\mu+}\partial_{+}r).
\end{aligned} \tag{4.46}$$

[10] We will use the fact that the only non-vanishing Christoffel symbols involving the null coordinates are $\Gamma^{+}{}_{++}$ and $\Gamma^{-}{}_{--}$. Also, the orientation is chosen such that $\epsilon = e^{-f}\ (d\xi^{-}\otimes d\xi^{+} - d\xi^{+}\otimes d\xi^{-})$.

And then, $K^\mu(\nabla_\mu K_\nu - \nabla_\nu K_\mu)$ equals to

$$\begin{aligned} K^+\big[&(-g_{\nu+}e^f\partial_+\partial_- r + g_{\nu-}e^f\partial_+\partial_+ r - g_{\nu-}e^f\Gamma^+{}_{++}\partial_+ r) \\ &\qquad\qquad - (-g_{++}e^f\partial_\nu\partial_- r + g_{+-}e^f\partial_\nu\partial_+ r - g_{+-}e^f\Gamma^+{}_{\nu+}\partial_+ r)\big] \\ &+ K^-\big[(-g_{\nu+}e^f\partial_-\partial_- r + g_{\nu+}e^f\Gamma^-{}_{--}\partial_- r + g_{\nu-}e^f\partial_-\partial_+ r) \\ &\qquad\qquad - (-g_{-+}e^f\partial_\nu\partial_- r + g_{-+}e^f\Gamma^-{}_{\nu-}\partial_- r + g_{--}e^f\partial_\nu\partial_+ r)\big]. \end{aligned} \tag{4.47}$$

Despite of the long expression, when studying each each component separately we observe a simplification (also making use of (4.41)):

$$K^\mu(\nabla_\mu K_+ - \nabla_+ K_\mu) = K^-\big[2g_{+-}e^f\partial_+\partial_- r\big] = -2e^f\partial_+ r\partial_+\partial_- r, \tag{4.48}$$

$$K^\mu(\nabla_\mu K_- - \nabla_- K_\mu) = K^+\big[-2g_{-+}e^f\partial_+\partial_- r\big] = -2e^f\partial_- r\partial_+\partial_- r. \tag{4.49}$$

This is valid on all spacetime, but we are interested in what happens on a future trapping horizon since this one is related to black holes. By definition, the expansion tensor in outgoing direction vanishes: $\theta_+ = 0$. And as a result, from (4.43), $\partial_+ r \stackrel{h}{=} 0$:

$$K^\mu(\nabla_\mu K_+ - \nabla_+ K_\mu) \stackrel{h}{=} 0, \tag{4.50}$$

$$K^\mu(\nabla_\mu K_- - \nabla_- K_\mu) \stackrel{h}{=} -2e^f\partial_- r\partial_+\partial_- r. \tag{4.51}$$

Furthermore, notice that on a trapping horizon $K_\mu = g_{\mu\nu}K^\nu \stackrel{h}{=} g_{\mu+}K^+$. The only non-null component being

$$K_- \stackrel{h}{=} -g_{-+}e^f\partial_- r \stackrel{h}{=} \partial_- r. \tag{4.52}$$

Therefore, we finally see that, working on the double null coordinate system, on a trapping horizon we have the following relation

$$\frac{1}{2}K^\mu(\nabla_\mu K_\nu - \nabla_\nu K_\mu) \stackrel{h}{=} -e^f\partial_+\partial_- r K_\nu. \tag{4.53}$$

Comparing (4.53) with (4.45) we are led to define the **geometric surface gravity** κ_G on trapping horizons indirectly via

$$\frac{1}{2}g^{\mu\nu}K^\rho\big(\nabla_\rho K_\mu - \nabla_\mu K_\rho\big) \stackrel{h}{=} \kappa_G K^\nu. \tag{4.54}$$

And if the Killing and the Kodama vector fields coincide, for instance in the Reissner-Nordström spacetime, the usual surface gravity and the geometric surface gravity are the same. Therefore, in this situations, the generalized surface gravity is indeed a generalization of the usual one when considering spherically symmetric geometries.

Equation (4.54) does not give a practical way to calculate the geometric surface gravity. An equivalent, but more direct and useful definition of κ_G is [21]:

$$\kappa_G = \nabla_a \nabla^a r = \frac{1}{2\sqrt{h}} \partial_a \big(\sqrt{h} h^{ab} \partial_b r \big), \tag{4.55}$$

with h_{ab} being the metric on the 2-dimensional effective surface defined on (4.36).

One interesting feature of the geometric surface gravity is that it can be used to classify trapping horizons. To show that, we compute the geometric surface gravity using the metric in the coordinate system of (4.40):

$$\kappa_G = -\frac{e^f}{2} \big[\partial_+ (e^{-f} e^f \partial_- r) + \partial_- (e^{-f} e^f \partial_+ r) \big] = -e^f \partial_+ \partial_- r. \tag{4.56}$$

But from (4.43):

$$\kappa_G = -\frac{1}{2} e^f \partial_- (r\theta_+) = -\frac{1}{2} e^f \left[(\partial_- r)\theta_+ + r\partial_- \theta_+ \right] = -\frac{1}{2} e^f \left(\frac{1}{2} r\theta_- \theta_+ + r\mathcal{L}_- \theta_+ \right). \tag{4.57}$$

Then, on a future trapping horizon, recalling that $\theta_+ = 0$, we have

$$\kappa_G = -\frac{1}{2} r e^f \mathcal{L}_- \theta_+. \tag{4.58}$$

Alternatively, we could write $\kappa_G = -\frac{1}{2} e^f \partial_+ (r\theta_-)$ and evaluate it on a past trapping horizon, where θ_- vanishes, finding

$$\kappa_G = -\frac{1}{2} r e^f \mathcal{L}_+ \theta_-. \tag{4.59}$$

From the sign of the derivatives $\mathcal{L}_- \theta_+$ and $\mathcal{L}_+ \theta_-$ in (4.58) and (4.59), we can classify each kind of trapping horizon according to the sign of the geometric surface gravity. The result is presented in the Table 4.3.

Table 4.3

	Future trapping horizon		**Past trapping horizon**	
	Outer	**Inner**	**Outer**	**Inner**
Geometric surface gravity κ_G	Positive	Negative	Positive	Negative

4.3.3 Misner-Sharp mass

In General Relativity there are distinct and non-equivalent ways to define the mass of a compact object. The most common ones are the Kodama and ADM masses, which both involve an integration on spatial infinity in order to be defined [47]. As it has been discussed, the Hayward thermodynamics is defined on trapping horizons, which are quasi-local objects. For this reason, it is natural to seek a quasi-local definition for the mass of the black hole. The one which is used in the Hayward thermodynamics is the **Misner-Sharp mass**:

$$M_{\text{MS}} \equiv \frac{r}{2}(1 - \nabla^\mu r \nabla_\mu r), \tag{4.60}$$

from where we see that it depends only on the value of the areal radius and its neighborhood to be defined.

The physical meaning of the Misner-Sharp mass is still not clear just from its definition (4.60) and our next task is to clarify its physical interpretation (it will be seen that it is in close relation with the Kodama vector field). In order to do that, following the presentation given by Hayward in [29], we will work with the spherically symmetric spacetime in the following coordinate system:

$$ds^2 = -d\tau^2 + e^\lambda d\zeta^2 + r^2 d\Omega^2, \tag{4.61}$$

where r and λ are functions of τ and ζ only.

In this coordinate system the components of the Kodama vector field are [29]

$$K^\tau = e^{-\frac{\lambda}{2}} \partial_\zeta r, \tag{4.62}$$
$$K^\zeta = -e^{-\frac{\lambda}{2}} \partial_\tau r, \tag{4.63}$$

the others vanishing. And for reasons that will soon become clear, it is also defined the vector field $J^\mu \equiv T^{\mu\nu} K_\nu$, where $T^{\mu\nu}$ is the energy-momentum tensor. The non-zero components are

$$J^\tau = \frac{e^{-\frac{\lambda}{2}}}{4\pi r^2} \partial_\zeta M_{\text{MS}}, \tag{4.64}$$
$$J^\zeta = -\frac{e^{-\frac{\lambda}{2}}}{4\pi r^2} \partial_\tau M_{\text{MS}}. \tag{4.65}$$

Furthermore, it can be shown that the divergent of K^μ and J^μ are null [3]:

$$\nabla_\mu K^\mu = 0, \tag{4.66}$$
$$\nabla_\mu J^\mu = \nabla_\mu (K_\nu T^{\mu\nu}) = 0. \tag{4.67}$$

As in Electrodynamics, equations (4.66) and (4.67) imply that both K^μ and J^μ are conserved currents. Then, from Stokes's theorem, each of them will generate a conserved charge. In other words, the quantities

$$\int_\Sigma \epsilon_\Sigma \; n_\mu K^\mu, \tag{4.68}$$

$$\int_\Sigma \epsilon_\Sigma \; n_\mu J^\mu, \tag{4.69}$$

where n^μ is the unit normal vector field orthogonal to Σ, are independent of the spacelike hypersurface Σ chosen.

In the next subsection, where the notion of black-hole volume will be discussed, the implications of (4.68) are going to be presented. For now, we will focus on (4.69) since this is the one related to the Misner-Sharp mass.

We calculate the integral over the hypersurface Σ of constant time-coordinate τ and areal radius between zero and a fixed value r:

$$\begin{aligned} -\int_\Sigma \epsilon_\Sigma \; J^\mu(\partial_\tau)_\mu = -\int_\Sigma \epsilon_\Sigma \; J^\mu g_{\mu\tau} = \int_\Sigma e^{\frac{\lambda}{2}} \; d\zeta d\Omega \; \frac{e^{-\frac{\lambda}{2}}}{4\pi r^2}\partial_\zeta M_{\mathrm{MS}} = \int_{\zeta_0}^{\zeta} d\zeta \; \partial_\zeta M_{\mathrm{MS}} \\ = M_{\mathrm{MS}}, \end{aligned} \tag{4.70}$$

where we have used that ζ_0 represents the coordinate ζ at zero areal radius, where we assume $M_{\mathrm{MS}} = 0$[11]. From (4.70) we have the physical interpretation of the Misner-Sharp mass as an amount of the conserved charge (4.69) within a region of some fixed radius at a given instant of time.

In Subsection 4.3.1 we saw that the norm of the Kodama vector and the sign of the geometric surface gravity could be used to characterize surfaces in a spherically symmetric spacetime. It turns out that we can also use the Misner-Sharp mass in order to give a condition for a 2-surface to be trapped, marginal or untrapped. For this task, we use the double-null coordinate system (4.40):

$$M_{\mathrm{MS}} = \frac{1}{2}r(1 - \nabla^\mu r \nabla_\mu r) = \frac{1}{2}r(1 - 2g^{+-}\partial_+ r \partial_- r) = \frac{r}{2} + \frac{e^f r^3 \theta_+ \theta_-}{4}. \tag{4.71}$$

Then, we can classify if a 2-sphere of radius r is a trapped, marginal or untrapped surface according to the value of the Misner-Sharp mass contained inside this surface. In Table 4.4 this description is presented, along with the classification according to the norm of the Kodama vector field.

[11] More generally, we have ΔM_{MS} for (4.70)

Table 4.4

	Trapped surface	**Marginal surface**	**Untrapped surface**
Kodama vector	Spacelike	Null	Timelike
Misner-Sharp mass M_{MS}	$2M_{\mathrm{MS}} > r$	$2M_{\mathrm{MS}} = r$	$2M_{\mathrm{MS}} < r$

4.3.4 Black-hole volume

In classical thermodynamics, one of the extensive parameters that is frequently used to characterize a system is its volume. Such term, or a relativistic analogue, is not present in the Bekenstein-Hawking thermodynamics but will appear in the Hayward's theory. However, how to define a spatial volume in a spacetime in an unambiguous form is usually not clear. And for this reason, before we get into Hayward's definition of volume, it is woth seeing in some details why it is not trivial to define a spatial volume in a Lorentzian geometry.

Minkowski space provides the first and most clear example to our discussion. A set of observers $\mathcal{O}$ with no motion with respect to each other could define a spatial volume V according to a fixed time on their synchronized clocks. Now we suppose that another set of observers $\mathcal{O}'$ travels with a velocity u with respect to $\mathcal{O}$. In their perspective, they can also define a spatial volume V' following the same procedure of $\mathcal{O}$. Then, how V and V' are related to each other? This is a simple question from special relativity. The answer is that they are related by a Lorentz contraction on the direction of motion. Therefore, each set of observers perceives the volume defined by the other set of observers contracted by an amount of $\sqrt{1-u^2}$. This conclusion could also be stated in terms of coordinate systems. If two coordinate systems are distinct by a Lorentz transformation, then the respective spatial volumes also differ by a Lorentz transformation. Therefore, the definition of spatial volume is ambiguous in the sense that it is dependent on the choice of a coordinate system.

For the case of a general Lorentzian geometry, a coordinate transformation will not keep a 3-volume invariant in general. Thus, for each foliation taken, that is, for a fixed time coordinate, the 3-volume may be different. Hence, the ambiguity is present. For instance, the paper [19] shows that for a Schwarzschild black hole its spatial volume, defined by fixing a time coordinate and integrating the areal radius from the singularity to the event horizon (and integrating on the angular coordinates), has different values depending on the coordinate system chosen.

After this prelude, we consider how the spatial volume is going to be defined in the Hayward thermodynamics. We recall that the divergence of the Kodama vector field K^μ

is zero (4.66) and from Stokes's theorem a conserved charge would be generated, which means that the integral (4.68) is independent of the spacelike hypersurface of integration, Σ. We did not explore this fact in details when defining the Misner-Sharp mass, however, we will do it here and also show how it is related to the spatial volume.

First we prove that (4.68) is indeed a conserved charge. So, we want to integrate $\nabla_\mu K^\mu$ and use Stokes's theorem to analyse the fluxes on the hypersurfaces of contant time. What we are going to do is integrate inside a region of fixed radius r (this is the region N in Figure 4.1) whose boundary is the union of Σ_p, Σ_f and C. Therefore, we have

$$\int_N \epsilon_N \nabla_\mu K^\mu = \int_{\Sigma_f} \epsilon_{\Sigma_f} (\partial_\tau)_\mu K^\mu - \int_{\Sigma_p} \epsilon_{\Sigma_p} (\partial_\tau)_\mu K^\mu + \int_C \epsilon_C \frac{\nabla_\mu r}{\sqrt{\nabla_\nu r \nabla^\nu r}} K^\mu. \tag{4.72}$$

The minus sign before the second term on the right hand side is due to the fact that on the hypersurface Σ_p the normal vector field points on the opposite direction of $(\partial_\tau)^\mu$. However,

$$\nabla_\mu r K^\mu = \epsilon^{\mu\nu} \nabla_\nu r \nabla_\mu r = 0 \tag{4.73}$$

since we are contracting the indices of a symmetric tensor with the indices of an anti-symmetric one. Then, because $\nabla_\mu K^\mu = 0$:

$$\int_{\Sigma_f} \epsilon_{\Sigma_f} (\partial_\tau)_\mu K^\mu = \int_{\Sigma_p} \epsilon_{\Sigma_p} (\partial_\tau)_\mu K^\mu, \tag{4.74}$$

which shows that the quantity

$$\int_\Sigma \epsilon_\Sigma \ (\partial_\tau)_\mu K^\mu \tag{4.75}$$

is independent of the hypersurface Σ of constant time-coordinate τ and of areal radius limited to r.

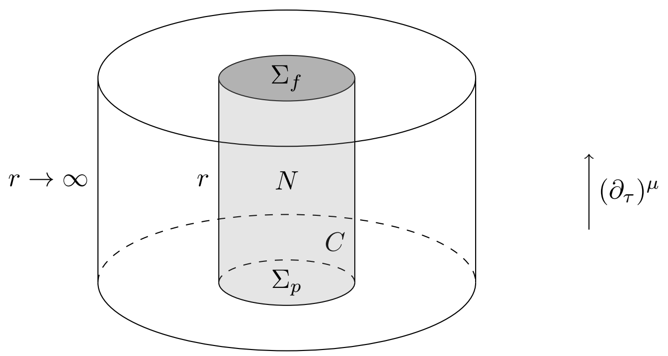

Figure 4.1: Representation of the region being integrated between two surfaces of constant τ. The boundary of N is composed by the future and past hypersurfaces, respectively, Σ_f and Σ_p and the cylinder C of constant radius r. On the right side we have an arrow representing the direction of the vector field $(\partial_\tau)^\mu$.

We now show that the conserved charge (4.69) defines a spatial volume. For that, consider the coordinate system of (4.61) and take a hypersurface Σ of constant coordinate τ and areal radius going from zero to r :

$$\begin{aligned} -\int \epsilon_\Sigma\ (\partial_\tau)_\mu K^\mu = -\int \epsilon_\Sigma\ g_{\mu\tau} K^\mu = \int e^{\frac{\lambda}{2}}\ d\zeta d\Omega\ e^{-\frac{\lambda}{2}} \partial_\zeta r = 4\pi \int_{\zeta_0}^{\zeta} d\zeta\ r^2 \partial_\zeta r \\ = \frac{4\pi r^3}{3}. \end{aligned} \tag{4.76}$$

What we are showing is that (4.68) defines not only a global conserved charge, but a quasi-local one. This is physically reasonable as we expect that for any time the region inside a fixed areal radius gives the same spatial volume.

4.3.5 Quantities associated to the energy-momentum tensor

It was seen how the Kodama vector replaces the Killing one and how it defines a geometric surface gravity analogue to the usual surface gravity. The definitions presented in Hayward's work of energy and volume for spherically symmetric spacetimes were also discussed in formal ways but keeping physical intuition close. In order to finally get to the Hayward thermodynamics, it is left for us to discuss about two quantities which are associated with the energy-momentum tensor. These are two invariants of the bidimensional effective surface and are called the work-density scalar and the energy-flux vector field.

Since they will be needed in the rest of this subsection, we already write the Einstein field equations for a spherically symmetric spacetime in double null coordinates [30]:

$$\begin{aligned} &\partial_\pm \partial_\pm r - \partial_\pm \ln(-g_{+-}) \partial_\pm r = -4\pi r T_{\pm\pm}, \\ &r \partial_+ \partial_- r + \partial_+ r \partial_- r - \frac{1}{2} g_{+-} = 4\pi r^2 T_{+-}, \\ &r^2 \partial_+ \partial_- \ln(-g_{+-}) - 2\partial_+ r \partial_- r + g_{+-} = 8\pi r^2 (g_{+-} T^\theta_\theta - T_{+-}). \end{aligned} \tag{4.77}$$

An appropriate manner to introduce the work-density scalar and the energy-flux vector field is to show where they come from. So, we will use the double null coordinates to evaluate the rate of change of the Misner-Sharp mass on the bidimensional effective surface in terms of the energy-momentum Tensor [30]:

$$\partial_\pm M_{\text{MS}} = -A g^{+-} (T_{+-} \partial_\pm r - T_{\pm\pm} \partial_\mp r). \tag{4.78}$$

Now, it is defined the **energy-flux vector field** ψ^μ and the **work-density scalar**

w, whose physical interpretation will be soon discussed, as:

$$\psi^{\mu} \equiv T^{\mu\nu}\nabla_{\nu} r + w\nabla^{\mu} r, \tag{4.79}$$

$$w \equiv -\frac{1}{2} h_{ab} T^{ab}, \tag{4.80}$$

which in the double-null coordinate system read:

$$\psi_{+} = T_{++} g^{+-} \partial_{-} r, \qquad \psi_{-} - T_{--} g^{+-} \partial_{+} r, \tag{4.81}$$

$$w = -g^{+-} T_{+-}. \tag{4.82}$$

From the definitions (4.79) and (4.80), we can write the rate of change of the Misner-Sharp mass of (4.78) as

$$\partial_{\pm} M_{\mathrm{MS}} = A\psi_{\pm} + w\partial_{\pm} V. \tag{4.83}$$

Or in a covariant form:

$$\nabla_{\mu} M_{\mathrm{MS}} = A\psi_{\mu} + w\nabla_{\mu} V. \tag{4.84}$$

The above equation (4.84) is of enormous importance as it will lead directly to the Hayward First Law of black-hole mechanics. Moreover, the expression gives some insights toward the physical meaning of the quantities just defined. Comparing with the left hand size of (4.84), the work-density scalar, w, clearly represents some energy density as it appears together with the derivative of the spatial volume. Further investigation, for instance analysing a spherically symmetric electromagnetic field tensor [30] and the FLRW cosmology [20] shows that this scalar indeed behaves as expected for a work term. For the energy-flux vector, since it is accompanied with only the spatial area, we can infer that it does represent some kind of energy flux. Furthermore, in analogy to the first law of classical thermodynamics, it seems natural that the change in energy can be separated in work plus energy-flux terms. Therefore, we have justified the names of the new quantities and why separate the derivative of the Misner-Sharp mass in this form.

4.3.6 The generalized laws of black-hole mechanics

In this subsection the generalized laws of black-hole mechanics, published by S. Hayward in 1994 [28] and in 1998 [30], are presented followed by their proof or, at least, a comment about it. Comparing his laws with the Bekenstein-Hawking thermodynamics or with classical thermodynamics suggests a reinterpretation of his work as thermodynamic laws. However, only in the next subsection this subject is going to be explored.

The **Hayward Zeroth Law** for black-hole mechanics states that for an equilibrium state, regarded as the stationarity configuration of the spacetime, the geometric surface gravity is constant on the trapping horizon.

Proof. In a static and spherically symmetric spacetime, we can write the line element in Schwarzschild-like coordinates (4.38) such that no component of the metric tensor depends on the time nor the angular coordinates. Therefore, since the trapping horizon must be the union of 2-spheres for all values of time due to the spherical symmetry, we see from (4.55) that the derivatives of the geometric surface gravity with respect to the time or the angular coordinates must be zero. Therefore, κ_G is constant on the trapping horizon. □

The **Hayward First Law** of the Hayward black-hole mechanics gives the rate of change of the Misner-Sharp mass of the black hole along its trapping horizon in the form:

$$M'_{\rm MS} = \frac{\kappa_G A'}{8\pi} + wV', \tag{4.85}$$

where f' denotes the derivative of the scalar f in any direction z^μ tangent to the trapping horizon: $f' \equiv z^\mu \nabla_\mu f$.

Proof. The second term on the right hand side of (4.85) comes directly from (4.84). We are left to prove that

$$Az^\mu \psi_\mu = \frac{\kappa_G}{8\pi} z^\mu \nabla_\mu A. \tag{4.86}$$

In order to do that, we will work on double null coordinates following the steps suggested in [30]. First we want to show the last equality of the following equation is true:

$$0 = (\nabla_+ r)' = z^\mu \nabla_\mu \partial_+ r = z^+ \partial_+ \partial_+ r + z^- \partial_- \partial_+ r = g_{+-}\kappa_G z^- - 4\pi r T_{++} z^+. \tag{4.87}$$

The term with the z^+ component comes directly from the first equation of (4.77) evaluated at a future trapping horizon, where $\partial_+ r = 0$. For the other term, with z^-, we use the second equation of (4.77). For that, we must notice that

$$T_{+-} = -\frac{w}{g^{+-}} = -wg_{+-}, \tag{4.88}$$

$$\frac{g_{+-}}{2r} = \frac{M_{\rm MS}}{r^2} g_{+-}. \tag{4.89}$$

Then, we find the relation

$$\partial_+ \partial_- r = g_{+-}\Big(\frac{M_{\rm MS}}{r^2} - 4\pi r w\Big) = g_{+-}\kappa_G{}^{12}. \tag{4.90}$$

And this completes the proof of (4.87).

[12] As it can be checked writing the geometric surface gravity, the work-density scalar and the Misner-Sharp mass in double-null coordinates, the second Einstein equation of (4.77) can also be written as $\kappa_G = \frac{M_{\rm MS}}{r^2} - 4\pi r w$.

Now we have all the ingredients needed to prove the First Law (4.85):

$$
\begin{aligned}
Az^\mu \psi_\mu = Az^\mu (T_{\mu +} g^{+-} \partial_- r + w \partial_\mu r) = Az^+ T_{++} g^{+-} \partial_- r = r\kappa_G z^- \partial_- r = r\kappa_G r' \\
= \frac{\kappa_G A'}{8\pi},
\end{aligned}
\tag{4.91}
$$

where in the third equality we used (4.87) and in order to get the final result we have used that, as it can be readily verified, $A' = 8\pi r r'$. Therefore, we have finally proven the First Law of the Hayward black-hole mechanics (4.85). □

The **Hayward Second Law** was published four years before the other two in 1994 [28] and states that, given that the null-energy condition is true, the area of the trapping horizon $\mathcal{H}$ is

> non-decreasing if $\mathcal{H}$ is future outer or past inner,

> non-increasing if $\mathcal{H}$ is future inner or past outer.

The cases in which the area is constant all happening when $\mathcal{H}$ is a null hypersurface.

Some aspects of the proof for the Hayward Second Law are too specific and we shall not present it here. However, the main idea is intuitive: we must find out the sign of the rate of change of the area element in a direction tangent to $\mathcal{H}$ and normal to the foliation of marginal surfaces.

We now recall the physical interpretation of each kind of trapping horizons. We have seen that a future outer trapping horizon is typical of black holes. In some cases it may even coincide with its event horizon. Therefore, the fact that its area is non-decreasing is what we would expect for an analogous of the usual Second Law of the Bekenstein-Hawking black-hole mechanics. On the other hand, a past outer trapping horizon is related to white holes, for which, not surprisingly, has an opposite dynamics. It was also previously seen that future and past inner trapping horizons can be taken as the definition of the cosmological horizon for a contracting and an expanding cosmology, respectively. Then, it is clear that the Second Law gives the expected behavior for the trapping horizon given these physical scenarios.

A third law for black-hole mechanics was not proposed by S. Hayward in his works [28, 30] and nor it is presented in most texts in the literature about this subject. Therefore, we end here the generalized laws of black-hole mechanics and in the next section we study how they can be reinterpreted as thermodynamic laws.

4.3.7 Hayward black-hole thermodynamics

At this point, we are in a similar situation after presenting the Bekenstein-Hawking black-hole mechanics. We have some laws which show interesting similarities with the laws of classical thermodynamics, but we have not even talked about temperature, entropy or any other characteristic parameter of a thermodynamic theory yet. Therefore, our current task is to define these quantities.

We begin recalling that in the usual black hole mechanics, the thermodynamics had its validation in S. Hawking's work, which showed that the surface gravity of the event horizon of a stationary black hole is the temperature it emits through, what is nowadays called, the Hawking radiation. Again, we are not going to enter in the details of how to precisely connect the geometric surface gravity to the temperature of a trapping horizon because it requires a semi-classical treatment beyond the purpose of this work. When Hayward published his Laws of black-hole mechanics, there were no formal proofs connecting the geometric surface gravity with the temperature of a trapping horizon (as he made clear in [30]). Since then, some effort were put in the attempt of filling this gap and researchers found success in applying a technique developted by Parikh and Wilczek [45] in which the Hawking Radiation is seen as a tunneling process. For instance, S. Hayward *et al.* used this method for the case of future outer trapping horizons in spherically symmetric spacetimes [32]. A brief review about how this method is applied can be found in [34]. In what follows, we summarize some of its main conclusions.

The geometric surface gravity κ_G is positive for outer trapping horizons and negative for inner ones. The temperature obtained via the Hawking Radiation as a tunneling effect [34] is proportional to $\frac{\kappa_G}{2\pi}$ for future trapping horizons and proportional to $-\frac{\kappa_G}{2\pi}$ for past ones (with the constant of proportionality being positive in both cases and given by universal constants). Therefore, it is concluded that future outer and past inner trapping horizons present a positive temperature and we can expect to be able to apply the Hayward thermodynamics in a physically reasonable way. However, according to these results, past outer and future inner ones would present a negative temperature. Such horizons will not be considered in this work and this odd result may be caused by different reasons. For instance, it may be that the method for obtaining the Hawking Radiation as a tunneling effect is failed for such cases for unknown reasons, or past outer and future inner trapping horizons may be physically impossible [34]. Other possibilities could exist, for instance, maybe we should consider only the absolute value of the temperature found. However, we will not go any further in this subject and in this work we will be interested in future outer and past inner trapping horizons, which are the ones related, respectively, to black holes and expanding cosmologies.

Given a connection between the geometric surface gravity and the temperature of a trapping horizon, we are led to interpret the laws of the Hayward black-hole mechanics as thermodynamic laws. Doing so, the entropy of the trapping horizon is given by $\frac{A}{4}$, where A is the area of the trapping horizon and, again, we have a similar relation with the usual black-hole thermodynamics.

Despite the similarities of the Hayward black-hole thermodynamics with the

Bekenstein-Hawking approach, they are very different in two important ways. For instance, the Hayward construction is quasi-local. We recall that, in opposition to an event horizon, whose definition requires a global knowledge of the spacetime, a trapping horizon depends only on its position (its areal radius in spherically symmetric spacetimes) and its neighborhood in order to be defined. Also, we have a thermodynamics of non-equilibrium. By that we mean that the temperature of our system is defined for arbitrary dynamical spherically symmetric spacetimes with trapping horizons and not only for stationary or quasi-stationary configurations, as it is the case of the Bekenstein-Hawking black-hole thermodynamics.

Nevertheless, in Hayward thermodynamics we are restricted to spherically symmetric spacetimes, where we can define the Kodama vector field. On the other hand, we are able to deal with dynamical spacetimes. Examples of systems where the Hayward thermodynamics can be applied include: the future outer trapping and cosmological horizons of the Vaidya and Vaidya-de Sitter spacetimes, this one being topic of the present work. Of course, we can also apply Hayward thermodynamics to the situations where the mass parameter is constant in the previous geometries. That is, the event horizon of the Schwarzschild and Schwarzschild-de Sitter spacetimes, where the Kodama vector and the geometric surface gravity coincide with the Killing vector and the usual surface gravity and, thus, we recover the results of Bekenstein-Hawking black-hole thermodynamics. One last interesting example we give is the FLRW cosmology. It was showed in [4] that the First Law of the Hayward thermodynamics can be written in a differential form as it is the case for the usual black-hole thermodynamics. This was accomplished by considering an ensemble of FLRW cosmologies with the same temperature and pressure but slightly different (Misner-Sharp) mass, volume and entropy. Then, taking the differential form of the Friedmann equation, they were able to find the relation $dM = TdS + wdV$, where w is the work-density scalar.

We finish this section comparing the main features of Bekenstein-Hawking black-hole thermodynamics to the ones of the Hayward theory in Table 4.5.

Table 4.5

	Black-Hole Thermodynamics	
	Bekenstein-Hawking	**Hayward**
Background	Event horizon of a stationary geometry	Future outer and past inner trapping horizons of a spherically symmetric spacetime
Construction	Global	Quasi-local
Energy / Temperature / Entropy	Komar or ADM / $\frac{\kappa}{2\pi}$ / $\frac{A}{4}$	Misner-Sharp / $\frac{\kappa_G}{2\pi}$ / $\frac{A}{4}$
Zeroth Law	Surface gravity κ is constant on the event horizon for a stationary black hole	Geometric surface gravity κ_G is constant on the trapping horizon for a stationary black hole
First Law	$dM = \frac{\kappa}{8\pi} dA + \Omega_{\mathcal{H}} dJ + \Phi_{\mathcal{H}} dQ$	$M' = \frac{\kappa A'}{8\pi} + wV'$
Second Law (mechanics law)	$\delta S_G \geq 0 \quad (\delta A \geq 0)$	$\Delta S_G \geq 0 \quad (A' \geq 0)$

Chapter 5

Applications of Hayward thermodynamics

The goal of this chapter is to apply the Hayward thermodynamics to concrete scenarios. We are mainly interested in the Vaidya-de Sitter spacetime which models a dynamical black hole whose mass changes in time and it is immersed in a not asymptotically-flat cosmological background. This geometry is not compatible with the Bekenstein-Hawking treatment. On the other hand, by S. Hayward's theory we will be able to study the thermodynamics of the future outer trapping horizon due to the presence of the black hole and also of the past inner trapping horizon due to the expansion of the background cosmology.

However, before we get into the Vaidya-de Sitter spacetime itself, the static case, in which the mass of the black hole is constant, that is, the Schwarzschild-de Sitter spacetime, will be first studied. That way we first get familiar to a simpler scenario so that we then generalize it.

In order to investigate the thermodynamics of each of these environments, we will discuss individually both spacetimes highlighting the important features. For this reason, this chapter is organized in the following way: Section 5.1 is about the Schwarzschild-de Sitter spacetime and in Section 5.2 the thermodynamics of the Schwarzschild black hole and of the cosmological horizon are studied. Similarly, in Section 5.3 we present the Vaidya-de Sitter spacetime in details and then, in Section 5.4, Hayward's black-hole thermodynamics is applied.

5.1 The Schwarzschild-de Sitter spacetime

The **Schwarzschild-de Sitter spacetime**, as the name suggests, describes a Schwarzschild object in a de Sitter space. That is, a stationary and spherically symmetric object of mass M immersed in a vacuum cosmological background with positive cosmological constant Λ.

The metric tensor for this geometry can be written in diagonal Shwarzschild-like coordinates [23]:

$$ds^2 = -f(r)dt^2 + f(r)^{-1}dr^2 + r^2 d\Omega^2, \tag{5.1}$$

such that

$$f(r) \equiv 1 - \frac{2M}{r} - \frac{\Lambda r^2}{3}, \tag{5.2}$$

with ranges

$$\begin{gathered} -\infty < t < \infty, \qquad 0 < \theta < \pi, \qquad 0 < \phi < 2\pi, \\ \text{for the radius coordinate, } r\text{, it depends on the roots of } f(r). \end{gathered} \tag{5.3}$$

The causal structure of this spacetime depends on the zeros of $f(r)$, which rely on the values of the parameters Λ and M. In order to study the different cases, first we write

$$g_{tt} = \frac{1}{r}\left(\frac{\Lambda r^3}{3} - r + 2M\right) \tag{5.4}$$

and take the derivative of what is inside parenthesis to find the local maximums and minimums. It is straightforward to see they will be located at $r = \pm\sqrt{1/\Lambda}$. From the asymptotic behavior of this function $\left(r \to \pm\infty \implies \frac{\Lambda r^3}{3} - r + 2M \to \pm\infty\right)$, the positive r must be a local minimum and the negative one a local maximum. And, to discover how many positive roots there are, we substitute $r = \sqrt{\frac{1}{\Lambda}}$ at

$$\frac{\Lambda r^3}{3} - r + 2M \tag{5.5}$$

to find

$$\frac{-2}{3\sqrt{\Lambda}} + 2M. \tag{5.6}$$

Thus, defining the extreme cosmological constant $\Lambda_{\text{ext}} \equiv \frac{1}{9M^2}$, we have three different cases (Figure 5.1 shows the behavior of $f(r)$ for each situation analysed):

∘ $0 < \Lambda < \Lambda_{\text{ext}}$: the function $f(r)$ has two positive roots r_H and r_C, with $r_H < r_C$, and a negative root $r_- = -(r_H + r_C)$. This is the case of non-extreme Schwarzschild-de Sitter spacetime, where the spherical object produces a horizon at $r = r_H$ and the de Sitter universe produces a cosmological horizon at $r = r_C$. It can be shown that r_H and r_C satisfy the following limits

$$\Lambda \longrightarrow 0 \implies r_H \longrightarrow 2M, \quad r_C \longrightarrow \infty, \tag{5.7}$$

$$\Lambda \longrightarrow \frac{1}{9M^2} = \Lambda_{\text{ext}} \implies r_H, r_C \longrightarrow 3M. \tag{5.8}$$

Therefore,

$$2M < r_H < 3M < r_C \tag{5.9}$$

for the non-extreme Shwarzschild-de Sitter spacetime. Unless otherwise specified, this situation will be assumed.

∘ $\Lambda = \Lambda_{\text{ext}}$: the function $f(r)$ has one positive root. This is the extreme case, where both horizons coincide at the same radius on this coordinate system, $r_H = r_C$.

∘ $\Lambda > \Lambda_{\text{ext}}$: the function $f(r)$ has no positive root. There is no black-hole, but a naked singularity.

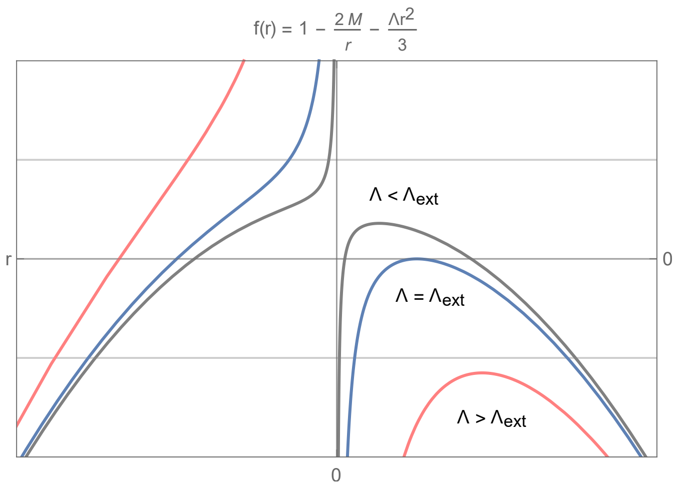

Figure 5.1: Each line represents the qualitative behavior of $f(r)$ for: (gray) non-extreme $\Lambda < \Lambda_{\text{ext}}$, (blue) extreme $\Lambda = \Lambda_{\text{ext}}$ and (red) $\Lambda > \Lambda_{\text{ext}}$.

Considering the non-extreme case, since no component of (5.1) is a function of the time coordinate, ∂_t is a Killing vector field and it is timelike between horizons. Hence, the Schwarzschild-de Sitter is a stationary geometry and we can compute the surface gravity on the horizon, κ_H, and on the cosmological horizon, κ_C. In order to do that, we can generalize the calculations that led to (3.40) so that

$$\kappa_i = \frac{1}{2}\left|\partial_r f(r_i)\right|. \tag{5.10}$$

For latter calculations purposes, it is useful to express $f(r)$ in terms of the position of the horizons [23]:

$$f(r) = \frac{1}{a^2 r}(r_C - r)(r - r_H)(r + r_H + r_C), \qquad a^2 = \frac{3}{\Lambda}. \tag{5.11}$$

Then,

$$f(r) = \frac{1}{a^2 r}[-r^3 + r(r_C^2 + r_H r_C + r_H^2) - r_H r_C (r_H + r_C)], \tag{5.12}$$

from which, comparing with (5.2), we can read the parameters a and M as functions of r_H and r_C :

$$a^2 = r_H^2 + r_H r_C + r_C^2, \qquad 2Ma^2 = r_H r_C (r_H + r_C). \tag{5.13}$$

We can also determine an expression of the surface gravity in terms of r_H and r_C. For that, we use (5.10) in (5.11) in order to find

$$\kappa_i = \frac{1}{2a^2 r_i^2}\big| - 2r_i^3 + r_H r_C (r_H + r_C)\big|. \tag{5.14}$$

The surface gravities on both horizons are given by:

$$\kappa_H = \frac{\big|(r_C - r_H)(2r_H + r_C)\big|}{2a^2 r_H} = \frac{1 - \Lambda r_H^2}{2r_H}, \tag{5.15}$$

$$\kappa_C = \frac{\big|(r_H - r_C)(2r_C + r_H)\big|}{2a^2 r_C} = \frac{\Lambda r_C^2 - 1}{2r_C}. \tag{5.16}$$

The coordinate system we are using to describe the Schwarzschild-de Sitter spacetime does not cover the entire manifold. One possible extension of (5.1) is, again, the tortoise coordinates, defined by $\frac{dr_*}{dr} = \frac{1}{f(r)}$. We could also perform a Eddington-Finskeltein-like transformation, defining the new coordinates $u = t - r_*$ and $v = t + r_*$. However, for a maximal extension of the spacetime, which means all geodesics being defined for all the values of the affine parameter, from $-\infty$ to ∞, unless it ends on a curvature singularity [63], it is necessary to glue together an infinite amount of Schwarzschild-de Sitter spacetimes described in these coordinates. In Figure 5.2 we present the Penrose diagram for the maximally extended Schwarzschild-de Sitter spacetime [23] and below we point out its main features.

∘ Curvature singularities at $r = 0$ are behind the horizon of black and white holes (BH and WH).

∘ The asymptotic structure, is the same one of the de Sitter spacetime, that is, conformal infinities are space-like ($\mathcal{I}^-$ and $\mathcal{I}^+$). Such surfaces are asymptotic boundaries of, respectively, the cosmological past and cosmological future (Cp and Cf).

∘ Regions between horizons (I and II) are causally disconnected.

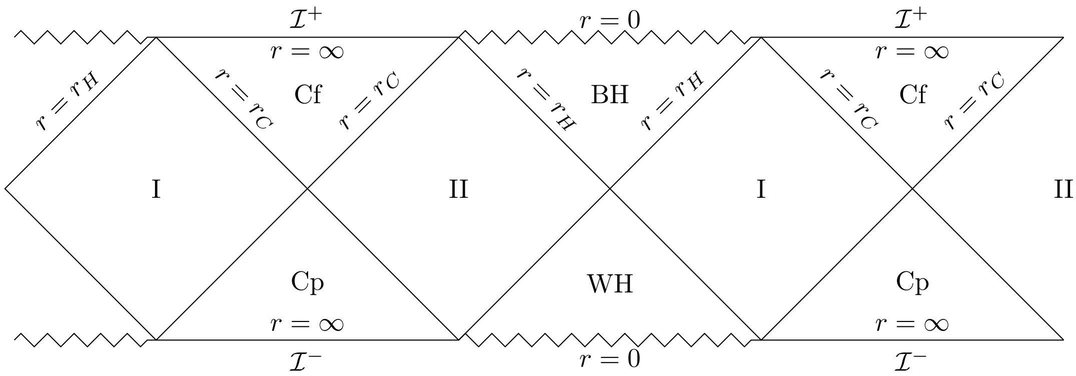

Figure 5.2: Penrose diagram for the maximally extended non-extreme Schwarzschild-de Sitter spacetime.

Despite the Schwarzschild-like coordinates being the most common ones to describe the geometry of the Schwarzschild-de Sitter spacetime, they are not well behaved at the horizons. When we change to Eddington-Finkelstein-like coordinates, it will become clear that at r_H it is located a future horizon due to a black hole or a past horizon due to a white hole. Similarly, the cosmological horizon at r_C can be relative to an expanding or a contracting spacetime. Such distinctions are not clear in the coordinate system we worked so far and it gives rise to ambiguities on the classification of the trapping horizons.

What we going to do, then, is to make use of outgoing and ingoing Eddington-Finkelstein-like coordinates in order to classify some surfaces and hypersurfaces of the Schwarzschild-de Sitter spacetime according to the terminology of trapped surfaces. Each one of the coordinate systems will cover a region in the maximally extended Schwarzschild-de Sitter spacetime and we shall analyse their distinctions and what they physically represent. Then, we will locate the trapping horizons so that we can apply the Hayward black-hole thermodynamics.

We start our analysis with the Schwarzschild-de Sitter spacetime in ingoing Eddington-Finkestein-like coordinates, in which the line element is written in the form

$$ds^2 = -f(r)dv^2 + 2dvdr + r^2(d\theta^2 + \sin^2\theta d\phi^2), \tag{5.17}$$

with $f(r)$ defined as (5.2) and ranges

$$\begin{aligned} -\infty < v < \infty, \qquad & 0 < r < \infty, \\ 0 < \theta < \pi, \qquad & 0 < \phi < 2\pi. \end{aligned} \tag{5.18}$$

We can find the radial null curves setting the line element of (5.17) equal to zero and not allowing any angular variation. Then, we are left with the equation

$$2dvdr = f(r)dv^2, \tag{5.19}$$

which has two solutions: a curve of constant time coordinate v and the solution of the differential equation:

$$\frac{dt}{dr} = \frac{f^{-1}(r)}{2}. \tag{5.20}$$

This gives the ingoing and outgoing null vector fields:

$$n^\mu = -\partial_r, \tag{5.21}$$

$$l^\mu = \partial_v + \frac{1}{2}\left(1 - \frac{2M}{r} - \frac{\Lambda}{3}r^2\right)\partial_r. \tag{5.22}$$

These vector fields are also generators of geodesics and satisfy $l^\mu n_\mu = -1$. They can be used to find the cross-sectional metric tensor $h_{\mu\nu}$ on the surface orthogonal to both l^μ and n^μ (A.4). The line element obtained for $h_{\mu\nu}$ is

$$ds^2 = r^2 d\theta^2 + r^2 \sin^2\theta d\phi^2, \tag{5.23}$$

which, as expected, characterizes a 2-sphere and has an area element equal to $r^2 \sin\theta$.

Then, we can use calculate the expansion scalars in outgoing and ingoing directions via (A.13):

$$\theta_l = \frac{1}{r}\left(1 - \frac{2M}{r} - \frac{\Lambda}{3}r^2\right) = \frac{1}{r}f(r), \tag{5.24}$$

$$\theta_n = -\frac{2}{r}, \tag{5.25}$$

from where we see that θ_n is always negative and θ_l is positive between horizons and negative otherwise. And in order to classify the trapping horizons, we also calculate the rate of change of θ_l along n^μ:

$$\mathcal{L}_n\theta_l = \frac{1}{r^2}f(r) - \frac{1}{r}\left(\frac{2M}{r^2} - \frac{2\Lambda}{3}r\right). \tag{5.26}$$

And evaluating at a marginal surface characterized by $\theta_l = 0$:

$$\mathcal{L}_n\theta_l\big|_{\theta_l=0} = -\left[\frac{2}{r^3}\left(M - \frac{\Lambda}{3}r^3\right)\right]_{\theta_l=0}. \tag{5.27}$$

However

$$\theta_l = 0 \implies f(r) = 0 \implies -\frac{\Lambda r^3}{3} = 2M - r, \tag{5.28}$$

which can be used to write the previous expression as

$$\mathcal{L}_n\theta_l\Big|_{\theta_l=0} = -\left[\frac{2}{r^3}(3M-r)\right]_{\theta_l=0}. \tag{5.29}$$

Due to (5.9), we conclude that

$$\mathcal{L}_n\theta_l\Big|_{r_H} < 0, \tag{5.30}$$

$$\mathcal{L}_n\theta_l\Big|_{r_C} > 0. \tag{5.31}$$

In what follows, we have the classification of surfaces for the non-extreme Schwarzschild-de Sitter spacetime according to the terminology of trapped surfaces and trapping horizons. In Figure 5.3 it is presented the maximally extended non-extreme Schwarzschild-de Sitter spacetime, where it is highlighted in blue the region covered by the ingoing Eddington-Finkelstein-like coordinates. It gives a helpful way to visualize the surfaces that we are going to discuss and also the behavior of the ingoing and outgoing radial null vector fields. Important features are:

∘ For a fixed time coordinate v, any 2-sphere of radius between $0 < r < r_H$ or $r_C < r < \infty$ is a future trapped surface.

∘ For a fixed time coordinate v, the 2-spheres of radius r_H and r_C are marginally future trapped surfaces.

∘ The union of all marginally future trapped surfaces, that is, for all time v, are marginally future trapped tubes: $\cup_v r_H$ and $\cup_v r_C$.

∘ The marginally trapped tube at r_H is a future outer trapping horizon, which is in agreement to our previous statement that a future outer trapping horizon is typical of black holes. The marginally trapped tube at r_C is a future inner trapping horizon. And as we know, this hypersurface is the cosmological horizon of a contracting spacetime.

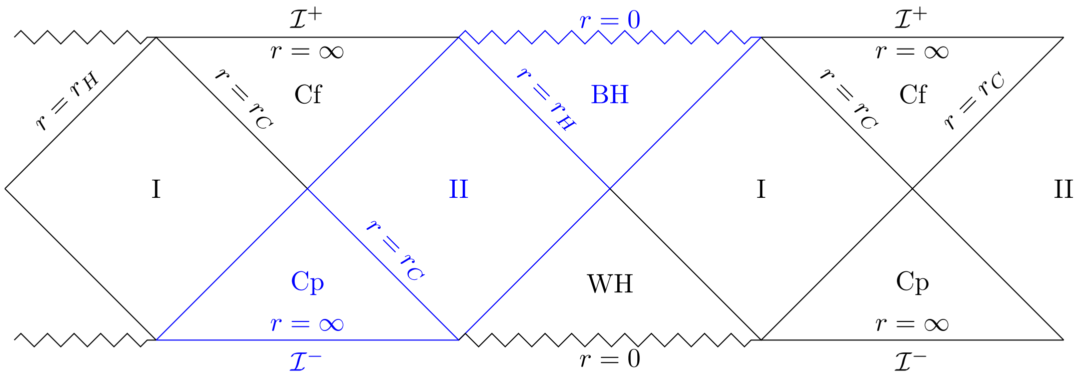

Figure 5.3: The region highlighted in blue on the Penrose diagram for the maximally extended non-extreme Schwarzschild-de Sitter spacetime represents the submanifold covered by the ingoing Eddington-Finkelstein-like coordinates.

Now we are going to work with the non-extreme Schwarzschild-de Sitter spacetime in outgoing Eddington-Finkestein-like coordinates. Our approach is the same as it was done for the ingoing coordinates. For this reason, we will be more direct in our treatment since most ideas remain the same. In the outgoing coordinates, the metric tensor reads

$$ds^2 = -f(r)du^2 - 2dudr + r^2(d\theta^2 + \sin^2\theta d\phi^2). \tag{5.32}$$

In order to characterize the causal structure for this spacetime through trapped surfaces, first we write the outgoing and ingoing radial null vector fields:

$$l^\mu = \partial_r, \tag{5.33}$$

$$n^\mu = \partial_u - \frac{1}{2}\left(1 - \frac{2M(u)}{r} - \frac{\Lambda}{3}r^2\right)\partial_r, \tag{5.34}$$

which satisfy $l^\mu n_\mu = -1$ and are geodesic generators.

The metric tensor defined for the cross sectional surface is again that of a 2-sphere (5.23). The expansion scalars can then be calculated:

$$\theta_l = \frac{2}{r}, \tag{5.35}$$

$$\theta_n = -\frac{1}{r}\left(1 - \frac{2M(u)}{r} - \frac{\Lambda}{3}r^2\right) = -\frac{1}{r}f(r). \tag{5.36}$$

We will also need the Lie derivative of θ_n in the outgoing direction:

$$\mathcal{L}_l\theta_n\big|_{\theta_n=0} = -\left[\frac{2}{r^3}(3M - r)\right]_{\theta_n=0}. \tag{5.37}$$

Similarly to what was previously done, we present the classification of surfaces of this patch of the Schwarzschild-de Sitter spacetime according to the terminology of trapped surfaces and trapping horizons (Figure 5.4 highlights in red the region covered by the outgoing Eddington-Finkelstein-like coordinates in the maximally extended spacetime):

∘ For a fixed time coordinate u, any 2-sphere of radius between $0 < r < r_H$ or $r_C < r < \infty$ is an past trapped surface.

∘ For a fixed time coordinate u, the 2-spheres of radius r_H and r_C are marginally past trapped surfaces.

∘ The union of all marginally past trapped surfaces, that is, for all time u, are marginally past trapped tubes: $\cup_u r_H$ and $\cup_u r_C$.

∘ The marginally trapped tube at r_H is a past outer trapping horizon, which agrees to our assertion that a past outer trapping horizon is typical of white holes. The marginally trapped tube at r_C is a past inner trapping horizon. This is the cosmological horizon of an expanding cosmology.

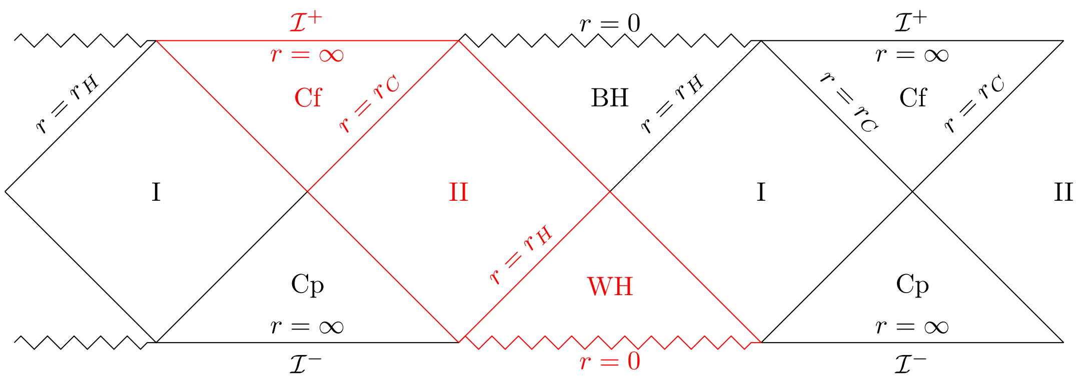

Figure 5.4: The region highlighted in red on the Penrose diagram for the maximally extended non-extreme Schwarzschild-de Sitter spacetime represents the submanifold covered by the outgoing Eddington-Finkelstein-like coordinates.

5.2 Thermodynamics of Schwarzschild-de Sitter

In this section Hayward thermodynamics is applied to the Schwarzschild-de Sitter spacetime. The study will always start with the ingoing Eddington-Finkelstein-like coordinates and, then, be finished with the outgoing ones. The goal is to calculate and analyse the relevant thermodynamic quantities.

5.2.1 Misner-Sharp mass

The Misner-Sharp mass for Schwarzschild-de Sitter evaluated at a fixed radius is given by (4.60):

$$\begin{aligned} M_{\mathrm{MS}}^{\mathrm{SdS}} = \frac{r}{2}(1 - g^{\mu\nu}\partial_\nu r \partial_\mu r) = \frac{r}{2}(1 - g^{rr}) = \frac{r}{2}\left[1 - \left(1 - \frac{2M}{r} - \frac{\Lambda}{3}r^2\right)\right] \\ = M + \frac{\Lambda}{6}r^3. \end{aligned} \tag{5.38}$$

It is noticed that the Misner-Sharp mass for this spacetime is the sum of a term due to the energy of the central spherical object and a term associated to the cosmological constant. These are also, respectively, the Misner-Sharp masses for the Schwarzschild and de Sitter spacetimes. In order to physically understand the contribution that comes from Λ, we analyse the acceleration of a static observer in the static region. First, we recall that in Schwarzschild a static observer has a velocity and an acceleration of (working in Schwarzschild-like coordinates), respectively,

$$U_{\mathrm{S}}^{\mu} = \frac{(\partial_t)^\mu}{\sqrt{1 - \frac{2M}{r}}}, \qquad a_{\mathrm{S}}^{\nu} \equiv U_{\mathrm{S}}^{\mu} \nabla_\mu U_{\mathrm{S}}^{\nu} = \frac{M}{r^2\left(1 - \frac{2M}{r}\right)}(\partial_r)^\nu. \tag{5.39}$$

Similarly, in de Sitter the velocity and the acceleration of the static observer are

$$U_{\mathrm{dS}}^{\mu} = \frac{(\partial_t)^\mu}{\sqrt{1 - \frac{\Lambda r^2}{3}}}, \qquad a_{\mathrm{dS}}^{\mu} = -\frac{\Lambda r}{3\left(1 - \frac{\Lambda r^2}{3}\right)}(\partial_r)^\mu. \tag{5.40}$$

The acceleration can be written in terms of the Misner-Sharp energy in de Sitter, $M_{\mathrm{MS}}^{\mathrm{dS}}$, as

$$a_{\mathrm{dS}}^{\mu} = -\frac{2M_{\mathrm{MS}}^{\mathrm{dS}}}{r^2\left(1 - \frac{2M_{\mathrm{MS}}^{\mathrm{dS}}}{r}\right)}(\partial_r)^\mu. \tag{5.41}$$

Then, it is in a similar form to the acceleration of the static observer in Schwarzschild.

However, there are still two differences between (5.41) and (5.39). The first one is the minus sign which is present in de Sitter as the cosmological constant has a negative pressure and acts to expand the spacetime. The second one is that the absolute value of the acceleration is twice bigger the one which would be felt by a static observer at a fixed radius r in a Schwarzschild spacetime that has a mass parameter equal to the Misner-Sharp mass of de Sitter evaluated at the same r. This result is explained due to the fact that each observer experiences the other one accelerating away as the spacetime expands. So, in order to account for both effects, it is reasonable that a static observer must maintain an acceleration two times bigger.

5.2.2 Work-density and energy-flux

For the purpose of obtaining the quantities associated to the energy-momentum tensor, we will need the components of the Einstein tensor, which are zero with exception of

$$G_{vv} = \Lambda\left(1 - \frac{2M}{r} - \frac{\Lambda}{3}r^2\right) = \Lambda f(r), \tag{5.42}$$

$$G_{vr} = G_{rv} = -\Lambda, \tag{5.43}$$

$$G_{\theta\theta} = -\Lambda r^2, \tag{5.44}$$

$$G_{\phi\phi} = -\Lambda r^2 \sin^2\theta. \tag{5.45}$$

The work-density scalar can be calculated from (4.80):

$$w = -\frac{1}{2}h^{ab}\frac{G_{ab}}{8\pi} = -\frac{1}{16\pi}(h^{vv}G_{vv} + 2h^{vr}G_{vr} + h^{rr}G_{rr}) = -\frac{1}{8\pi}h^{vr}G_{vr} = \frac{\Lambda}{8\pi}, \tag{5.46}$$

and the energy-flux vector field from (4.79):

$$\begin{aligned}\psi_\mu = \frac{G_{\mu\nu}}{8\pi}g^{\nu\rho}\partial_\rho r + w\partial_\mu r = \frac{G_{\mu\nu}}{8\pi}g^{\nu r} + w\partial_\mu r &= \frac{G_{\mu v}}{8\pi}g^{vr} + \frac{G_{\mu r}}{8\pi}g^{rr} + w\partial_\mu r \\ &= \frac{G_{\mu v}}{8\pi} + \frac{G_{\mu r}}{8\pi}f(r) + w\partial_\mu r.\end{aligned} \tag{5.47}$$

The angular components of the energy-flux vector are zero. It turns out that the other two components also vanish:

$$\psi_t = \frac{\Lambda}{8\pi}f(r) - \frac{\Lambda}{8\pi}f(r) = 0, \tag{5.48}$$

$$\psi_r = -\frac{\Lambda}{8\pi} + \frac{\Lambda}{8\pi} = 0. \tag{5.49}$$

Before we proceed, it is worth considering the physical interpretation of the previous results. We have found that in the Schwarzschild-de Sitter there is no energy flux, which is expected for a static spacetime. For the work-density scalar, it can be used in order to write (5.38) as

$$M_{\text{MS}}^{\text{SdS}} = M + \frac{4\pi r^3}{3}w, \tag{5.50}$$

which supports the physical interpretation of w as an energy density quantity. Furthermore, the cosmological constant is responsible for the expansion of the spacetime. Then, it is natural for it to be interpreted as a work quantity.

In the outgoing Eddington-Finkelstein-like coordinates, we need the new components of the Einstein tensor. They are equal to those ones from ingoing coordinates, with the exception of G_{ur} and G_{ru}:

$$G_{uu} = \Lambda\left(1 - \frac{2M}{r} - \frac{\Lambda}{3}r^2\right) = \Lambda f(r), \tag{5.51}$$

$$G_{ur} = G_{ru} = \Lambda, \tag{5.52}$$

$$G_{\theta\theta} = -\Lambda r^2, \tag{5.53}$$

$$G_{\phi\phi} = -\Lambda r^2 \sin^2\theta. \tag{5.54}$$

Because the components h_{ur} and h_{ru} of the metric in the outgoing coordinates also have a reverse sign with respect to h_{vr} and h_{rv}, it can be checked that the calculations we have previously made for the quantities associated to the energy-momentum tensor give the same results.

5.2.3 Temperature and entropy

In order to define the temperature at the trapping horizons, our first task is to calculate the geometric surface gravity from (4.55):

$$\kappa_G = \frac{1}{2\sqrt{h}}\partial_a(\sqrt{h}h^{ab}\partial_b r) = \frac{1}{2}\partial_r h^{rr} = \frac{1}{2}\partial_r\left(1 - \frac{2M}{r} - \frac{\Lambda}{3}r^2\right) = \frac{1}{2}\partial_r f(r), \tag{5.55}$$

where h_{ab} is the metric in the 2-dimensional effective surface as defined in (4.36). As expected, the result coincides with the usual surface gravity (up to a sign), which is given by (5.10). Therefore, the geometric surface gravity on the future outer trapping horizon is positive and equal to (5.15). And for the future inner trapping horizon the geometric surface gravity is negative and equal to minus (5.16). Because for a future trapping horizon the temperature is $\frac{\kappa_G}{2\pi}$, we have that a physically reasonable temperature can be associated to the future outer trapping horizon:

$$\text{Temperature for the future outer trapping horizon} = \frac{1 - \Lambda r_H^2}{4\pi r_H}. \tag{5.56}$$

The temperature associated to this trapping horizon is clearly constant, which is in accordance with the Zeroth Law of black hole thermodynamics.

Given a temperature for the future outer trapping horizon, we can also associate an entropy to the black hole as one fourth of its surface area:

$$\text{Entropy for the future outer trapping horizon} = \pi r_H^2. \tag{5.57}$$

Classically, this is a non-decreasing entropy as it should be (we recall that if we take into account the Hawking Radiation, then it is the generalized entropy that is non-decreasing).

Actually, the entropy is constant as it is expected from what says the Hayward Second Law for a null trapping horizon.

We, then, turn our attentions to the outgoing Eddington-Finkelstein-like coordinates. We give only a summary of the results since the calculations are a lot similar to the ones in ingoing coordinates. First, it is straightforward to find that the geometric surface gravity is again given by (5.55). Therefore, the geometric surface gravity on the past outer trapping horizon is positive and equal to (5.15). And for the past inner trapping horizon the geometric surface gravity is negative and equal to minus (5.16). As for a past trapping horizon the temperature is $-\frac{\kappa_G}{2\pi}$, we can associate a meaningful temperature to the latter hypersurface:

$$\text{Temperature for the past inner trapping horizon} = \frac{\Lambda r_C^2 - 1}{4\pi r_C}. \tag{5.58}$$

And given a temperature for the past inner trapping horizon, we can also associate an entropy to the cosmological horizon as one fourth of its surface area:

$$\text{Entropy for the past inner trapping horizon} = \pi r_C^2. \tag{5.59}$$

5.3 The Vaidya-de Sitter spacetime

As the Vaidya spacetime generalizes Schwarzschild for a dynamical spherical object, the **Vaidya-de Sitter spacetime** is an analogous generalization of Schwarzschild-de Sitter. Its discovery is due to R. Mallet in 1985 [42]. In his paper, the line element for the Vaidya-de Sitter geometry was written in Schwarzschild-like coordinates as

$$ds^2 = \frac{\dot{M}^2}{M'^2}\frac{1}{g(t,r)}dt^2 - \frac{1}{g(t,r)}dr^2 + r^2(d\theta^2 + \sin^2 d\phi^2), \tag{5.60}$$

where

$$g(t,r) \equiv 1 - \frac{2M(t,r)}{r} - \frac{\Lambda r^2}{3}, \tag{5.61}$$

$M(t,r)$ being interpreted as the mass of the spherical object and Λ a positive cosmological constant. The dot $(\cdot)$ and the apostrophe $(')$ above M mean, respectively, the derivatives with respect to the time and the radius coordinates. And the ranges taken for the coordinates are

$$\begin{gathered} 0 < \theta < \pi, \qquad 0 < \phi < 2\pi, \\ \text{for } t \text{ and } r\text{, it depends on the roots of } g(t,r). \end{gathered} \tag{5.62}$$

Since the Vaidya-de Sitter is a dynamical geometry, there is no timelike Killing vector field and, therefore, the usual surface gravity cannot be defined. For this reason, in order to analyse the thermodynamics of this geometry, the Bekenstein-Hawking theory is not suitable. On the other hand, (5.60) gives a relevant example of a spacetime where Hayward's work is useful and the study of the thermodynamics of the trapping horizons on Vaidya-de Sitter is the topic of study in the next section.

Despite being the first coordinate system used to describe the Vaidya-de Sitter spacetime, the Schwarzschild-like coordinates are not the ones in which this geometry is usually presented in the literature. The most common ones are the Eddington-Finkelstein-like coordinates and, as it will be seen, the physical interpretation for this spacetime is a lot clearer in the latter coordinates. Moreover, following the same approach done for Schwarzschild-de Sitter, before considering the thermodynamics, we must locate the trapping horizons, which will be covered in these coordinates.

After R. Mallet's discovery of the Vaidya-de Sitter geometry, in the same year D. Vick presented this metric in outgoing Eddington-Finkelstein-like coordinates [60]:

$$ds^2 = -f(u,r)du^2 - 2dudr + r^2(d\theta^2 + \sin^2\theta d\phi^2), \tag{5.63}$$

where

$$f(u,r) = 1 - \frac{2M(u)}{r} - \frac{\Lambda r^2}{3}, \tag{5.64}$$

with ranges

$$\begin{aligned} -\infty < u < \infty, \qquad & 0 < r < \infty, \\ 0 < \theta < \pi, \qquad & 0 < \phi < 2\pi. \end{aligned} \tag{5.65}$$

The energy-momentum tensor for the Vaidya-de Sitter spacetime in outgoing Eddington-Finkelstein-like coordinates coincides with the one for Vaidya in the same coordinates [37], that is,

$$T^{\mu\nu} = -\frac{1}{4\pi r^2}\frac{dM(u)}{du}(\partial_r)^\mu(\partial_r)^\nu, \tag{5.66}$$

which leads to an equivalent physical interpretation we have already discussed in details in Section 3.4. That is, the line element (5.63) represents a spherically symmetric object, immersed in a de Sitter universe, losing its mass due to the radiation of light-speed particles of radial trajectory.

The causal structure of this spacetime depends on the zeros of the function $f(u,r)$. However, differently from the Schwarzschild-de Sitter spacetime, the mass parameter is now a function of the time coordinate u. As a consequence, it may happen that the mass of the spherical object reaches a specific value such that the spacetime has its causal structure changed. Therefore, in order to study the different situations, it makes more sense now to define an extreme mass parameter

$$M_{\text{ext}} \equiv \frac{1}{3\sqrt{\Lambda}} \tag{5.67}$$

and analyse each case for a given value of the cosmological constant Λ.

∘ $0 < M(u) < M_{\text{ext}}$: the function $f(u,r)$ has two positive roots $r_H(u)$ and $r_C(u)$, defined such that $r_H(u) < r_C(u)$, and a negative root $r_-(u) = -\big[r_H(u)+r_C(u)\big]$. This is the case of non-extreme Vaidya-de Sitter spacetime, where there is a radiating spherical object with with a horizon at $r_H(u)$ immersed in a de Sitter universe with a cosmological horizon at $r(u) = r_C(u)$. We have the following relation for the horizons:

$$2M(u) < r_H(u) < 3M(u) < r_C(u) \qquad \text{for the non-extreme case.} \tag{5.68}$$

Unless otherwise stated, this is the situation considered when we refer to the Vaidya-de Sitter spacetime in outgoing Eddington-Finkelstein-like coordinates.

∘ $M(u) = M_{\text{ext}}$: the function $f(u,r)$ has only one positive root and the horizons coincide at the same radius. This is the extreme case.

∘ $M(u) > M_{\text{ext}}$: no positive root for $f(u,r)$. There is a naked singularity.

In order to study this spacetime through the terminology of trapped surfaces, we follow the same approach done for Schwarzschild-de Sitter. First, we need the outgoing and ingoing null vector fields:

$$l^\mu = \partial_r, \tag{5.69}$$

$$n^\mu = \partial_u - \frac{1}{2}\left(1 - \frac{2M(u)}{r} - \frac{\Lambda}{3}r^2\right)\partial_r, \tag{5.70}$$

which satisfy $l^\mu n_\mu = -1$ and are generators of radial geodesics.

Again and as expected from the spherical symmetry, the cross-sectional metric on the surface ortoghonal to l^μ and n^μ is the one of a 2-sphere (5.23). The expansion scalars in outgoing and ingoing directions can, then, be calculated via (A.13):

$$\theta_l = \frac{2}{r}, \tag{5.71}$$

$$\theta_n = -\frac{1}{r}\left(1 - \frac{2M(u)}{r} - \frac{\Lambda}{3}r^2\right) = -\frac{1}{r}f(u,r). \tag{5.72}$$

In order to classify the trapping horizons, we must also calculate the derivative of θ_n in the outgoing direction and evaluate it on the hypersurface of vanishing θ_n. Since this is a generalization of the calculation from Section 5.1, we just present the result:

$$\mathcal{L}_l\theta_n\big|_{\theta_n=0} = -\left[\frac{2}{r^3}\left[3M(u) - r\right]\right]_{\theta_n=0}. \tag{5.73}$$

Then, we have the following classification for the surfaces and hypersurfaces of our interest:

∘ For a fixed time coordinate u, any 2-sphere of radius between $0 < r(u) < r_H(u)$ or $r_C(u) < r(u) < \infty$ is a past trapped surface.

∘ For a fixed time coordinate u, the 2-spheres of radius $r_H(u)$ and $r_C(u)$ are marginally past trapped surfaces.

∘ The union of all marginally past trapped surfaces, that is, for all time u, are marginally past trapped tubes: $\cup_u r_H(u)$ and $\cup_u r_C(u)$.

∘ The marginally trapped tube at $r_H(u)$, due to the presence of a radiating white hole, is a past outer trapping horizon. The marginally trapped tube at $r_C(u)$ is a past inner trapping horizon. This is defined as the cosmological horizon due to the expanding spacetime.

Now we change our attentions to the Vaidya-de Sitter spacetime in ingoing Eddington-Finkestein-like coordinates, which line element is written as

$$ds^2 = -f(v,r)dv^2 + 2dvdr + r^2(d\theta^2 + \sin^2\theta d\phi^2), \tag{5.74}$$

with

$$f(v,r) \equiv 1 - \frac{2M(v)}{r} - \frac{\Lambda}{3}r, \tag{5.75}$$

and ranges

$$\begin{aligned} -\infty < v < \infty, \qquad & 0 < r < \infty, \\ 0 < \theta < \pi, \qquad & 0 < \phi < 2\pi. \end{aligned} \tag{5.76}$$

The energy-momentum tensor for the Vaidya-de Sitter spacetime in ingoing Eddington-Finkelstein-like coordinates also coincides with the one for Vaidya in these coordinates:

$$T^{\mu\nu} = \frac{1}{4\pi r^2}\frac{dM(v)}{dv}(\partial_r)^\mu(\partial_r)^\nu, \tag{5.77}$$

leading to the same physical interpretation discussed in details in Section 3.4, that is, the metric (5.74) represents a spherically symmetric object, immersed in a de Sitter universe, increasing its mass due to the accretion of light-speed particles of radial trajectory.

As we know, the causal structure of this spacetime depends on the zeros of the function $f(v,r)$. Since this is only a replacement of the previous time coordinate u for the new time coordinate v, we have the same situations previoulsy described. That is, the non-extreme case $0 < M(v) < M_{\text{ext}}$, the extreme case $M(v) = M_{\text{ext}}$ and the case in which $M(v) > M_{\text{ext}}$. The difference here, however, is that at $r_H(v)$ is the horizon of an accreting spherical object.

Since the process to find the trapping horizons and to classify other surfaces according to the terminology of trapped surfaces was done many times by now, we are going to be more straightforward this time.

The outgoing and ingoing radial null vector fields are

$$l^\mu = \partial_v + \frac{1}{2}\left(1 - \frac{2M(v)}{r} - \frac{\Lambda}{3}r^2\right)\partial_r, \tag{5.78}$$

$$n^\mu = -\partial_r, \tag{5.79}$$

which give the expansions:

$$\theta_l = \frac{1}{r}\left(1 - \frac{2M(v)}{r} - \frac{\Lambda}{3}r^2\right) = \frac{1}{r}f(v,r), \tag{5.80}$$

$$\theta_n = -\frac{2}{r}, \tag{5.81}$$

and the rate of change of θ_n along l on the trapping horizon of vanishing θ_l is

$$\mathcal{L}_n\theta_l\Big|_{\theta_l=0} = -\left[\frac{2}{r^3}\left[3M(v) - r\right]\right]_{\theta_l=0}. \tag{5.82}$$

Some features of the Vaidya-de Sitter geometry are presented in the following:

◦ For a fixed time coordinate v, any 2-sphere of radius between $0 < r(v) < r_H(v)$ or $r_C(v) < r(v) < \infty$ is a future trapped surface.

◦ For a fixed time coordinate v, the 2-spheres of radius $r_H(v)$ and $r_C(v)$ are marginally future trapped surfaces.

◦ The union of all marginally future trapped surfaces, that is, for all time v, are marginally future trapped tubes: $\cup_v r_H(v)$ and $\cup_v r_C(v)$.

◦ The marginally trapped tube at $r_H(v)$, due to the presence of an accreting black hole, is a future outer trapping horizon. The marginally trapped tube at $r_C(v)$ is a future inner trapping horizon. This is the cosmological horizon due to the contracting spacetime.

5.4 Thermodynamics of Vaidya-de Sitter

In the previous section, we have presented the trapped surfaces for the Vaidya-de Sitter spacetime and have also located the trapping horizons. Now, we study the thermodynamics on the future outer and past inner trapping horizons. As we will work with a general mass parameter function, this spacetime is not under the Bekenstein-Hawking theory applicability and, therefore, it opens the way for the Hayward black-hole thermodynamics. Furthermore, a realistic black hole may undergo a strong accretion process or quickly radiate away before vanishing in the final period of its lifetime. Both of these processes, for instance, could be expected to be too dynamical such that they cannot be considered quasi-stationary and, hence, Hayward's work presents itself as a viable alternative in order to study the thermodynamics of these systems.

Table 5.1

	Vaidya-de Sitter Thermodynamics	
	Ingoing coordinates	**Outgoing coordinates**
Metric tensor	$ds^2 = -f(v,r) + 2dvdr + r^2 d\Omega^2$	$ds^2 = -f(u,r) - 2dudr + r^2 d\Omega^2$
Einstein tensor $G_{\mu\nu}$ (non-zero components)	$G_{vv} = \Lambda f(v,r) + \frac{2}{r^2}\frac{dM(v)}{dv}$ $G_{vr} = G_{rv} = -\Lambda$ $G_{\theta\theta} = -\Lambda r^2$ $G_{\phi\phi} = -\Lambda r^2 \sin^2\theta$	$G_{uu} = \Lambda f(u,r) - \frac{2}{r^2}\frac{dM(u)}{du}$ $G_{ur} = G_{ru} = \Lambda$ $G_{\theta\theta} = -\Lambda r^2$ $G_{\phi\phi} = -\Lambda r^2 \sin^2\theta$
Work-density scalar w	$\frac{\Lambda}{8\pi}$	$\frac{\Lambda}{8\pi}$
Energy-flux covector ψ_μ (non-zero components)	$\psi_v = \frac{1}{4\pi r^2}\partial_v M(v)$	$\psi_u = \frac{1}{4\pi r^2}\partial_u M(u)$
Misner-Sharp mass M_{MS}	$M(v) + \frac{\Lambda r^3}{6}$	$M(u) + \frac{\Lambda r^3}{6}$
Geometric surface gravity κ_G	at a trapping horizon $\frac{M(v)}{r_i^2(v)} - \frac{\Lambda r_i(v)}{3}$	at a trapping horizon $\frac{M(u)}{r_i^2(u)} - \frac{\Lambda r_i(u)}{3}$
Temperature	at the future outer trapping horizon $\frac{M(v)}{2\pi r_H^2(v)} - \frac{\Lambda r_H(v)}{6\pi} = \frac{1-\Lambda r_H^2(v)}{4\pi r_H(v)}$	at the inner past trapping horizon $-\frac{M(u)}{2\pi r_C^2(u)} + \frac{\Lambda r_C(u)}{6\pi} = \frac{\Lambda r_C^2(u)-1}{4\pi r_C(u)}$
Entropy	at the future outer trapping horizon $\pi r_H^2(v)$	at the inner past trapping horizon $\pi r_C^2(u)$

All the relevant quantities for Hayward's theory are presented in advance in Table 5.1 and, in the subsections that follow, important results are derived for the thermodynamics of the Vaidya-de Sitter spacetime. The calculations that lead to the values that appear in Table 5.1 can be found in Appendix C, where we work with a even more general situation since the whole f function that appears in the Eddington-Finkelstein-like coordinates is considered arbitrary.

5.4.1 Misner-Sharp mass, work-density and energy-flux

From Table 5.1, we see that the work-density scalar, as it was the case for the Schwarzschild-de Sitter spacetime, is essentially the cosmological constant. This result corroborates with the physical interpretation given to this quantity (4.80) since it is the cosmological constant which is responsible for the expansion of the spacetime.

Moreover, the energy-flux vector field is no longer zero for the Vaidya-de Sitter geometry as it was for its static configuration. In both coordinate systems, the time-component for the energy-flux at a position r is the rate of change of the mass parameter with respect to the time coordinate over the area of a 2-sphere of radius r. This is a expected result for a flux of energy in a spacetime in which the dynamics is dictated by how the mass of a spherical object changes in time. Furthermore, accordingly to what was presented in Section 3.4, by the null energy condition

$$\frac{\partial M(v)}{\partial v} \geq 0, \tag{5.83}$$

$$\frac{\partial M(u)}{\partial u} \leq 0. \tag{5.84}$$

And, therefore, a positive energy-flux refers to energy entering the black hole, while a negative energy-flux refers to energy leaving the white hole.

5.4.2 Temperature

In this section we analyse the temperature on the future outer and past inner trapping horizons as well as some of their most interesting features. We notice from Table 5.1 that the geometric surface gravity assumes the same form for all kinds of horizons, not only on those where a temperature is defined, and for both coordinate systems. On the other hand, the temperature on the inner past trapping horizon has an opposite sign with respect to the one from the future trapping horizon. As already discussed, this is due to the fact that the geometric surface gravity is negative in the former horizon.

When S. Hayward published his generalized laws of black-hole mechanics in the 1990s [28, 30], he highlighted that at the time there was no proof of a connection between the geometric surface gravity and a temperature emitted from the trapping horizon. As commented in the introduction of the this chapter, this missing connection would be solved latter applying a method for deriving the Hawking Radiation as a tunneling phenomenon developed by M. Parikh and F. Wilczek in 2000 [45]. From this method, S. Hayward *et al.* showed in 2009 that the particle production by a dynamical black hole takes a thermal spectrum for a temperature of $\frac{\kappa_G(r_H)}{2\pi}$ at the future outer trapping horizon [32]. However, according to this work, the actual temperature that is measured by observers following integral curves generated by the Kodama vector field is actually

$$T = \frac{\kappa_G(r_H)}{2\pi\sqrt{1 - \frac{2M(v)}{r}}}, \tag{5.85}$$

at first order near the horizon. When $r \to 2M(v)$, that is, for an observer as near as possible from the trapping horizon, the temperate measured diverges and, then, S. Hayward *et al.* argued that we can interpret $\frac{\kappa_G(r_H)}{2\pi}$ as a renormalized temperature which is finite as $r \to 2M(v)$.

For the Schwarzschild black hole, (5.85) agrees to what was already derived for the Hawking Radiation. The square root on the denominator is a red-shift correction for an observer that is not located infinitely far away from the horizon and, although for a dynamic black hole this term appears for the same reason, in [32] is not clear whether an observer at infinity would measure a temperature of $\frac{\kappa_G(r_H)}{2\pi}$.

Until here we have talked about the temperature defined on the future outer trapping horizon. Then, it is left to give the physical interpretation for the temperature defined for the past inner trapping horizons. If we consider the de Sitter space only, Hayward thermodynamics coincides with the Bekenstein-Hawking approach and, therefore, the temperature $\frac{\kappa_G(r_C)}{2\pi}$ is measured by an observer moving along a timelike geodesic as derived by G. Gibbons and S. Hawking in 1976 [22].

The semi-classical derivation for the temperature for a dynamic black hole in a de Sitter cosmology follows the work of M. Parikh and F. Wilczek [38]. However, the physical interpretation in terms of what is measured by observers is not discussed in this paper.

An interesting feature is that the temperature of the future outer trapping horizon is always bigger than that of the past inner one. In order to show this, we recall that the position of the cosmological horizon can be written with respect to r_H via (5.13)

$$r_C^2 + r_H r_C + r_H^2 - a^2 = 0, \qquad a^2 = \frac{3}{\Lambda}, \tag{5.86}$$

giving

$$r_C = \frac{-r_H + \sqrt{4a^2 - 3r_H^2}}{2}. \tag{5.87}$$

Then, we evaluate the difference between the temperatures of the horizons, which can be found in Table 5.1:

$$\frac{1-\Lambda r_H^2}{2r_H} - \frac{\Lambda r_C^2 - 1}{2r_C}, \tag{5.88}$$

making use of (5.87). It is found that the function (5.88) is always positive for any value of r_H between zero and $\sqrt{\frac{3}{\Lambda}}$. Nonetheless, because the physical value for the position of the future outer trapping horizon, r_H, is actually between zero and $\frac{1}{\sqrt{\Lambda}}$, we conclude that the temperature on the trapping horizon due to the black hole is indeed always bigger than the one of the cosmological horizon. There is, however, a situation where the temperatures tend to coincide and that happens when $r_H \to r_C$, which is approaching to the extreme Schwarzschild-de Sitter spacetime. This represents an almost thermal equilibrium situation and it is further investigated in Subsection 5.4.5.

5.4.3 Entropy

After discussing the temperatures, we change our attentions to the entropy of each trapping horizon, which, as it is presented in Table 5.1, is one fourth of the area of the respective horizon. Since the Hayward Second Law of black-hole mechanics is the only one which we have not presented the formal and general proof of it, in what follows, we prove that it indeed holds for the Vaidya-de Sitter spacetime.

A necessary condition for a horizon at some radius r_i, where r_i stands for r_H or r_C, is

$$f(M) = 1 - \frac{2M}{r_i} - \frac{\Lambda r_i^2}{3} = 0. \tag{5.89}$$

Since this is true for any value of the mass parameter M, which may change in time, $\frac{\partial f}{\partial M} = 0$. We must be careful taking this derivative since the position of the horizon is also a function M. But, from these two expressions, we find

$$\frac{\partial r_i}{\partial M} = \frac{r_i}{3M - r_i}. \tag{5.90}$$

Furthermore, we recall that the positions for the horizons satisfy

$$2M < r_H < 3M < r_C \tag{5.91}$$

and if the null energy condition holds then $M(v)$ never decreases and $M(u)$ never increases (5.83 - 5.84). Therefore, from (5.90) the area for the future outer trapping horizon can only increase, while the area for the past inner trapping horizon can only decrease. This is in accordance with the Second Law of the Hayward black-hole mechanics presented in Subsection 4.3.6. However, we recall that this is a law for the black-hole mechanics and in the thermodynamics, when the semi-classical treatment is fundamental, it is the generalized entropy that is non-decreasing.

5.4.4 Heat capacity and no phase transition

All quantities relevant for the Hayward black-hole thermodynamics have already been discussed for the Vaidya-de Sitter spacetime. Also, all three of Hayward's laws were checked for this geometry. In the rest of this chapter, we shall present two interesting behaviors for the horizons as the mass parameter varies. The first one is that, given some assumptions about how M changes in time, we can show that no phase transition will occur during the process. The second one is that a connection between the thermodynamics and the Hawking radiation can be proposed analysing the total entropy and total energy for this spacetime.

By a (first order) phase transitions, we will be considering a divergence in the heat capacity, which measures the rate of change of the internal energy of the system with respect to its temperature. In the Vaidya-de Sitter spacetime, the energy is given by the Misner-Sharp mass evaluated at each horizon and the heat capacity, C, is given by

$$\text{Heat capacity for the future outer trapping horizon} = 2\pi \frac{\partial M_{\mathrm{MS}}}{\partial M}\frac{\partial M}{\partial \kappa_G}(r_H), \tag{5.92}$$
$$\text{Heat capacity for the past inner trapping horizon} = -2\pi \frac{\partial M_{\mathrm{MS}}}{\partial M}\frac{\partial M}{\partial \kappa_G}(r_C). \tag{5.93}$$

When taking the derivative, it is important to be careful since the position of the horizon, r_i, varies with the value of the mass parameter M. We will also consider that the inverse function theorem applies to $\frac{\partial M}{\partial \kappa_G}$, meaning that M, as a function of the temperature, is at least of class C^1 and its derivative exists and does not vanish in any point. Then, we start calculating each term:

$$\frac{\partial M_{\mathrm{MS}}}{\partial M} = 1 + \frac{\Lambda r_i^2}{2}\frac{\partial r_i}{\partial M}, \tag{5.94}$$
$$\frac{\partial \kappa_G}{\partial M} = \frac{1}{r_i^2} - \frac{2M}{r_i^3}\frac{\partial r_i}{\partial M} - \frac{\Lambda}{3}\frac{\partial r_i}{\partial M}. \tag{5.95}$$

Since we are interested in evaluating those quantities at the horizons, we use the value of the derivative of r_i with respect to M already calculated (5.90):

$$\frac{\partial M_{\mathrm{MS}}}{\partial M} = \frac{2(3M - r_i) + \Lambda r_i^3}{2(3M - r_i)}, \tag{5.96}$$
$$\frac{\partial \kappa_G}{\partial M} = \frac{3(3M - r_i) - 6M - \Lambda r_i^3}{3r_i^2(3M - r_i)}. \tag{5.97}$$

Furthermore, at the horizons necessarily $\Lambda r_i^3 = 3(r_i - 2M)$:

$$\frac{\partial M_{\text{MS}}}{\partial M} = \frac{r_i}{2(3M - r_i)}, \tag{5.98}$$

$$\frac{\partial \kappa_G}{\partial M} = \frac{3M - 2r_i}{r_i^2(3M - r_i)}. \tag{5.99}$$

Due to (5.91), the numerator of (5.99) is always negative, which means that these derivatives have opposite signs as both have the same sign in the denominator. We conclude that (5.92) is always negative for the future outer trapping horizon, which is a generalization of the result already found in Subsection 4.2.3 for Schwarzschild. On the other hand, the heat capacity for the past inner trapping horizon is always positive (5.93). We also see that given our assumptions and definitions, no phase transition occurs:

$$\text{Heat capacity for the future outer trapping horizon} = \frac{\pi r_H^3}{3M - 2r_H}, \tag{5.100}$$

$$\text{Heat capacity for the past inner trapping horizon} = \frac{\pi r_C^3}{2r_C - 3M}. \tag{5.101}$$

One important point to highlight here is that, as already stated, in other thermodynamic theories the energies associated to the black hole and to the cosmological horizon may not be equivalent to the Misner-Sharp ones. For instance, in the work [57] from 2002, the internal energies considered for each of these horizons are, respectively, M and $-M$. From this consideration, the heat capacities are analysed and it is found that they are both negative. A more recent example is [41] from 2017, where it is considered a unique effective temperature, which is a function of both horizons, and the single heat capacity for the whole spacetime is found to be always positive. Despite the differences, no phase transition is found.

5.4.5 Unstable equilibrium

When discussing the entropy of a horizon, we were careful in distinguishing the black-hole mechanics law, in which the null energy condition is supposed to hold, and the black-hole thermodynamics law, where, due to the Hawking Radiation, it is a generalized entropy that is non-decreasing. However, on a multiple-horizon spacetime, we could wonder if it is possible to define a total entropy which (only) takes into account the entropy of each horizon and such that it does not decrease as the black hole evaporates. It turns out that if the entropies of both horizons in the Vaidya-de Sitter spacetime are combined, then the resulted quantity possess this kind of behavior. When defining this total entropy, we are conjecturing a possible extension of Hayward's approach which gives a single thermodynamics for geometries with multiple horizons. Similar treatments are already known for different thermodynamics [67].

The calculations are straightforward but they lead to the interesting assumption that the near-extreme Schwarzschild-de Sitter spacetime represents an unstable equilibrium and that the Hawking Radiation makes the dynamics of the Vaidya-de Sitter spacetime tend to a configuration of maximum total entropy and minimum total energy. First, we define what is meant by "total entropy":

$$S^{\mathrm{T}} = S_H + S_C = \pi(r_H^2 + r_C^2), \tag{5.102}$$

and, in order to find the maximums and minimums, we take its derivative making use of (5.13) to write r_C in terms of r_H :

$$r_C = \frac{-r_H + \sqrt{4a^2 - 3r_H^2}}{2}. \tag{5.103}$$

Then, it is found that:

$$\text{the total entropy is minimized for } r_H \to \frac{1}{\sqrt{\Lambda}} \text{ and } r_C \to r_H, \tag{5.104}$$

$$\text{the total entropy is maximized for } r_H \to 0 \text{ and } r_C \to \sqrt{\frac{3}{\Lambda}}. \tag{5.105}$$

These are, respectively, the extreme Schwarzschild-de Sitter and the de Sitter spacetimes. Then, one conclusion is that the total entropy, defined as the sum of the entropy of both horizons, is non-decreasing for a black hole that shrinks due to the Hawking Radiation.

Since in the limit of the extreme situation the temperatures of both trapping horizons coincide and we have just found that the entropy is minimized, we are led to similarly analyse the behavior of the total energy of the system. This is defined as the sum of the Misner-Sharp masses evaluated at each horizon:

$$M_{\mathrm{MS}}^{\mathrm{T}} = M + \frac{\Lambda r_H^3}{6} + M + \frac{\Lambda r_C^3}{6}, \tag{5.106}$$

and we take its derivative, where (5.13) can be used to write the mass parameter as a function of the position of the horizons:

$$M = \frac{r_H r_C (r_H + r_C)}{2a^2}. \tag{5.107}$$

It is found an opposite behavior:

$$\text{the total Misner-Sharp mass is maximized for } r_H \to \frac{1}{\sqrt{\Lambda}} \text{ and } r_C \to r_H, \tag{5.108}$$

$$\text{the total Misner-Sharp mass is minimized for } r_H \to 0 \text{ and } r_C \to \sqrt{\frac{3}{\Lambda}}. \tag{5.109}$$

The way the total entropy (5.102) and the total energy (5.106) behaves as functions of the positions of the trapping horizons are represented in Figure 5.5. From it and as just described, we have that, at the limit of a near-extreme Schwarzschild-de Sitter spacetime, the horizons tend to thermal equilibrium, the total entropy is minimized and the total energy is maximized. This might suggest that such situation represents an unstable equilibrium configuration. Moreover, this conclusion seems to be in accordance with a semi-classical result derived by R. Bousso and S. Hawking in 1998 in which the near-extreme Schwarzschild-de Sitter spacetime (called the Nariai solution in their paper) is unstable due to quantum perturbations that disturb this equilibrium [11].

Furthermore, it is interesting that the Hawking Radiation acts to increase the total entropy and to decrease the total energy of the Vaidya-de Sitter spacetime, driving the geometry away from the extreme situation and towards the configuration of maximum total entropy and minimum total energy as it would be expected from a classical thermodynamic system. In order to further explore a possible connection between Hayward thermodynamics and semi-classical effects, it would be necessary a treatment according to quantum field theory in curved geometries, which is beyond the study developted during the production of this work.

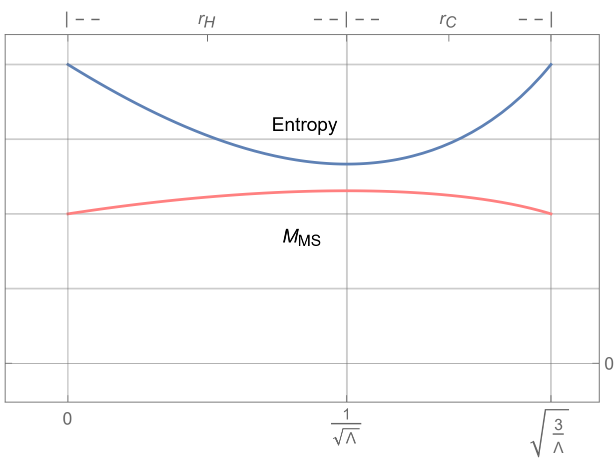

Figure 5.5: The blue and red lines represent, respectively, the qualitative behavior of the total entropy and total energy as functions of the position of the horizons.

Chapter 6

Primordial black holes

In this chapter, we propose the application of the Hayward black-hole thermodynamics in the modelling of primordial black holes. Since these hypothetical black holes should be originated during the early stages of the universe, such objects would be interfering in their environment since the radiation dominated era. For instance, a tiny black hole, around an asteroid mass, that undergoes a relative strong evaporation via the Hawking Radiation could change abruptly its mass due to an accretion process. It was the possibility of such a strong accretion on the radiation dominated era studied by Y. Zel'dovich and I. Novikov in 1967, for instance, that drew attention to the possible existence of primordial black holes [66]. It is due to this importance of the background cosmology that in the first section of this chapter, Section 6.1, the most relevant elements of the ΛCDM model are briefly reviewed.

Even though the existence of primordial black holes is still debatable since no conclusive evidence has yet been observed, the merger of two black holes detected via gravitational waves by the LIGO-Virgo collaboration in 2015 [2], known as the GW150914 event, has recently risen the research in such objects. Two of the reasons that justify this increased interest in primordial black holes are the unexpectedly large mass of the black holes detected in 2015 [1, 52] and the agreement of the merger rate estimated by LIGO with models in which primordial black holes constitute part of the dark matter [51].

If primordial black holes do exist, than it is hoped that some of their interactions with the environment could be detected. On the other hand, the lack of observations would represent constraints on the amount of primordial blacks in the universe. Many recent works investigate how the current observations of the universe constraints the ratio of which primordial black can represent the dark matter. The discussion presented here is mainly based on [13], which compiles some of the up models of constraints, but also looking at [14, 15] that we give an overview of the current understanding of primordial black holes in Section 6.2. After understanding what primordial black holes are and reviewing some of the important up-to-date developments, in Section 6.3 we propose a model representing the dynamics of a black hole in a de Sitter universe.

6.1 Elements of the ΛCDM cosmological model

The ΛCDM cosmological model is a widely-accepted proposal emerged in the 1990s to explain cosmological phenomenons such as, among many others, the present stage of accelerated expansion of the universe and the cosmic microwave background. In the theory and with the current known data, the universe is not a static spacetime, but it is actually dynamical, transitioning through different configurations in which the responsible factor to describe its evolution are the parametrized contents in the universe, which currently the main contributions comes from the dark energy (cosmological constant, Λ) and the cold dark matter (CDM).

One of the assumptions of the ΛCDM model, known as the cosmological principle, is that on large scales our universe should look the same for all observers. More precisely, this means that it can be foliated by homogeneous and isotropic spacelike hypersurfaces. Such solutions for the Einstein Equation are known as the FLRW spacetimes and can be classified according to their close ($\tilde{\kappa} = 1$), open ($\tilde{\kappa} = -1$) and flatness ($\tilde{\kappa} = 0$) [23]:

$$ds^2 = -dt^2 + R^2(t)d\omega^2, \tag{6.1}$$

where $R(t)$ is a scale factor with dimensions of spacetime and

$$d\omega^2 = \frac{d\tilde{r}^2}{1 - \tilde{\kappa}\tilde{r}^2} + \tilde{r}^2 d\Omega^2. \tag{6.2}$$

The ranges taken for the coordinates are:

$$\begin{gathered} -\infty < t < \infty, \qquad 0 < \theta < \pi, \qquad 0 < \phi < 2\pi, \\ \text{for } \tilde{r}, \text{ it depends on the value of } \tilde{\kappa}. \end{gathered} \tag{6.3}$$

A coordinate system in which the line element is written with a -1 component in the dt^2 term and no time-space cross terms, such as (6.1), is known as comoving and the observers who follow the integral curves of ∂_t are said to be comoving observers. These are the ones who perceive the cosmology as isotropic and homogeneous and, moreover, measure a proper time interval of Δt, with respect to which the age of the universe is referred to.

This coordinate system is one of the most used in order to write the FLRW spacetimes. Nonetheless, the geometric intuition to justify the previous classification in terms of the values of $\tilde{\kappa}$ is hidden and it can be favored performing coordinate transformations such that each situation is written apart:

○ $\tilde{\kappa} = 1$: The metric tensor on the spacelike hypersurface is that of a 3-sphere:

$$d\omega^2 = d\chi^2 + \sin^2\chi d\Omega^2, \qquad 0 < \chi < \pi. \tag{6.4}$$

○ $\tilde{\kappa} = -1$: The metric tensor on the spacelike hypersurface is that of a hyperbolic 3-space:

$$d\omega^2 = d\chi^2 + \sinh^2\chi d\Omega^2, \qquad 0 < \chi < \infty. \tag{6.5}$$

○ $\tilde{\kappa} = 0$: The metric tensor on the spacelike hypersurface is that of Euclidean space:

$$d\omega^2 = d\chi^2 + \chi^2 d\Omega^2, \qquad 0 < \chi < \infty. \tag{6.6}$$

Many coordinate systems were already presented and each of them serves a specific purpose. However, the one we will work with comes from a slightly modification in (6.1) so that the new scale factor, $a(t)$, is dimensionless:

$$ds^2 = -dt^2 + a^2(t)\left(\frac{dr^2}{1-\kappa r^2} + r^2 d\Omega^2\right), \tag{6.7}$$

and $\tilde{\kappa}$ is replaced by $\kappa \equiv \frac{\tilde{\kappa}}{R^2(0)}$, which can take any real value.

The energy-momentum tensor for which the FLRW metric (6.7) is a solution of the Einstein Equation is that of a perfect fluid:

$$T_{\mu\nu} = (\rho + p)U_\mu U_\nu + p\ g_{\mu\nu}, \tag{6.8}$$

which represents a fluid whose particles travel with a 4-velocity U^μ with no heat conduction ($T^{i0} = T^{0i} = 0$ for any spatial index), no viscosity ($T^{ij} = 0$), density ρ and pressure p.

There are only two non-trivial and non-distinct Einstein equations which are then called Friedmann equations and describe the dynamics of the scale parameter when given a certain perfect fluid, that is, specifying its density and pressure [17]:

$$H^2 = \frac{8\pi\rho}{3} - \frac{\kappa}{a^2}, \tag{6.9}$$

$$\frac{\ddot{a}}{a} = -\frac{4\pi}{3}(\rho + 3p), \tag{6.10}$$

where it was defined the Hubble parameter

$$H \equiv \frac{\dot{a}}{a}. \tag{6.11}$$

It is also common to define the density parameter, Ω, and the critical density, $\rho_{\rm crit}$, as

$$\Omega \equiv \frac{8\pi\rho}{3H^2} \equiv \frac{\rho}{\rho_{\rm crit}}. \tag{6.12}$$

Hence, the Friedmann equation (6.9) is written as

$$\Omega - 1 = \frac{\kappa}{H^2 a^2}, \tag{6.13}$$

from where it can be seen that if the fluid in the cosmology has its density exactly equal to the critical density, then the spacetime is spatially flat. Moreover, if the density is bigger or lower than the critical density, then the spacetime is, respectively, closed or open.

However, it is expected that the content of the universe is constituted by a set of perfect fluids such that the total density energy can be decomposed as the sum of each constituent,

$$\rho = \sum \rho_i, \tag{6.14}$$

and, therefore, so it can be the density parameter:

$$\Omega = \sum \Omega_i. \tag{6.15}$$

In order to simplify (6.13), it is usual to treat the curvature term in the same way as a fluid so that we define a curvature density

$$\rho_{\rm curv} = -\frac{3\kappa}{8\pi a^2} \tag{6.16}$$

and similarly a curvature density parameter $\Omega_{\rm curv}$. Therefore, (6.13) is simply written as

$$\sum_i \Omega_i = 1. \tag{6.17}$$

Until this point, we have discussed the FLRW spacetimes and how the Friedmann equation can be written in the simple form (6.17), where the curvature and each fluid present in the universe gives some contribution to the dynamics of the scalar factor. In order for the ΛCDM cosmological model to provide predictions in accordance with our universe, we must know the fluids that will enter (6.17) and in which percentage they contribute. According to recent observations, the content of the universe is divided between radiation, baryonic matter, cold dark matter and dark energy (cosmological constant) in the current following proportion [56]:

$$\begin{aligned}
&\Omega_{\mathrm{R}\ 0} \sim 10^{-5},\\
&\Omega_{\mathrm{BM}\ 0} \sim 0.05,\\
&\Omega_{\mathrm{CDM}\ 0} \sim 0.26,\\
&\Omega_{\Lambda\ 0} \sim 0.69.
\end{aligned} \tag{6.18}$$

Moreover, the observable universe is close to being spatially flat [56]:

$$\Omega_{\mathrm{curv}\ 0} \sim -0.005. \tag{6.19}$$

The density and, hence, the density parameter of each of the contents is a function of the scale factor. The matter density decreases with volume $\rho_{\mathrm{M}} \propto a^{-3}$, the radiation density decreases with $\rho_{\mathrm{R}} \propto a^{-4}$ due to the change in volume plus the change in wavelength and the density of the dark matter is not altered by the scalar factor $\rho_{\Lambda} \propto a^{0}$. Knowing the current contribution of each content of the universe and how it evolves in time, the description of the universe for all times is a matter of solving a differential equation. This is a calculation that is not going to be presented here, but in the rest of this section we comment some of the main results.

It is found out that there is a time in the past when our universe becomes singular. Thus, it is said that our universe has a beginning, that is, a big bang. When the universe was small enough, it can be seen from the discussion in the previous paragraph that the main contribution for the total density comes from the radiation. For that reason, it is said that in the first 47 Ka[1] the universe was in the radiation dominated era. After this period, the most relevant contribution becomes the baryonic and the dark matter until 9.8 Ga and this is known as the matter dominated era. During this epoch, the expansion of the universe stops to slow down and it begins to accelerate. The discovery of the accelerated expansion of the universe comes from the late 1990s and it was a surprising result since there was no known content present in the universe capable to such consequences. At the present time, it is believable that this acceleration comes from a positive cosmological constant which might be a result of some form of "dark energy". After the matter dominated era, passing through the current age of the universe of 13.8 Ga, the universe is in the dark energy dominated era and, asymptotically in the future, when the only contribution comes from Λ, the universe tends to the de Sitter spacetime.

We gave a brief review about the chronology of our universe and in order to end this section about the ΛCDM, it is worth mentioning that there is one addition to the model, which is called inflation. It is a brief period after the big bang, around only 10^{-32}s, when it is believed that the universe expanded at an enormous accelerated rate. The point in

[1] The term Ka stands for kilo-annum, that is, 10^{6} years. Similarly, Ga is giga-annum, or, 10^{9} years.

making this addition to the model is to solve known cosmological problems. For instance, the universe seems to be currently flat although for a universe dominated by radiation or matter it is expected that the cosmology evolves away from flatness. Therefore, the universe must have been almost perfectly flat just after the big bang. The other problem that inflation proposes to solve is called the horizon problem. The point is that, in the ΛCDM model alone, there are causally disconnected regions of the observable universe that appear to have been in thermal equilibrium at some point in the past [17]. Our goal is not to present how inflation solves each of these problems, but to motivate why this proposal is added to the model discussed.

In this section we talked about some of the most important elements of the ΛCDM cosmological model. As it will be seen, there is a class of black holes that may exist during all the different epochs of the universe and, therefore, would be subjected to their distinct characteristics. After giving an overview about these black holes, this work is finished with a thermodynamic model for primordial black holes.

6.2 An overview of primordial black holes

Black holes are called primordial given that they are hypothesized to be originated during the early universe (sometimes taken as the first one second after the big bang [15]) at the inflationary period or, more commonly, at the radiation dominated epoch. There is still no conclusive evidence for their existence, nevertheless, the interest on such objects started more than fifty years ago when Y. Zel'dovich and I. Novikov showed in 1967 that a black hole could go through an extreme accretion of radiation at the early stages of the universe [66]. However, a theoretical suggestion for the existence of such black holes came only a few years latter, in 1971, when S. Hawking proposed a model for their creation with a mass range starting at only 10^{-5}g [24].

In the literature, the formation of primordial black holes is proposed in a variety of ways during inflation or the radiation dominated era [13]. The main perspective is the existence of an inhomogeneity able to stop the natural expansion of an overdense region and to make it collapse. In 1974, B. Carr and S. Hawking showed that for an early universe during the radiation dominated era, when the energy density satisfies $\rho \sim G^{-1}t^{-2}$ (where t is the cosmological time such that the big bang happens when $t = 0$), the gravitational collapse happens on a spherically symmetric region of radius equal to ct (that is, the size of the particle horizon) [16]. Thus, the primordial black hole originated at an early time t has its initial mass of order [13]

$$M \sim \frac{c^3 t}{G} \sim 10^{15} \left(\frac{t}{10^{-23}\ \mathrm{s}} \right) \mathrm{g}. \tag{6.20}$$

And given further details about the nature of the formation of the black hole, the expression (6.20) can be made more accurate [13]. From (6.20), we immediately see that primordial black holes can, in principle, come in an enormous range of masses. For instance, for those originated just at the end of inflation, 10^{-32}s, the black hole would have an initial mass of only 10^6g and, on the other hand, those originated at $1s$ would have a mass of 10^{38}g, which corresponds to 10^5 solar masses.

A lot of the current interest in primordial black holes comes from the detection of gravitational waves originated by a binary black hole merger [2] in 2015. What drew the attention of researchers is the fact that both black holes were about 30 times heavier than the sun and black holes that big were not known to form via stellar collapses. For instance, as it was made clear by the own LIGO-Virgo collaborators in a latter paper [1], this was the best evidence, until that time, of the existence of such a heavy stellar-mass black hole. In the same article, an explanation for the origin the black holes observed is proposed and other hypothesis about their origin are rejected. However, the idea that those objects are in fact primordial black holes were discussed in many subsequent papers, for instance [51, 48].

One reason why primordial black holes are so interesting is that they are natural candidates for dark matter. For a long time, the existence of unknown weakly interacting massive particles, abbreviated to WIMPs, is a strong candidate as a solution to the question: what is the dark matter? Another possible solution for the same question resides on the massive compact halo objects, MACHOs. These are astronomical bodies present in galaxy halos with few or negligible radiation emission. Then, it is proposed by some researchers that the primordial black holes could be the hypothesized MACHOs needed in order to explain at least part of the dark matter [13]. However, as it is just about to be commented, the eventual fraction of dark matter in the form of primordial black holes is heavily constrained due to the lack of observations. This turns this objects far from being an unanimous idea in explaining the lack of matter perceived in the universe.

If an observation is expected for primordial black holes having some mass but they are not detected, this represents a constraint on their existence at this circumstance. An up-to-date review on the current known constraints on primordial black holes is [13] and other useful references in the subject include [14, 15]. The former paper is also being used in order to produce the rest of this section where we review some of, what we consider, its most interesting results.

For primordial black holes generated with a mass less than 10^{15}g, which are those that have been already completely evaporated or are on the verge of vanishing, one of the main constraints comes from the analysis of the cosmic microwave background. For instance, for a mass of 10^{15}g, this constraint says that the primordial black holes could correspond only a fraction of 10^{-8} of the dark matter. The cosmic microwave background is also the main constraint on those black holes which have not yet evaporated and whose initial mass is less than 10^{17}g [13].

Another kind of constraint for non-evaporated primordial black holes that has gained a lot of attention lately are those from the detection of gravitational waves. For instance, the merger rate of binary systems of black holes obtained by LIGO is compared to the expected one given that primordial black holes provide some fraction of the dark matter. For the still existing primordial black holes, we have a large number of different constraints such that between 10^{15}g and 10^{55}g most mass ranges could represent, at most (and usually a lot less), ten per cent of the dark matter. Some of the interesting mass intervals in the study of primordial black holes are the 10^{15}g, which is highly constrained but would make the Hawking radiation relevant in observations, the asteroid range, that is, the interval 10^{17} to 10^{23}g, which is still not constrained, and the interval of 10 to 10^2 solar masses, which, despite being also highly constrained, is in agreement with the GW150914 event [13].

6.3 A model for the thermodynamics of primordial black holes

As pointed out, the topic of primordial black holes is one of the subjects of most interest among physicists in recent years. Moreover, we have already seen that there are proposals of primordial black holes being formed at a large spectrum of masses and those of order 10^{15} g would be close to vanish by now. For these black holes, the temperature is high and the Hawking Radiation strong enough so that a dynamical approach, in order to study their thermodynamics, should be preferable to the Bekenstein-Hawking theory.

If a primordial black hole is originated at the radiation dominated era and, if it is massive enough, it will exist during the matter dominated era and will spend most of its lifetime during the dark energy epoch until it completely evaporates. Therefore, a more interesting model for the thermodynamics for this kind of black hole should take into account its cosmological environment. In this work, we propose a dynamical black-hole model in a de Sitter background, that is, the Vaidya-de Sitter spacetime. In the ΛCDM, de Sitter is the asymptotic geometry for our universe in the far future and, therefore, our model will be more realistic for latter times. It is also expected that a primordial black hole undergoes accretion processes during its lifetime and its dynamics would not only be due to its evaporation via Hawking Radiation. Thus, in the proposed scenario it is chosen a function for the mass parameter and compare the results with a black hole that is only submitted to evaporation.

The construction of the model is based on the work of W. Hiscock of 1981 [35] (also adapted latter by Hayward [31]) where the geometry of the evaporating black hole can be described outside and inside the future outer trapping horizon by, respectively, the portion of the Vaidya geometry in outgoing and ingoing coordinates such that, at the horizon, $M(u) = M(v)$ (see Figure 6.1). For this reason and because the past inner trapping horizon describing the cosmological horizon of an expanding spacetime is covered by the outgoing coordinates, we work in this coordinate system.

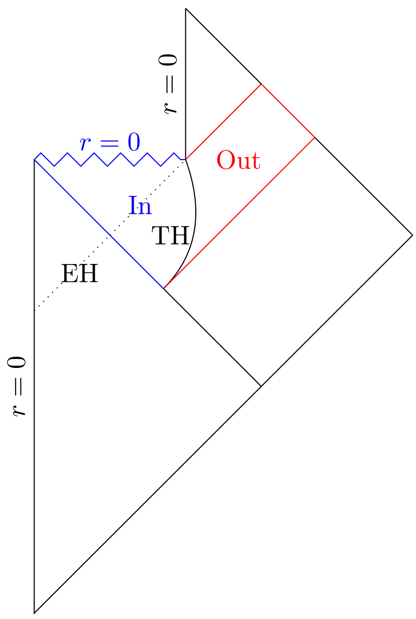

Figure 6.1: Penrose diagram for the formation and evaporation of a black hole in vacuum. The blue and red region are submanifolds of the Vaidya spacetime and they are covered, respectively by ingoing and outgoing Eddington-Finkelstein-like coordinates. The dotted line represents the event horizon, while the curved line represents part of the future outer trapping horizon.

We propose a simple model for the study of the thermodynamics of dynamical primordial black holes. The idea is not to consider a very realistic scenario, but, instead, to obtain some experience and knowledge on how to study the thermodynamics, via Hayward's theory, of such systems so that more detailed models could be explored latter. The dynamics for the mass parameter proposed is

$$M(u) = \frac{M_f - M_i}{\pi} \arctan\left(\frac{u}{\lambda}\right) + \frac{M_f + M_i}{2}. \tag{6.21}$$

In (6.21), there are three parameters we must choose. They are not entirely free as there are constraints from the theory. Neither the initial mass parameter M_i nor the final mass parameter, M_f, can match or exceed $\frac{1}{3\sqrt{\Lambda}}$ in order for the spacetime to remain non-extreme. Furthermore, we ask for $M_i > M_f$ to represent a situation in which the black hole is evaporating.

The last parameter, λ, dictates how fast $M(u)$ changes in time. Since the evaporation is only due to the Hawking Radiation, it makes no physical sense to set its value so that it makes the black hole to evaporate faster than expected from this phenomenon. Therefore, in order to have a base parameter, we will look at the Hawking Radiation of black hole in vacuum[2], for which the rate of change of the mass parameter is estimated as [46]

$$\frac{dM}{du} = -\frac{\hbar c^4}{15360\pi G^2 M^2}. \tag{6.22}$$

It can be calculated that choosing a value for λ greater than around 10^{18}s makes the mass parameter of our model decrease faster than what is given by the Hawking Radiation at $u = 0$. Therefore, we have the following constraint: $\lambda \geq 10^{18}$s.

In Table 6.1 are summarized the constraints that the free parameters must satisfy and, moreover, the chosen values they will assume. The reasons that explain the chosen values shall now be justified. First, we set $M_f = 0$ in order for the mass parameter to approximate to zero as much as possible. We want a black hole small enough so that its evaporation is too fast and, thus, its configuration should not be considered quasi-stationary. Therefore, with this intention we choose M_i to be 5×10^{11} kg, which is a primordial black hole nearly to be completely evaporated by now. As discussed in Section 6.2, primordial black holes of this mass are not the most likely ones to exist according to the current constraints. However, they are small enough to make their evaporation sufficiently strong so that the Hayward black-hole thermodynamics is more appropriate than the Bekenstein-Hawking one. Moreover, there dynamics can be studied on a timescale compatible with the current age of the universe. Lastly, we are going to set $\lambda = 10^{18}$s so that at $u = 0$ the mass parameter in our model changes in the same rate as given by (6.22). This can be interpreted as meaning that when the black hole is formed its dynamics is only driven by the Hawking Radiation emission, but it begins to accrete matter and, then, its evaporation is slowed down (see Figure 6.5).

Table 6.1

	$\boldsymbol{M_i}$	$\boldsymbol{M_f}$	$\boldsymbol{\lambda}$
Constraint	$> M_f$	$< \frac{1}{3\sqrt{\Lambda}}$	$\geq 10^{18}$s
Chosen value	5×10^{11}kg	0	10^{18}s

As we want our model to describe the dynamics of a primordial black hole, it is important to be able to measure the evolution of the mass parameter (and also of the

[2]This is a reasonable approximation for the rate of evaporation of a Vaidya-de Sitter black hole if the cosmological constant given that the cosmological constant and the black hole mass are small enough [65].

relevant thermodynamic quantities) with respect to the time coordinate used in cosmology. That means, it is necessary to compare the u time coordinate of the outgoing Eddington-Finkelstein-like coordinates with the cosmological time, which is measured by the observers that are comoving with the expansion of the universe.

In order to find such coordinate change, first consider that far enough from the black hole (to be quantified latter) the spacetime is approximately de Sitter. Than, our task is to make a transition from the comoving coordinates to the outgoing ones. This can be done first making use of (3.29), (3.32) and (3.26) to find the coordinate change from comoving to Schwarzschild-like coordinates in both disconnected regions, that is, $0 < r < a$ and $a < r < \infty$. Then, we can find the transformation to the outgoing Eddington-Finkelstein-like coordinates via (3.35).

Setting $\theta = 0$ and χ and ϕ to be constant, we have the following relation between the cosmological time, τ, and u:

$$\text{for}\quad 0 < r < a \qquad u = a\,\text{arcsinh}\left(\frac{a}{\sqrt{a^2 - r^2}}\sinh\frac{\tau}{a}\right) - \frac{a}{2}\ln\left|\frac{r+a}{r-a}\right| + C, \tag{6.23}$$

$$\text{for}\quad a < r < \infty \qquad u = a\,\text{arccosh}\left(\frac{a}{\sqrt{r^2 - a^2}}\sinh\frac{\tau}{a}\right) - \frac{a}{2}\ln\left|\frac{r+a}{r-a}\right| + C, \tag{6.24}$$

where

$$r = a\cosh\frac{\tau}{a}\sin\chi, \qquad a = \sqrt{\frac{3}{\Lambda}}, \tag{6.25}$$

and C is a constant that we set to be

$$C \equiv \frac{a}{2}\ln\left|\frac{a\sin\chi + a}{a\sin\chi - a}\right|, \tag{6.26}$$

so that $u = 0$ when $\tau = 0$.

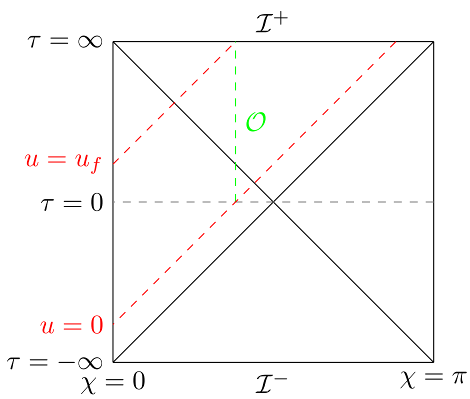

Figure 6.2: Representation of a comoving observer (dashed green line), $\mathcal{O}$, in the Penrose diagram of the de Sitter geometry. The dashed red lines represent the time of the outgoing coordinates, u, at $\tau = 0$ and $\tau \to \infty$.

As commented, we expect the Vaidya-de Sitter spacetime, for a small enough mass parameter, to be nearly de Sitter for large values of radius, r. From (6.25) and considering that the universe has a beginning at $\tau = 0$, we must have χ not too far from $\frac{\pi}{2}$. Therefore, we are interested in an observer $\mathcal{O}$ that has a world line similar to the one of Figure 6.2.

In this work, we are going to choose $\chi = \frac{4}{5}\frac{\pi}{2}$. Then, (6.23) and (6.24) relate the time u, which is used in the model for the dynamics of the mass parameter, and the cosmological time τ, which is measured by this comoving observer. In Figure 6.3 and Figure 6.4 are, respectively, the plots of u with respect to τ around the point when the observer crosses the cosmological horizon and near to the current age of the universe (approximately 4×10^{17}s).

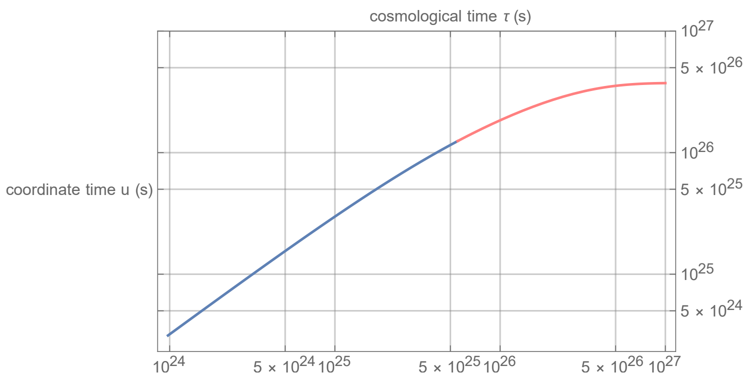

Figure 6.3: Graph of coordinate time u of outgoing coordinates as a function of the cosmological time τ for $\chi = \frac{4\pi}{10}$, $\theta = 0$ and ϕ constant. The blue line comes from (6.23) and the red line from (6.24).

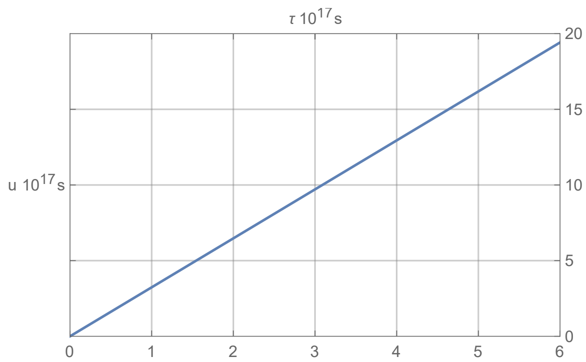

Figure 6.4: Graph of coordinate time u of outgoing coordinates as a function of the cosmological time τ for $\chi = \frac{4\pi}{10}$, $\theta = 0$ and ϕ constant. The curve comes from (6.23).

Knowing how to relate the time u with the cosmological time τ, we calculate the dynamics of some of the relevant quantities in the Hayward black-hole thermodynamics and present the results as functions of both time coordinates. For that, we shall use SI units:

$$
\begin{aligned}
c &= 1 \longrightarrow 3 \times 10^{8} \text{ m s}^{-1}, \\
\hbar &= 1 \longrightarrow 1.05 \times 10^{-34} \text{ m}^2 \text{ kg s}^{-1}, \\
G &= 1 \longrightarrow 6.67 \times 10^{-11} \text{ m}^3 \text{ kg}^{-1} \text{ s}^{-2}, \\
k_B &= 1 \longrightarrow 1.38 \times 10^{-23} \text{ m}^2 \text{ kg s}^{-2} \text{ K}^{-1}.
\end{aligned}
\tag{6.27}
$$

The value for the cosmological constant, Λ, is also needed, which is of order [56]

$$
\Lambda = 10^{-52} \text{ m}^{-2}. \tag{6.28}
$$

First, in Figure 6.5 the evolution of the mass parameter is represented for (6.21) in the color red as function of u and τ in a timescale compatible with the current age of the universe. In the same figure, the evolution of the mass parameter of a black hole submitted only to the Hawking Radiation in vacuum (6.22) is represented in blue. The colors in the background are a reminder that the primordial black hole exists during different cosmological epochs. We consider it is originated at the radiation dominated era (qualitatively in purple color) just after the big bang, it goes through the matter dominated era (gray color) and it transitions to the dark energy dominated era (light blue color), where it exists during most of its lifetime. Since our model only contemplates the de Sitter background, it should be more accurate in the latter region.

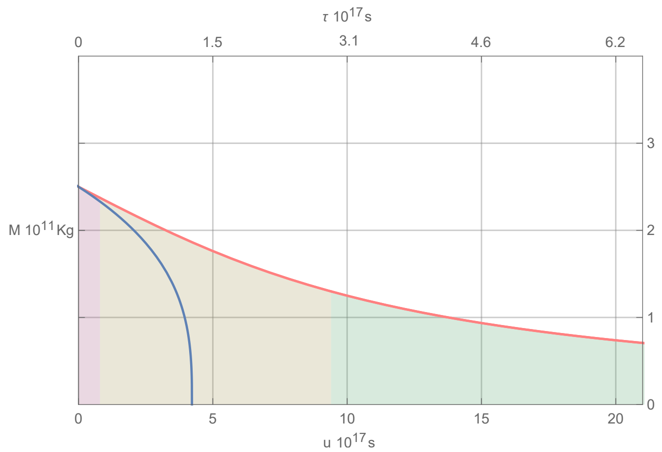

Figure 6.5: Graphs of the mass parameter as a function of, both, the coordinate time in outgoing coordinates and the cosmological time for (red) the simplified model of a dynamic primordial black hole in a de Sitter cosmology (6.21) and for (blue) an evaporating black hole in vacuum (6.22). The purple color in the background represents, qualitatively, the radiation dominated era and the gray and light blue colors represent the transition from matter to dark energy dominated era.

We also want to analyse the behavior of the horizons, which are necessary in order to compute the evolution of the thermodynamic quantities of interest. For that, the position of the horizons, which are the zeros of (5.2) for a time-changing mass parameter, is written as a function of the time coordinate [53]:

$$r_H(u) = \frac{2}{\sqrt{\Lambda}} \cos\left(\frac{\pi + \psi(u)}{3}\right), \tag{6.29}$$

$$r_C(u) = \frac{2}{\sqrt{\Lambda}} \cos\left(\frac{\pi - \psi(u)}{3}\right), \tag{6.30}$$

where $\psi(u) = \arccos\left[3M(u)\sqrt{\Lambda}\right]$ and we take the mass parameter function of our simplified model (6.21) with the free parameters assuming the values discussed.

In Figure 6.6a, the dynamics of each horizon is presented following the same previous definitions for the colors. It can be noticed that the size of the black hole horizon is tiny, even (a bit) smaller than the radius of the nucleus of a hydrogen atom. Furthermore, it is seen that the variations on the position of the horizons are both of order 10^{-16}m. Although the fluctuation is quite small and we should not take them too seriously due to uncertainties in the values we are assuming for the constants, it is enough to see that the black hole horizon contracts a bit more than the cosmological horizon expands. This difference is small, but relevant for the thermodynamic quantities to behave as studied in Section 5.4.

The temperature, Misner-Sharp mass and entropy evaluated at both horizons are also presented in, respectively, Figures 6.6b, 6.6c and 6.6d. As can be observed from Table 5.1, they are all dynamic for being functions of the coordinate time u. For such a small cosmological constant, as it is the case of our universe, taking into account Λ in the calculations result in a tiny correction for the thermodynamic quantities when considering the black hole in vacuum. For instance, the correction in the temperature, which is more relevant for larger black holes, is of order 10^{-27} percent for a black hole one billion times heavier than the sun. One notable result that can be seen from Figure 6.6b is that the temperature for the black hole horizon is a lot greater than the one for the cosmological horizon. This could be expected since we already knew that the area of the former horizon is a lot smaller than the area of the latter one. Furthermore, it justifies our earlier assertion that a black hole that small has a strong Hawking Radiation and, hence, should be treated as a dynamical system.

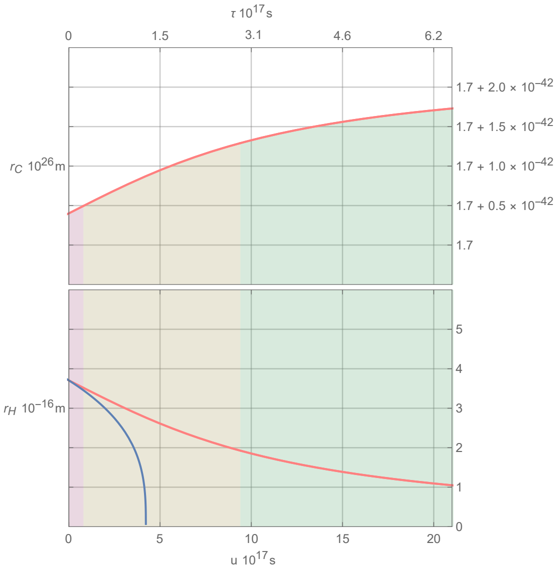

(a) Graphs of the positions of the trapping horizons as a function of, both, the coordinate time in outgoing coordinates and the cosmological time.

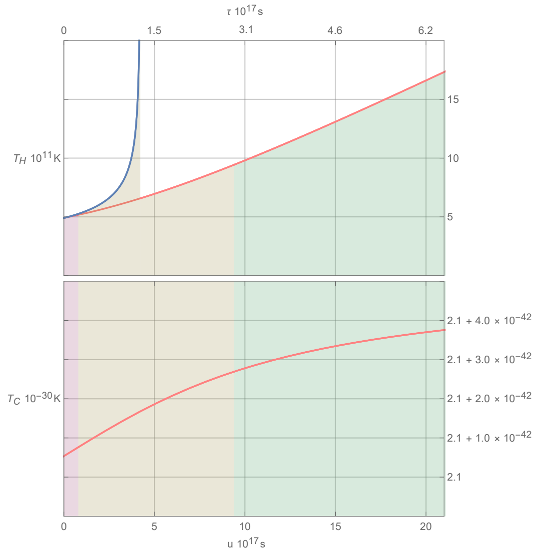

(b) Graphs of the temperatures of the trapping horizons as a function of, both, the coordinate time in outgoing coordinates and the cosmological time.

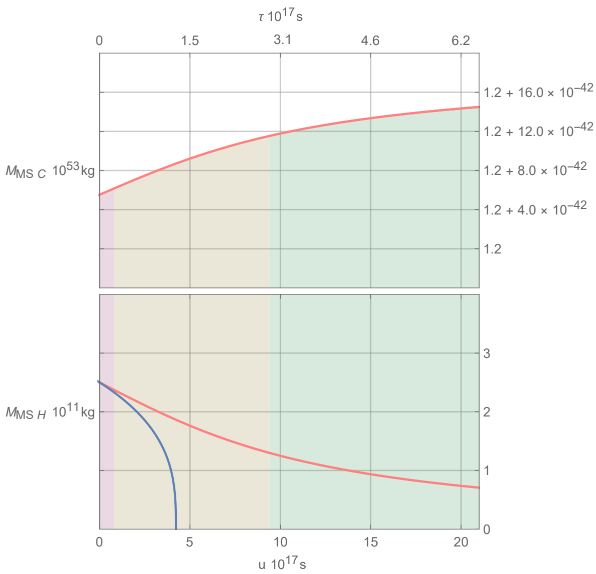

(c) Graphs of the Misner-Sharp masses of the trapping horizons as a function of, both, the coordinate time in outgoing coordinates and the cosmological time.

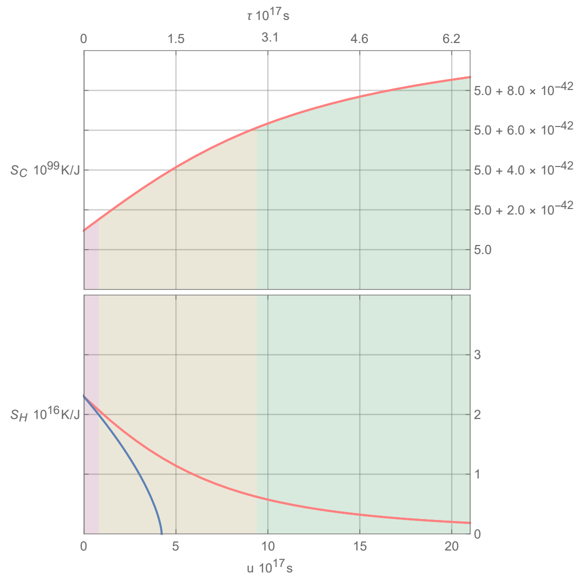

(d) Graphs of the entropies of the trapping horizons as a function of, both, the coordinate time in outgoing coordinates and the cosmological time.

Figure 6.6: In red is the curve for the simplified model of a dynamic primordial black hole in a de Sitter cosmology (6.21) for $M_f = 0$, $M_i = 5 \times 10^{11}$kg and $\lambda = 10^{18}$s. In blue is the curve for an evaporating black hole in vacuum (6.22). In order to relate the distinct time coordinates, it is assumed $\chi = \frac{4\pi}{10}$, $\theta = 0$ and ϕ constant.

Chapter 7

Conclusion

In the present work, we studied the thermodynamics of Vaidya-de Sitter via the Hayward black-hole thermodynamics for general mass functions and also for a more concrete scenario. An important part was the detailed presentation of Hayward's approach. In order for the generalized mechanics laws to be stated and proved, we have explored how important quantities used to develop the theory replace their respective counterpart from the Bekenstein-Hawking thermodynamics. The Kodama vector field, which reduced to the timelike Killing vector field for a class spherically symmetric spacetimes, defined a geometric surface gravity on trapping horizons. This is in a role equivalent to the one assumed by the usual surface gravity on event horizons. It was commented that it is also from the Kodama vector that energy (Misner-Sharp mass) and volume, contained within a trapping horizon, are defined as conserved charges in Hayward's description

Quantities associated to the energy-momentum tensor appeared when defining the generalized Hayward First Law. The rate of change of the Misner-Sharp mass was decomposed as the sum of a term containing the work-density scalar and another with the energy-flux vector field. The other two generalized laws of black-hole mechanics presented were: the Hayward Zeroth Law, which states that the geometric surface gravity is constant on a trapping horizon, and the Hayward Second Law, asserting that the behavior (that is, whether it is non-decreasing, non-increasing or constant) of a given trapping horizon is predicted by its classification (future/past and outer/inner).

The transition to a proper thermodynamics was possible due to the existence of the Hawking Radiation, which associates a physical temperature for the black hole. The semi-classical treatment was not a part of this work, but it was commented that instead of S. Hawking's derivation for the phenomenon on event horizons, it is based on a work of M. Parikh and F. Wilczek that it is shown that the radiation can be seen as a tunneling process on a trapping horizon. It is also interesting that a positive temperature is only derived from this method to future outer and past inner trapping horizons. These being the ones related to a black hole and to a cosmological horizon of an expanding spacetime.

How to interpret the negative "temperatures" is not clear as it was commented in this work and also in [34]. Given a temperature, the entropy of the black hole was defined as one fourth of the area of the trapping horizon.

After studying the Hayward black-hole thermodynamics, the theory was applied to Schwarzschild-de Sitter and Vaidya-de Sitter. First, the trapping horizons for these geometries were found and classified. Then, the thermodynamic quantities were evaluated at the horizons where a positive temperature is defined. Comments were made about the physical interpretation of such quantities. Moreover, two results are relevant to be summarized. From the calculation of the heat capacity, and assuming further conditions, it was proved that no phase transition occurs. This result was derived in the context of Hayward's work and, therefore, the Misner-Sharp mass is understood as the energy of the system. However, the absence of a phase transition is also obtained when considering other thermodynamics and, therefore, different energy definitions [41, 57].

It was also shown that the Hawking Radiation takes the Vaidya-de Sitter spacetime to a configuration of minimum energy and maximum entropy, as it would be expected from a classical thermodynamic system. Furthermore, it is found that the limit of the near-extreme configuration would represent an unstable equilibrium. This result seems to be in accordance to studies where the complete evaporation of black holes, even if it starts in the quasi-extreme Vaidya-de Sitter geometry, is predicted considering quantum effects [11, 12]. This also opens up a possible extension for the present work. We have not studied the semi-classical treatment of Hawking Radiation, but only cited well-known results. Therefore, we can hope that, in an analysis of quantum effects in the Vaidya-de Sitter spacetime, we would be able to explore in more details the interesting relation between the thermodynamic behavior of this geometry and quantum phenomenons related to the evaporation of the black hole.

This work was concluded applying the results obtained for Vaidya-de Sitter to a simple model for the dynamics of a primordial black hole. Furthermore, it was found a way to relate the time used in the model, which is written in outgoing Eddington-Finkelstein-like coordinates, to the cosmological time, that is measured by observers that are comoving with the expansion of the spacetime and with respect to which the chronology of the universe is studied.

The goal of our simplified model was not to represent a realistic situation but, actually, to learn how Hayward's theory can be used to study the thermodynamics of such concrete scenarios. This also indicates another possible extension of our work. There are proposals for the dynamics of primordial black holes specifying the conditions of its formation and which kinds of particles it accretes. For instance, this is done in [50], where it is used a McVittie solution to study the black hole in a cosmological background. Such geometry is also spherically symmetric, contains trapping horizons and, therefore, Hayward's formalism could be employed. Another example is the model presented in [44], which is a lot simpler and also closer to what we have considered. It models the dynamics of the black hole via a Vaidya solution which accretes radiation from the cosmic microwave background. Our work could also be complemented by taking into account the other constituents of the universe. Then, the cosmological environment would not be described by a de Sitter solution, but we would also consider how radiation and matter affects the thermodynamic quantities in the periods they have dominated the universe.

Appendix A

Congruence of null geodesics

If a family of curves fills a region $\mathcal{O}$ of the spacetime, in the sense that on each point of $\mathcal{O}$ one (and only one) curve passes through it, then this family is called a **congruence** in $\mathcal{O}$. In the theory of black-holes, congruences of null curves play a crucial role in the study of the evolution of event-horizons and in the proof of singularity theorems.

Consider we have a congruence of null geodesics generated by the vector field n^μ. Moreover, let us take a one-parameter family of geodesics which is a subset of the congruence such that each curve is designated by a parameter s (in a smooth way) and affinely parametrized by t along its path. If we have a local coordinate system x^μ, then we define the deviation vector from one curve to another by

$$\xi^\mu \equiv \frac{\partial x^\mu}{\partial s}. \tag{A.1}$$

As it is shown in [63], we can always affinely reparametrize the congruence in such a way that the deviation vector is ortoghonal to the curves. Therefore, we may consider $\xi^\mu n_\mu = 0$. And because partial derivatives commute: $\partial_t \xi^\nu = \partial_s n^\mu$, which can be written in an explicit covariant form as

$$n^\mu \nabla_\mu \xi^\nu = \xi^\mu \nabla_\mu n^\nu. \tag{A.2}$$

From ($A.2$) we see that the rate of change of the deviation vector ξ^μ is dictated by

$$\nabla_\mu n^\nu \equiv B^\nu{}_\mu. \tag{A.3}$$

We can also say that $B^\nu{}_\mu$ measures, in some sense, the failure of ξ^ν to be parallel-transported. Since this can be done for any subset of one-parameter family of geodesics of the congruence, it is natural to expect that the tensor $B^\nu{}_\mu$ contains information about how the congruence behaves. In the rest of this appendix we show this is indeed the case.

Besides the null congruence generated by n^μ, let us take another congruence of null curves, of tangent vector field l^μ, such that they are parallel transported, $n^\mu \nabla_\mu l^\nu = 0$, and the new congruence is parametrized so that $n^\mu l_\mu = -1$. Then, we can use these vector fields to build a metric tensor $h_{\mu\nu}$, also called the **projection tensor**, which acts on the vector space spanned by tangent vectors orthogonal to l^μ and n^μ [17]:

$$h_{\mu\nu} = g_{\mu\nu} + l_\mu n_\nu + n_\mu l_\nu. \tag{A.4}$$

In order to understand how (A.4) works, apply it to multiple-scalar vectors of l^μ (or n^μ) and to vectors v^μ and w^μ orthogonal to both l^μ and n^μ:

$$\begin{aligned} h_{\mu\nu} l^\mu v^\nu &= g_{\mu\nu} l^\mu v^\nu - l_\nu v^\nu = g_{\mu\nu} l^\mu v^\nu = 0, \\ h_{\mu\nu} v^\mu w^\nu &= g_{\mu\nu} v^\mu w^\nu. \end{aligned} \tag{A.5}$$

Then we see that when acting on vector fields on the space orthogonal to both l^μ and n^μ, the metric $h_{\mu\nu}$ works just as $g_{\mu\nu}$, but when applied to a tangent vector proportional to l^μ or n^μ, it gives zero. There is another property that confirms the projection behavior of $h_{\mu\nu}$:

$$\begin{aligned} h^\mu_\nu h^\nu_\rho &= (\delta^\mu_\nu + l^\mu n_\nu + n^\mu l_\nu)(\delta^\nu_\rho + l^\nu n_\rho + n^\nu l_\rho) \\ &= \delta^\mu_\rho + l^\mu n_\rho + n^\mu l_\rho + l^\mu n_\rho - l^\mu n_\rho + n^\mu l_\rho - n^\mu l_\rho = h^\mu_\rho. \end{aligned} \tag{A.6}$$

If we return to (A.2), but considering a deviation vector in the projected space, $\xi^\mu = \hat{\xi}^\mu$, it turns out that we only need the projection of ${B^\nu}_\mu$ on the cross sectional surface defined by (A.4),

$${\hat{B}^\nu}_{\ \mu} \equiv h^\nu_\alpha h^\beta_\mu {B^\alpha}_\beta, \tag{A.7}$$

in order to measure the rate of change of the deviation vector along n^μ :

$$\begin{aligned} n^\mu \nabla_\mu \hat{\xi}^\nu = n^\mu \nabla_\mu \xi^\nu &= n^\mu \nabla_\mu h^\nu_\alpha \xi^\alpha \\ &= h^\nu_\alpha n^\mu \nabla_\mu \xi^\alpha \\ &= h^\nu_\alpha \xi^\mu \nabla_\mu n^\alpha \\ &= h^\nu_\alpha \xi^\mu {B^\alpha}_\mu \\ &= h^\nu_\alpha h^\mu_\rho \xi^\rho {B^\alpha}_\mu \\ &= {\hat{B}^\nu}_{\ \mu} \xi^\mu = {\hat{B}^\nu}_{\ \mu} \hat{\xi}^\mu. \end{aligned} \tag{A.8}$$

Inspired by fluid kinematics [47], we decompose $\hat{B}_{\mu\nu}$ as

$$\hat{B}_{\mu\nu} = \frac{1}{2}\theta h_{\mu\nu} + \hat{\sigma}_{\mu\nu} + \hat{\omega}_{\mu\nu}, \tag{A.9}$$

where

$$\theta \equiv \hat{B}^{\mu}{}_{\mu}, \tag{A.10}$$

$$\hat{\sigma}_{\mu\nu} \equiv \hat{B}_{(\mu\nu)} - \frac{1}{2}\theta h_{\mu\nu} = \frac{\hat{B}_{\mu\nu} + \hat{B}_{\nu\mu}}{2} - \frac{1}{2}\theta h_{\mu\nu}, \tag{A.11}$$

$$\hat{\omega}_{\mu\nu} \equiv \hat{B}_{[\mu\nu]} = \frac{\hat{B}_{\mu\nu} - \hat{B}_{\nu\mu}}{2}, \tag{A.12}$$

are, respectively, the **expansion scalar** and the shear and rotation tensors.

In our study of black holes, we will be mostly interested in the behavior of the expansion scalars as they are used to find trapped surfaces and trapping horizons. Therefore, it is important to have a physical interpretation for θ and this comes from the following result [47]:

$$\theta = \frac{1}{\sqrt{h}}\mathcal{L}_n\sqrt{h}. \tag{A.13}$$

Then, we see that the expansion scalar is directly related to the rate of change of the cross sectional area along the null geodesic congruence and ($A.13$) gives an easy way to compute it.

We can also calculate the rate of change of the expansion scalar along one (affinely-parametrized) congruence:

$$\begin{aligned}
n^{\mu}\nabla_{\mu}\theta &= n^{\mu}\nabla_{\mu}\hat{B}^{\nu}{}_{\nu} \\
&= n^{\mu}\nabla_{\mu}B^{\nu}{}_{\nu} \\
&= n^{\mu}\nabla_{\mu}\nabla_{\nu}n^{\nu} \\
&= n^{\mu}\nabla_{\nu}\nabla_{\mu}n^{\nu} + R^{\nu}{}_{\sigma\mu\nu}n^{\sigma}n^{\mu} \\
&= -(\nabla_{\nu}n^{\mu})(\nabla_{\mu}n^{\nu}) - R_{\sigma\mu}n^{\sigma}n^{\mu} \\
&= -B^{\mu}{}_{\nu}B^{\nu}{}_{\mu} - R_{\mu\nu}n^{\mu}n^{\nu} \\
&= -\hat{B}^{\mu}{}_{\nu}\hat{B}^{\nu}{}_{\mu} - R_{\mu\nu}n^{\mu}n^{\nu} \\
&= -\frac{1}{2}\theta^2 - \hat{\sigma}^{\mu\nu}\hat{\sigma}_{\mu\nu} + \hat{\omega}^{\mu\nu}\hat{\omega}_{\mu\nu} - R_{\mu\nu}n^{\mu}n^{\nu}.
\end{aligned} \tag{A.14}$$

In order to find the previous equation we have used $\hat{B}^{\nu}{}_{\nu} = B^{\nu}{}_{\nu}$ and $\hat{B}^{\mu}{}_{\nu}\hat{B}^{\nu}{}_{\mu} = B^{\mu}{}_{\nu}B^{\nu}{}_{\mu}$ [9]. The result ($A.14$) is known as **Raychaudhuri's equation**.

If the null geodesic congruence is not affinely-parametrized,

$$n^{\mu}\nabla_{\mu}n^{\nu} = \kappa_n n^{\nu}, \tag{A.15}$$

then we have [9]

$$\hat{B}^{\mu}{}_{\mu} = B^{\mu}{}_{\mu} + \kappa_n \tag{A.16}$$

$$\hat{B}^{\mu}{}_{\nu}\hat{B}^{\nu}{}_{\mu} = B^{\mu}{}_{\nu}B^{\nu}{}_{\mu} + \kappa_n^2. \tag{A.17}$$

Therefore, applying the necessary changes on the derivation of ($A.14$), Raychaudhuri's equation becomes

$$n^{\mu}\nabla_{\mu}\theta = -\frac{1}{2}\theta^2 - \hat{\sigma}^{\mu\nu}\hat{\sigma}_{\mu\nu} + \hat{\omega}^{\mu\nu}\hat{\omega}_{\mu\nu} - R_{\mu\nu}n^{\mu}n^{\nu} + \kappa_n\theta. \tag{A.18}$$

Appendix B

Radial null geodesics in Vaidya-de Sitter

In Chapter 5, we have frequently used the outgoing and ingoing null vector fields in order to study the behavior of the expansion scalars in the cross-sectional surface. However, it was said but never proven that the presented vector fields, n^μ and l^μ, indeed satisfies the normalization $n^\mu l_\mu = -1$ and are geodesic generators. The present appendix aims to fill this gap.

Since the Vaidya-de Sitter spacetime is a generalization of all spacetimes we have also worked with, we restrict ourselves to show that the remarked features for the radial outgoing and ingoing null vector fields are true in this geometry. Furthermore, as the calculations are similar in ingoing and outgoing Eddington-Finkelstein-like coordinates, we are going to consider here only latter ones.

We recall that the line element for the Vaidya-de Sitter spacetime in Eddington-Finkelstein-like coordinates is (5.74)

$$ds^2 = -f(v,r)du^2 + 2dvdr + r^2(d\theta^2 + \sin^2\theta d\phi^2), \tag{B.1}$$

where

$$f(v,r) = 1 - \frac{2M(v)}{r} - \frac{\Lambda r^2}{3}. \tag{B.2}$$

And also that the outgoing and ingoing radial null vector fields are (5.78 - 5.79)

$$l^\mu = \partial_v + \frac{1}{2}\left(1 - \frac{2M(v)}{r} - \frac{\Lambda}{3}r^2\right)\partial_r, \tag{B.3}$$

$$n^\mu = -\partial_r, \tag{B.4}$$

First, it is straightforward to show that $l^\mu n_\mu = -1$:

$$g_{\mu\nu} l^\mu n^\nu = -g_{\nu r} l^\nu = -g_{vr} l^v - g_{rr} l^r = -g_{rv} l^v = -1. \tag{B.5}$$

In order to show that both vector fields generate geodesics, we need the Christoffel symbols. They can be found in [43] and the non-zero ones are

$$\begin{aligned}
&\Gamma^v{}_{vv} = \frac{M(v)}{r^2} - \frac{\Lambda r}{3}, \qquad \Gamma^v{}_{\theta\theta} = -r, \qquad \Gamma^v{}_{\phi\phi} = -r\sin^2\theta, \\
&\Gamma^r{}_{vv} = f(v,r)\left(\frac{M(v)}{r^2} - \frac{\Lambda r}{3}\right) + \frac{1}{r}\frac{dM(v)}{dv}, \qquad \Gamma^r{}_{rv} = -\left(\frac{M(v)}{r^2} - \frac{\Lambda r}{3}\right), \\
&\qquad\qquad \Gamma^r{}_{\theta\theta} = -rf(v,r), \qquad \Gamma^r{}_{\phi\phi} = -r\sin^2\theta f(v,r), \\
&\Gamma^\theta{}_{r\theta} = \frac{1}{r}, \qquad \Gamma^\theta{}_{\phi\phi} = -\cos\theta\sin\theta, \\
&\Gamma^\phi{}_{r\phi} = \frac{1}{r}, \qquad \Gamma^\phi{}_{\theta\phi} = \cot\theta.
\end{aligned} \tag{B.6}$$

Since this coordinate system is adapted to the ingoing vector field n^μ, it is not hard to show that this vector is tangent to geodesics:

$$n^\mu \nabla_\mu n^\nu = n^\mu\left(\partial_\mu n^\nu + \Gamma^\nu{}_{\mu\rho} n^\rho\right) = \Gamma^\nu{}_{rr} = 0. \tag{B.7}$$

However, to show that the outgoing vector field is also tangent to geodesics requires some calculations:

$$\begin{aligned}
l^\mu \nabla_\mu l^\nu &= l^v \nabla_v l^\nu + l^r \nabla_r l^\nu \\
&= \Gamma^\nu{}_{v\rho} l^\rho + \partial_v l^\nu + \frac{1}{2} f(v,r)\left(\Gamma^\nu{}_{r\rho} l^\rho + \partial_r l^\nu\right) \\
&= \Gamma^\nu{}_{vv} + \frac{1}{2} f(v,r)\Gamma^\nu{}_{vr} + \partial_v l^\nu \\
&\qquad + \frac{1}{2} f(v,r)\left(\Gamma^\nu{}_{rv} + \frac{1}{2} f(v,r)\Gamma^\nu{}_{rr} + \partial_r l^\nu\right),
\end{aligned} \tag{B.8}$$

$$\begin{aligned}
\text{if } \nu = v \qquad &= \Gamma^v{}_{vv} + \frac{1}{2} f(v,r)\Gamma^v{}_{vr} + \partial_v l^v + \frac{1}{2} f(v,r)\left(\Gamma^v{}_{rv} + \frac{1}{2} f(v,r)\Gamma^v{}_{rr} + \partial_r l^\nu\right) \\
&= \Gamma^v{}_{vv} \\
&= \frac{M}{r^2} - \frac{\Lambda r}{3},
\end{aligned}$$

$$
\begin{aligned}
\text{if } \nu = r \qquad\qquad &= \Gamma^{r}{}_{vv} + \frac{1}{2}f(v,r)\Gamma^{r}{}_{vr} + \partial_v l^r + \frac{1}{2}f(v,r)\left(\Gamma^{r}{}_{rv} + \frac{1}{2}f(v,r)\Gamma^{r}{}_{rr} + \partial_r l^r\right)\\
&= f(v,r)\left(\frac{M}{r^2} - \frac{\Lambda r}{3}\right) + \frac{1}{r}\frac{dM}{dv} - \frac{1}{2}f(v,r)\left(\frac{M}{r^2} - \frac{\Lambda r}{3}\right) - \frac{1}{r}\frac{dM}{dv}\\
&\qquad\qquad + \frac{1}{2}f(v,r)\left[\frac{\Lambda r}{3} - \frac{M}{r^2} + \frac{1}{2}\left(\frac{2M}{r^2} - \frac{2\Lambda r}{3}\right)\right]\\
&= \frac{1}{2}f(v,r)\left(\frac{M}{r^2} - \frac{\Lambda r}{3}\right),
\end{aligned}
$$

$$
\text{if } \nu = \theta \qquad\qquad = 0,
$$

$$
\text{if } \nu = \phi \qquad\qquad = 0.
$$

Substituting all the components calculated in (B.8) we find

$$
l^{\mu}\nabla_{\mu}l^{\nu} = \left(\frac{M}{r^2} - \frac{\Lambda r}{3}\right)l^{\nu}. \tag{B.9}
$$

Therefore, it is proven that n^{μ} and l^{μ} are indeed generators of geodesics, such that, the first one is affinely-parametrized but the second one is not.

Appendix C

Thermodynamics for a general metric function in Vaidya-de Sitter

The purpose of this appendix is to generalize the results presented in Table 5.1 for a general f function in the Eddington-Finkelstein-like coordinates. Moreover, some important quantities that appear in the Hayward black-hole thermodynamics in the ingoing coordinates[1] are calculated in some details so that the results given in Table 5.1 and in Table C.1 can be checked.

The metric tensor we are considering is

$$ds^2 = -f(v,r)dv^2 + dvdr + r^2 d\Omega^2, \tag{C.1}$$

where $f(v,r)$ is an arbitrary smooth function of v and r. In what follows, we present all the calculations in a straightforward manner.

∘ Work-density scalar:

$$w = -\frac{1}{2}h^{ab}\frac{G_{ab}}{8\pi} = -\frac{1}{8\pi}h^{vr}G_{vr} = \frac{1 - f(v,r) - r\partial_r f(v,r)}{8\pi r^2}. \tag{C.2}$$

∘ Energy-flux vector field:

$$\psi_\mu = \frac{G_{\mu\nu}}{8\pi}g^{\nu\rho}\partial_\rho r + w\partial_\mu r = \frac{G_{\mu\nu}}{8\pi} + \frac{G_{\mu r}}{8\pi}f(v,r) + w\partial_\mu r, \tag{C.3}$$

with non-zero components:

$$\psi_v = -\frac{\partial_v f(v,r)}{8\pi r}, \tag{C.4}$$

$$\psi_r = 0. \tag{C.5}$$

[1]The calculations are similar for the outgoing Eddington-Finkelstein-like coordinates.

○ Misner-Sharp mass:

$$M_{\rm MS} = \frac{r}{2}(1 - g^{\mu\nu}\partial_\mu r \partial_\nu r) = \frac{r}{2}\big[1 - f(v,r)\big]. \tag{C.6}$$

○ Geometric surface gravity (at a possible trapping horizon at r_i):

$$\kappa_G = \frac{1}{2\sqrt{h}}\partial_a(\sqrt{h}h^{ab}\partial_b r) = \frac{1}{2}\partial_r h^{rr} = \frac{1}{2}\partial_r f(v,r_i). \tag{C.7}$$

Table C.1

	Ingoing coordinates	**Outgoing coordinates**
Metric tensor	$ds^2 = -f(v,r) + 2dvdr + r^2 d\Omega^2$	$ds^2 = -f(u,r) - 2dudr + r^2 d\Omega^2$
Einstein tensor $G_{\mu\nu}$ (non-zero components)	$G_{vv} = \frac{1}{r^2}\big[-f^2(v,r) + f(v,r) \times [1 - r\partial_r f(v,r)] - r\partial_v f(v,r)\big]$ $G_{vr} = G_{rv} = \frac{f(v,r) + r\partial_r f(v,r) - 1}{r^2}$ $G_{\theta\theta} = r\left[\partial_r f(v,r) + \frac{r}{2}\partial_r\partial_r f(v,r)\right]$ $G_{\phi\phi} = r\sin^2\theta\left[\partial_r f(v,r) + \frac{r}{2}\partial_r\partial_r f(v,r)\right]$	$G_{uu} = \frac{1}{r^2}\big[-f^2(u,r) + f(u,r) \times [1 - r\partial_r f(u,r)] + r\partial_u f(u,r)\big]$ $G_{ur} = G_{ru} = \frac{-f(u,r) + -r\partial_r f(u,r) + 1}{r^2}$ $G_{\theta\theta} = r\left[\partial_r f(u,r) + \frac{r}{2}\partial_r\partial_r f(u,r)\right]$ $G_{\phi\phi} = r\sin^2\theta\left[\partial_r f(u,r) + \frac{r}{2}\partial_r\partial_r f(u,r)\right]$
Work-density scalar w	$\frac{\Lambda}{8\pi}$	$\frac{\Lambda}{8\pi}$
Energy-flux covector ψ_μ (non-zero components)	$\psi_v = -\frac{1}{8\pi r}\partial_v f(v,r)$	$\psi_u = -\frac{1}{8\pi r}\partial_u f(u,r)$
Misner-Sharp mass $M_{\rm MS}$	$\frac{r}{2}\big[1 - f(v,r)\big]$	$\frac{r}{2}\big[1 - f(u,r)\big]$
Geometric surface gravity κ_G	$\frac{1}{2}\partial_r f(v,r)$	$\frac{1}{2}\partial_r f(u,r)$

Bibliography

[1] Benjamin P Abbott, Richard Abbott, TD Abbott, MR Abernathy, F Acernese, K Ackley, C Adams, T Adams, P Addesso, RX Adhikari, et al. Astrophysical implications of the binary black hole merger gw150914. *The Astrophysical Journal Letters*, 818(2):L22, 2016.

[2] Benjamin P Abbott, Richard Abbott, TD Abbott, MR Abernathy, Fausto Acernese, Kendall Ackley, Carl Adams, Thomas Adams, Paolo Addesso, RX Adhikari, et al. Observation of gravitational waves from a binary black hole merger. *Physical review letters*, 116(6):061102, 2016.

[3] Gabriel Abreu and Matt Visser. Kodama time: Geometrically preferred foliations of spherically symmetric spacetimes. *Physical Review D*, 82(4):044027, 2010.

[4] M Akbar and Rong-Gen Cai. Thermodynamic behavior of the friedmann equation at the apparent horizon of the frw universe. *Physical Review D*, 75(8):084003, 2007.

[5] James M Bardeen. Black holes do evaporate thermally. *Physical Review Letters*, 46(6):382, 1981.

[6] James M Bardeen, Brandon Carter, and Stephen W Hawking. The four laws of black hole mechanics. *Communications in Mathematical Physics*, 31(2):161–170, 1973.

[7] Jacob D Bekenstein. Black holes and entropy. *Physical Review D*, 7(8):2333, 1973.

[8] Richard L Bishop and Samuel I Goldberg. *Tensor analysis on manifolds*. Courier Corporation, 2012.

[9] Matthias Blau. *Lecture notes on general relativity*. Albert Einstein Center for Fundamental Physics, 2011.

[10] Ivan Booth. Black-hole boundaries. *Canadian journal of physics*, 83(11):1073–1099, 2005.

[11] Raphael Bousso. Adventures in de sitter space. *arXiv preprint hep-th/0205177*, 2002.

[12] Raphael Bousso and Stephen W Hawking. (anti-) evaporation of schwarzschild–de sitter black holes. *Physical Review D*, 57(4):2436, 1998.

[13] Bernard Carr, Kazunori Kohri, Yuuiti Sendouda, and Jun'ichi Yokoyama. Constraints on primordial black holes. *arXiv preprint arXiv:2002.12778*, 2020.

[14] Bernard Carr, Florian Kühnel, and Marit Sandstad. Primordial black holes as dark matter. *Physical Review D*, 94(8):083504, 2016.

[15] Bernard Carr and Joseph Silk. Primordial black holes as generators of cosmic structures. *Monthly Notices of the Royal Astronomical Society*, 478(3):3756–3775, 2018.

[16] Bernard J Carr and Stephen W Hawking. Black holes in the early universe. *Monthly Notices of the Royal Astronomical Society*, 168(2):399–415, 1974.

[17] Sean M Carroll. *Spacetime and geometry*. Cambridge University Press, 2019.

[18] Brandon Carter and James B Hartle. *Gravitation in Astrophysics: Cargèse 1986*, volume 156. Springer Science & Business Media, 2012.

[19] Brandon S DiNunno and Richard A Matzner. The volume inside a black hole. *General Relativity and Gravitation*, 42(1):63, 2010.

[20] Valerio Faraoni. Cosmological apparent and trapping horizons. *Physical Review D*, 84(2):024003, 2011.

[21] Valerio Faraoni. *Cosmological and black hole apparent horizons*. Springer, 2015.

[22] Gary W Gibbons and Stephen W Hawking. Cosmological event horizons, thermodynamics, and particle creation. In *EUCLIDEAN QUANTUM GRAVITY*, pages 281–294. World Scientific, 1993.

[23] Jerry B Griffiths and Jiří Podolskỳ. *Exact space-times in Einstein's general relativity*. Cambridge University Press, 2009.

[24] Stephen Hawking. Gravitationally collapsed objects of very low mass. *Monthly Notices of the Royal Astronomical Society*, 152(1):75–78, 1971.

[25] Stephen W Hawking. Black holes in general relativity. *Communications in Mathematical Physics*, 25(2):152–166, 1972.

[26] Stephen W Hawking. Particle creation by black holes. *Communications in mathematical physics*, 43(3):199–220, 1975.

[27] Stephen W Hawking and George Francis Rayner Ellis. *The large scale structure of space-time*, volume 1. Cambridge university press, 1973.

[28] Sean A Hayward. General laws of black-hole dynamics. *Physical Review D*, 49(12):6467, 1994.

[29] Sean A Hayward. Gravitational energy in spherical symmetry. *Physical Review D*, 53(4):1938, 1996.

[30] Sean A Hayward. Unified first law of black-hole dynamics and relativistic thermodynamics. *Classical and Quantum Gravity*, 15(10):3147, 1998.

[31] Sean A Hayward. Formation and evaporation of nonsingular black holes. *Physical review letters*, 96(3):031103, 2006.

[32] Sean A Hayward, R Di Criscienzo, Mario Nadalini, L Vanzo, and S Zerbini. Local hawking temperature for dynamical black holes. *Classical and Quantum Gravity*, 26(6):062001, 2009.

[33] Michal Heller. The manifold model for spacetime. *Acta Cosmologica*, 10:33, 1981.

[34] Alexis Helou. Dynamics of the four kinds of trapping horizons and existence of hawking radiation. *arXiv preprint arXiv:1505.07371*, 2015.

[35] William A Hiscock. Models of evaporating black holes. ii. effects of the outgoing created radiation. *Physical Review D*, 23(12):2823, 1981.

[36] Werner Israel. Third law of black-hole dynamics: a formulation and proof. *Physical review letters*, 57(4):397, 1986.

[37] Pankaj S Joshi. Global aspects in gravitation and cosmology. *ISMP*, 87, 1993.

[38] Sung-Won Kim. The hawking temperature of a dynamical black hole in de sitter spacetime. *Gravitation and Cosmology*, 20(4):247–251, 2014.

[39] Hideo Kodama. Conserved energy flux for the spherically symmetric system and the backreaction problem in the black hole evaporation. *Progress of Theoretical Physics*, 63(4):1217–1228, 1980.

[40] Peter T Landsberg. Is equilibrium always an entropy maximum? *Journal of Statistical Physics*, 35(1):159–169, 1984.

[41] Huai-Fan Li, Meng-Sen Ma, and Ya-Qin Ma. Thermodynamic properties of black holes in de sitter space. *Modern Physics Letters A*, 32(02):1750017, 2017.

[42] Ronald L Mallett. Radiating vaidya metric imbedded in de sitter space. *Physical Review D*, 31(2):416, 1985.

[43] Ronald L Mallett. Evolution of evaporating black holes in an inflationary universe. *Physical Review D*, 33(8):2201, 1986.

[44] Alex B Nielsen. The spatial relation between the event horizon and trapping horizon. *Classical and quantum gravity*, 27(24):245016, 2010.

[45] Maulik K Parikh and Frank Wilczek. Hawking radiation as tunneling. *Physical Review Letters*, 85(24):5042, 2000.

[46] Julius Piesnack and Klaus Kassner. The vaidya metric: expected and unexpected traits of evaporating black holes. *arXiv preprint arXiv:2103.08340*, 2021.

[47] Eric Poisson. *A relativist's toolkit: the mathematics of black-hole mechanics*. Cambridge university press, 2004.

[48] Martti Raidal, Ville Vaskonen, and Hardi Veermäe. Gravitational waves from primordial black hole mergers. *Journal of Cosmology and Astroparticle Physics*, 2017(09):037, 2017.

[49] David C Robinson. Uniqueness of the kerr black hole. *Physical Review Letters*, 34(14):905, 1975.

[50] F Ruiz, C Molina, and JAS Lima. Dynamical model for primordial black holes. *Physical Review D*, 102(12):123516, 2020.

[51] Misao Sasaki, Teruaki Suyama, Takahiro Tanaka, and Shuichiro Yokoyama. Primordial black hole scenario for the gravitational-wave event gw150914. *Physical review letters*, 117(6):061101, 2016.

[52] Misao Sasaki, Teruaki Suyama, Takahiro Tanaka, and Shuichiro Yokoyama. Primordial black holes—perspectives in gravitational wave astronomy. *Classical and Quantum Gravity*, 35(6):063001, 2018.

[53] S Shankaranarayanan. Temperature and entropy of schwarzschild–de sitter spacetime. *Physical Review D*, 67(8):084026, 2003.

[54] Larry Smarr. Mass formula for kerr black holes. *Physical Review Letters*, 30(2):71, 1973.

[55] Peter Szekeres. *A course in modern mathematical physics: groups, Hilbert space and differential geometry*. Cambridge University Press, 2004.

[56] Masaharu Tanabashi, K Hagiwara, K Hikasa, Katsumasa Nakamura, Y Sumino, F Takahashi, J Tanaka, K Agashe, G Aielli, Claude Amsler, et al. Review of particle physics. *Physical Review D*, 98(3), 2018.

[57] Claudio Teitelboim. Gravitational thermodynamics of schwarzschild-de sitter space. *arXiv preprint hep-th/0203258*, 2002.

[58] P Chunilal Vaidya. The gravitational field of a radiating star. In *Proceedings of the Indian Academy of Sciences-Section A*, volume 33, page 264. Springer, 1951.

[59] PC Vaidya. 'newtonian'time in general relativity. *Nature*, 171(4345):260–261, 1953.

[60] D Vick. The vaidya-de-sitter metric in retarded co-ordinates. *Lettere al Nuovo Cimento (1971-1985)*, 44(2):127–128, 1985.

[61] Robert M Wald. Black holes and thermodynamics. In *Black Hole Physics*, pages 55–97. Springer, 1992.

[62] Robert M Wald. The thermodynamics of black holes. *Living reviews in relativity*, 4(1):1–44, 2001.

[63] Robert M Wald. *General relativity*. University of Chicago press, 2010.

[64] David Wallace. The case for black hole thermodynamics part i: Phenomenological thermodynamics. *Studies in History and Philosophy of Science Part B: Studies in History and Philosophy of Modern Physics*, 64:52–67, 2018.

[65] Shi Yan, Tang-Mei He, and Jing-Yi Zhang. Corrected stefan—boltzmann law and lifespan of schwarzschild-de-sitter black hole. *Communications in Theoretical Physics*, 65(6):731, 2016.

[66] Ya B Zel'dovich and ID Novikov. The hypothesis of cores retarded during expansion and the hot cosmological model. *Astronomicheskii Zhurnal*, 43:758, 1966.

[67] L-Chun Zhang and R Zhao. The critical phenomena of schwarzschild-de sitter black hole. *EPL (Europhysics Letters)*, 113(1):10008, 2016.